THE
PHYSICAL REVIEW
A Journal of Experimental and Theoretical Physics
VOL. 46, NO. 7 OCTOBER 1, 1934 SECOND SERIES

Recent Advances in the Production of Heavy High Speed Ions Without the Use of High Voltages

DAVID H. SLOAN AND WESLEY M. COATES, *Radiation Laboratory, Department of Physics, University of California*
(Received August 2, 1934)

A description is given of improvements in the Sloan-Lawrence method of accelerating heavy ions. The new apparatus yields mercury ions with energies of 2,850,000 electron volts, while the previous apparatus yielded ions with energies of 1,260,000 electron volts. The intensity of the beam of ions is of the order of 10^{-8} amperes—only slightly less than in the previous tube which was considerably shorter. The new tube withstands the application of 79,000 volts while the previous tube was limited to 42,000 volts. This improvement is due principally to decreased heating of the electrodes as a result of lowering their resistance and capacity. The spacing of the electrodes has been increased to 20 percent of their length, and their diameter decreased from 13 mm to 6 mm. The number has been increased from 30 to 36 and the length of each is now 25 percent greater. The possibility of extending this method to the acceleration of lighter ions is discussed.

INTRODUCTION

IN previous papers by one of the authors and E. O. Lawrence,[1] an apparatus which produced mercury ions having kinetic energies up to 1,260,000 electron volts was described. The method required the use of no potentials higher than 42,000 volts due to the fact that the ions were made to fall through this potential difference 30 times. Recently, further improvements including the building of a larger tube have made it possible to produce mercury ions with energies of 2,850,000 electron volts.[2] In this case only 79,000 volts is applied to the tube and the ions fall through this potential difference 36 times. The present paper is an account of the changes which have made possible this extension of the method. Another paper will describe some of the properties of these high speed ions.

[1] Sloan and Lawrence, Phys. Rev. **38**, 2021 (1931); Lawrence and Sloan, Proc. Nat. Acad. Sci. **17**, 64 (1931).

[2] A brief account of this work was presented at the Pasadena meeting of the American Physical Society, Phys. Rev. **43**, 212 (1933).

THE METHOD OF ACCELERATING THE IONS

Since the method of accelerating the ions has been described in previous papers,[1] only a brief account will be given here. The apparatus is shown schematically in Fig. 1. The ions travel through a series of copper tubes, or "accelerators," which are connected alternately to the opposite ends of the inductance of an oscillatory circuit. At any instant, there are electric fields of opposite direction and equal magnitude between successive accelerators. If an ion finds itself between the first and second accelerators, it will be drawn into the second accelerator provided that the field is in the right direction. If the proper voltage has been applied, the time consumed while the ion passes through this tube will be exactly one half period of the oscillations. Hence, the ion will arrive between the second and third tubes with the field reversed in direction, so that the ion will receive an additional acceleration into the third tube. Obviously each tube should have a length equal to the square

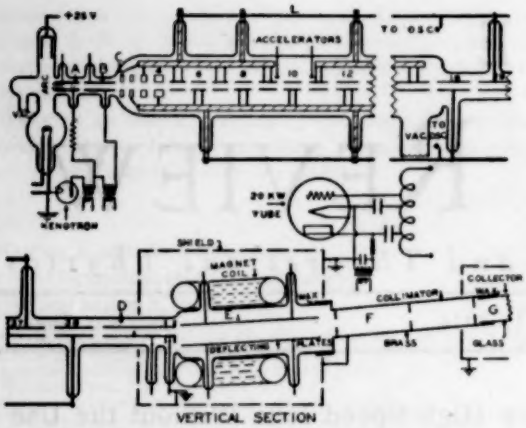

FIG. 1. Diagram of tube and oscillator circuit.

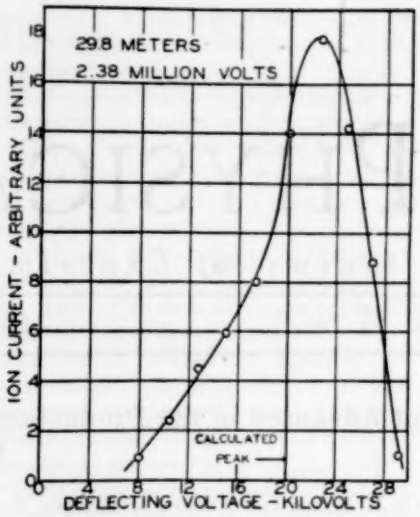

FIG. 2. Variation of ion current to collector with deflecting voltage.

root of its number in the series times the length of the first one (diminished so as to leave a gap between tubes) if each tube is to be traversed in a half period. Under these conditions, the ion will move through the series of accelerators in synchronism with the oscillating fields, gaining between each pair of accelerators an increase in kinetic energy corresponding to the applied voltage. For any given frequency of oscillation, there will be a voltage which gives synchronism between the moving ions and the oscillating fields. Thus, with the tube used in this work, oscillations at 29.8 meters require an applied potential of 79,000 volts and these conditions produce ions with final energies of 2,850,000 electron volts.

The final energy of the ions can be determined in three ways. It is equal to the average voltage between accelerators times the number of accelerators. (An average voltage must be used because the voltage changes while the ions are between accelerators.) Also, the final energy of the ions may be calculated from the period of the oscillations. The ions must of course pass through any accelerator in exactly one half period. Thus, the velocity (and hence the energy) may be calculated from the distance and time involved. Finally, the energy may be calculated from the value of the electrostatic field required to deflect the moving ions through a known angle. (See Fig. 1—*E* and *F*.)

The results of these three calculations are found always to be in quite satisfactory agreement. Fig. 2 shows a plot of the current of ions to the collector as a function of the deflecting voltage. (The collector, not shown in Fig. 1, is simply a Faraday cage.) The curve was taken for a frequency corresponding to 2.38 million electron volts. The deflecting voltage calculated for ions of this energy is 20 kv. It is seen that the peak of the curve is at a deflecting voltage about 10 percent higher. This result may indicate an error in measuring the angle of deflection. However, it is quite possible that the majority of the ions had more energy than that calculated from the frequency. The loading coil, which is inserted at *L* (Fig. 1) in order to increase the voltage on the first few accelerators, had only approximately the correct value when the data of Fig. 2 were taken. As has been pointed out in the previous paper of Sloan and Lawrence,[1] a loading coil which is too small may result in ions with energies in excess of the calculated value. At any rate, there can be no doubt but that the ions had at least the calculated energy of 2.38 million electron volts.

The width of the peak in Fig. 2 is rather great. This width is due partly to fairly wide slits in the collimator (Fig. 1—*F*), and partly to the presence of ions of more than one energy. This matter also has been discussed by Sloan and Lawrence. As they point out, the loading coil has an important effect on the width of the peak. It is quite possible that the peak could have been made sharper if that had been necessary.

The Present Experimental Arrangement

The present tube does not differ greatly in any one respect from the one previously described, but due to a number of small changes it is able to produce much faster ions. The principal changes were made in the accelerating system. The ion source, deflecting system, and pumping arrangements have not been modified in any important way.

The fundamental advantage of the new tube is that higher voltages can be applied to it (79,000 volts as compared to 49,000). The principal reason for this difference is the decreased heating of the electrodes due to decreasing the capacity and the resistance of the accelerator system. Also the gap between accelerators has been increased to 20 percent of the distance between their centers, except in the case of the first ten which are so short that the gap must be considerably more than 20 percent of their length. Another reason for the tube's ability to withstand higher voltages lies in the addition of two liquid air cooled glass bulbs which project into the region near the accelerators.

The accelerators in the new tube have been made 25 percent longer, thus allowing the ions to attain a higher velocity for the same frequency. The number has been increased from 30 to 36. As a result of these two changes the accelerating system is 185 cm long instead of 114 cm in the previous tube. The increased length makes the capacity greater, but this increase is more than offset by the increased spacing of the accelerators and by a reduction in their diameters. The tubes, formerly 13 mm in diameter, are now only 6 mm in diameter. In spite of this last change, the intensity of the beam is of the order of 10^{-8} ampere, and it appears that the focussing action is so strong that the present tube is as effective as the earlier one.

The electrical efficiency of the oscillatory circuit has been considerably improved by reducing the resistance of the connections between accelerators. The inductance coil was made of quarter inch copper tubing and arranged so as to have cooling water running through it. As a result of the increased efficiency it was possible to obtain 2.85 million volt ions with less than 10 kw input. In the previous tube, the same power produced only 1.26 million volt ions. The voltage applied to the tube is obtained from a Hartley circuit as described in the previous papers.

The design of the glass part of the tube seems worthy of mention. As shown in the figure, the first part of the tube was made of Pyrex glass four inches in diameter, while the latter part was made of two inch Pyrex tubing with each accelerator individually supported. The latter type of construction is simpler than the former and in operation, the smaller diameter part of the tube behaved in every way as well as the other part. When the accelerators are individually supported it is a simple matter to add more of them, and it is also possible to insert loading coils wherever desired. For these reasons it would be desirable to use the latter type of construction for the whole tube, except for the first few very short accelerators required in the case of the heavier ions.

Discussion

While this method of accelerating charged particles has so far been used only for mercury ions, it could readily be used for other ions. Lighter ions would travel faster for the same energy in proportion to the inverse square root of their masses. Nitrogen molecule ions (N_2^+) would travel somewhat less than three times as fast as mercury ions. The frequency of oscillation cannot be increased much over that so far used. It is, however, perfectly possible to make the accelerators longer, and in this case two and a half times the present length would be ample.

If the same number of accelerators were used, the tube would be two and a half times as long as at present. Such a tube could be operated by three oscillator tubes in parallel with a master oscillator to excite the grids. If, however, only one oscillator were used, as in the present work, the number of accelerators need not be reduced to less than twenty to leave the tube with the same length as at present, since the accelerators discarded are the long ones at the end of the series. With the smaller number of accelerators, the capacity would be less, so that higher

frequencies of oscillation would be possible. The accelerators, being longer, could have greater spacing and thus higher voltages could be applied. Hence it is feasible to produce nitrogen molecule ions with nearly two million electron volts energy by this method.

It is even possible to give considerable energy to very light ions by this method. Lithium ions could be accelerated to energies of at least one and a quarter million electron volts. Hydrogen or helium ions could be given about one million electron volts. Since this method requires no elaborate equipment it is a practical method even for such very light ions.

The comparative simplicity of this method should be emphasized. The principal requirements are the oscillator tube and the plate voltage transformer. If these two have a power rating of 5 kw, it is possible to produce mercury ions with nearly two million electron volts energy. To produce ions with energies of 2.85 million electron volts, the power rating must be 10 kw. The construction of the tube itself presents no difficulties, especially if one uses the type of construction where the accelerators are individually supported. With such modest equipment as this, it is possible to study the little known properties of very fast positive ions.

The authors take pleasure in expressing their gratitude to Professor Ernest O. Lawrence for his constant interest in this work and for his many valuable suggestions.

OCTOBER 1, 1934 PHYSICAL REVIEW VOLUME 46

The Production of X-Rays by Swiftly Moving Mercury Ions

WESLEY M. COATES, *Radiation Laboratory, Department of Physics, University of California*

(Received August 2, 1934)

A study has been made of the production of soft x-rays (4 to 9A) by mercury ions having energies up to 2.38 million electron volts. The ions were accelerated by the method of Sloan and Lawrence. It has been shown conclusively that the x-rays are actually produced by the ions and not by electrons. Through absorption measurements in aluminum and in air the wave-length of the radiation has been determined for the following targets: aluminum, sulfur, bromine, molybdenum, silver, tin and lead. No radiation could be detected from lithium, boron, carbon, oxygen, sodium, nickel or copper. The wave-lengths were characteristic of the target in the case of aluminum, sulfur, bromine, lead and probably molybdenum. The radiations from tin and silver were not characteristic either of the target or of mercury. The variation in x-ray intensity as a function of the energy of the ions has been studied for targets of lead, bromine, molybdenum, silver and aluminum. The x-ray intensity is found to increase very rapidly with the energy of the ions. No radiation could be detected from bromine, molybdenum, or aluminum when the ions had energies less than 700 kv, nor from lead or silver when the ions had energies less than 400 kv. It is found that at least one in every 2000 mercury ions produces an x-ray quantum when silver is bombarded. The ions in this case had 2.38 million electron volts and produced 2600 volt quanta. A theory is proposed to explain the excitation of x-rays by positive ions, wherein it is assumed that the ion and the target atom temporarily form a quasi-molecule. Loss of some of the inner electrons by one of the atoms as the molecule breaks up necessitates refilling of the empty levels and consequent radiation. Support for this theory is afforded by the agreement between the calculated and the experimental values for the minimum energy necessary for excitation.

INTRODUCTION

IT has been known for some time that x-rays can be produced by positively charged particles such as the alpha-particle[1] and the proton.[2] There has been, however, no observation of x-radiation produced by heavier particles. On the other hand, until recently there has not been available a method of giving large energies to heavy ions. Such a method has been developed by Sloan and Lawrence[3] and extended by Sloan and the author.[4] This method has made it possible to work with mercury ions having energies up to

[1] Chadwick, Phil. Mag. **24**, 594 (1912); Bothe and Fränz, Zeits. f. Physik **49**, 1 (1928); **52**, 466 (1928).

[2] Thomson, Phil. Mag. **28**, 620 (1914); Gerthsen, Ann. d. Physik **85**, 881 (1928); Barton, J. Frank. Inst. **209**, 1 (1930); Lawrence and Livingston, unpublished work.

[3] Sloan and Lawrence, Phys. Rev. **38**, 2021 (1931).

[4] Sloan and Coates, Phys. Rev., preceding article.

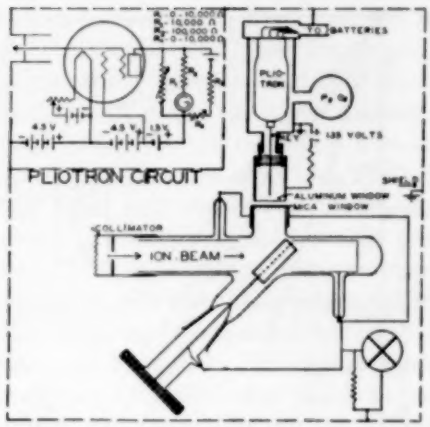

FIG. 1. Collector and ionization chamber with electrical circuit.

2.38 million electron volts. It has been shown in this work that these ions are able to produce an appreciable amount of x-radiation.

APPARATUS

For production of the ions

The method of producing the high speed ions has been described in previous papers.[3, 4] Fig. 1 of the preceding paper shows schematically the tube used. It will be desirable to refer to this figure, and point out the features which were designed to prevent spurious results.

The end of the accelerating system is a tube *D*, which is provided with two lead rings. These rings prevent x-rays or electrons from reaching the ion collector by travelling between the accelerator tubes and the glass walls. X-rays or electrons, which travel through the tube *D*, are stopped by the lead diaphragms in the collimator *F*. Electrons reaching the point *E* are deflected downward by the electrostatic field and also horizontally by the magnetic field. The horizontal deflection eliminates electrons reflected from the bottom deflecting plate. That these precautions were adequate to prevent spurious results was shown by experiments described below.

For detection and measurement of the x-rays

The apparatus used for the study of the x-rays is shown in Fig. 1 of the present paper. The collector for the ion beam which was made of Pyrex glass was waxed in to the brass collimator tube. The glass walls were shielded by metal so as to prevent charges from building up on them. The metal parts were all electrically connected so as to form a Faraday cage. The latter was connected to an electrometer which measured the intensity of the ion beam.

The targets were mounted on a rectangular metal box, which could be rotated by means of a ground joint. Thus it was possible to compare four different targets under identical conditions. One of the targets was always molybdenum which served as a standard. The position of the ion beam could be determined by observation of the fluorescence produced when the ions struck a zinc sulfide target. Thus the solid angle subtended by the ionization chamber could be readily calculated. In some of the earlier measurements this interchangeable target was not used. However it was found that targets could be changed by opening up the tube without appreciably altering conditions, since results could be repeated after changing from one target to another of the same material. Opposite the target a brass cap was waxed on to the glass. This cap was perforated by 59 holes each 2.5 mm in diameter. A sheet of thin mica (1.3 mg/cm^2) covered these holes so as to make the whole vacuum tight.

The radiation was first detected with a Geiger point counter, but the quantitative measurements were all made with an ionization chamber. The latter consisted of a copper cylinder surrounding and insulated from a No. 24 copper wire. The front was closed by thin aluminum (0.47 mg/cm^2). The chamber was filled with air at atmospheric pressure. The guard ring, as shown, was insulated by amber from the central electrode. The chamber was mounted on the brass shield enclosing the FP-54 pliotron by means of an ebonite sleeve. The whole formed a rigid unit which could be moved on a track so as to study the absorption in air. The whole apparatus was well shielded from other electrical circuits.

EXPERIMENTS SHOWING THE OBSERVED EFFECT TO BE GENUINE

Since x-radiation produced by mercury ions has not heretofore been observed it was necessary to show that the effect observed was really due to the ions and that it actually consisted of x-rays. First, it was shown that the observed results were not due to x-rays produced by electrons and scattered from the target. To prove this point,

the beam of ions was prevented from striking the target by a foil known to be transparent to the x-rays. Under these conditions, no x-rays whatever could be detected. Next, it was shown that the effect was not due to cathode rays producing x-rays at the target. It was found that the x-rays were never affected by the application of magnetic fields and retarding potentials which were more than sufficient to eliminate cathode rays from the path leading to the target. Finally, extensive studies of the absorption of the radiation in different substances made it obvious that the radiation was electromagnetic in character. In particular, it was shown that the radiation could not consist appreciably of particles.

The Wave-Length of the Radiation

The wave-length of the radiation was determined in each case by measuring the absorption coefficients in aluminum and in air. In some cases the absorption in mica and in gold was also studied. The absorption curves (Fig. 2) show the logarithm of the ionization current as a function of the thickness of aluminum. In no case do the curves show any evidence for continuous radiation. Moreover, the fact that certain targets of medium atomic number gave no appreciable radiation, while targets of lower and higher atomic numbers did, is strong evidence that the radiation was characteristic rather than continuous. It is of interest to note that Bothe and Fränz[5] found only characteristic radiation excited by alpha-particles.

Aluminum

An effective wave-length for the K radiation of any element may be calculated by taking the weighted mean of the wave-lengths of the individual lines in the K spectrum. From this effective wave-length an effective absorption coefficient may be obtained from the tables of such coefficients.[6] In Fig. 2, the straight line corresponding to the absorption coefficient for the aluminum K radiation has been drawn, and it is seen that the experimental points fit the curve quite well. The data have been multiplied by a constant factor so as to make the point for zero absorber lie on the curve. These results seem to indicate that the radiation observed was the

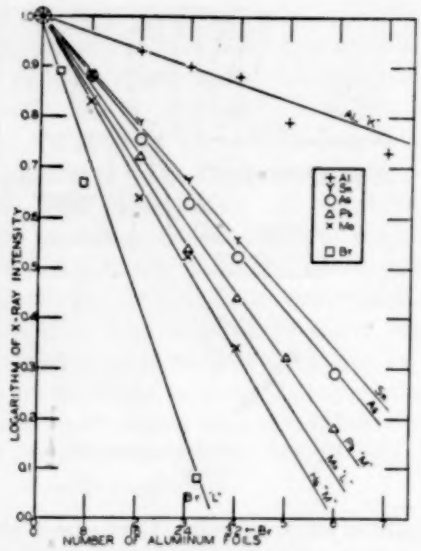

Fig. 2. Curves showing the absorption of the radiation in aluminum.

characteristic K radiation of aluminum (8.23A). A comparison with the other data in Fig. 2 (plotted on the same scale except in the case of bromine) brings out an interesting fact. The curves show that the aluminum foils were more transparent to the radiation from aluminum than to the shorter wave-length radiation from tin, silver, molybdenum, etc. These latter radiations had wave-lengths of from 4 to 5A. This result is of course necessary if the radiation from aluminum was really characteristic of aluminum. The absorption of this radiation in air was also measured. The measurement was rather inaccurate due to the necessity of using a very thin layer of air and of moving the ionization chamber. The result indicated a wave-length of 8.8A, which differs from 8.2A by less than the experimental error. Bothe and Fränz[5] observe that alpha-particles excite the aluminum K radiation with an intensity about 1000 times as great as that found in this work.

Sulfur

The sulfur K radiation involves more excitation energy than that of aluminum (2260 volts as compared to 1460 volts). Hence one might expect the probability of excitation and hence the intensity of the radiation to be less for sulfur than for aluminum under the same conditions. Such a result is found by Bothe and Fränz[5] in the case of

[5] See reference 1.
[6] Siegbahn, *Die Spektroskopie der Röntgenstrahlen* (1932).

alpha-particle excitation. They find less and less intense K radiation from different targets as the atomic number increases until finally no K radiation can be detected. When a sulfur target was bombarded by the mercury ions a small amount of radiation was observed. The intensity was less than half that from aluminum. The absorption in aluminum could not be measured because of lack of intensity. However, measurements in air gave a mass absorption coefficient of 290. The value to be expected for the sulfur K radiation (5.3A) is 301. The agreement is well within the experimental error and it seems quite certain that what was observed was actually the sulfur K radiation.

Nickel and copper

The K radiations for nickel and copper require still more excitation energy (about 8000 volts). Hence the intensity here might be expected to be extremely small and probably unmeasurable. The L radiations are much too soft (about 15A) to reach the ionization chamber. When each of these elements was bombarded by the 2.38 million volt ions no radiation could be detected. It is therefore believed that the ions could not excite an appreciable quantity of the K radiations of these elements.

Lithium, carbon, oxygen and boron

If elements of atomic number less than that of aluminum are bombarded, they might be expected to give the K radiation with large intensity. However the K radiations in these cases would be too soft to reach the ionization chamber. When the 2.38 million volt ions were made to bombard targets of lithium carbonate and boric acid, no radiation could be detected. It is believed that the K radiations were excited but were too soft to be observed.

Bromine

The bromine L radiation, unlike that of nickel and copper, is sufficiently hard (8A) to penetrate the window of the tube. The most prominent lines of the spectrum have wave-lengths of 8.36A, 8.34A, and 8.11A. The weighted mean is 8.3A. The target used was sodium bromide fused on to nickel. The sodium K radiation is quite soft (12A) and apparently was absorbed by the window. At any rate, it would be impossible to confuse the sodium and bromine radiations. Fig. 2 shows the absorption measurements. (The scale of abscissae is different from that for the other data.) The straight line has the slope corresponding to the absorption coefficient for 8.3A. It is seen that the points fit the line quite well. The measurements in air gave a mass absorption coefficient of 1000, whereas the value for 8.3A is 1050. There is little doubt but that the bromine L radiation was actually observed.

Molybdenum

The interpretation of the molybdenum results is complicated by the fact that the mercury M radiation has wave-lengths near those of the molybdenum L radiation. The possibility of exciting the mercury radiation must be considered since every collision in the target involves a mercury ion as well as a target atom. The strongest lines in the mercury M spectrum have wave-lengths of: 5.6, 5.4 and 5.0A. The weighted mean is 5.5A. In Fig. 2 a line has been drawn for this wave-length, as well as for 5.3A, the effective wave-length of the molybdenum L radiation. It is not possible to decide whether the experimental points fit the molybdenum curve or the mercury curve. It is even possible that both types of radiation were present. The intensity of the radiation from molybdenum was less than that from bromine. This fact is consistent with the hypothesis that the molybdenum L radiation was observed. The molybdenum L radiation requires more excitation energy than the bromine L radiation and would therefore be expected to have less intensity under the same conditions. With alpha-particle excitation, such is found to be the case.[5]

Silver and tin

The absorption data for silver and for tin are given in Fig. 2. The straight lines are merely those fitting the data best. These lines indicate, respectively, wave-lengths of 4.8 and 4.7A. The L radiations are at 4.0 and 3.5A, respectively. The significance of these results is not clear. Further investigation of these substances will be necessary.

Lead

The absorption measurements for the radiation from a lead target are shown in Fig. 2. The

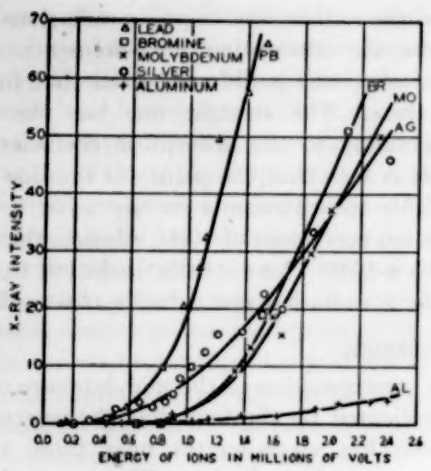

FIG. 3. Excitation curves.

straight line is that for 5.0A, the weighted mean of the wave-lengths of the lead M spectrum. The points lie nearer this line than the one for mercury. However it is not possible to say whether the radiation observed was the lead M radiation, or the mercury M radiation, or a mixture of both. The intensity from lead was greater than that from any other target—about four times that from molybdenum (see Fig. 3).

THE VARIATION IN X-RAY INTENSITY WITH THE ENERGY OF THE IONS

Excitation curves are plotted in Fig. 3 for five targets: aluminum, bromine, molybdenum, silver and lead. The abscissae represent the energy of the mercury ions as measured by the electrostatic field required to deflect them through a known angle. The ordinates represent the x-ray intensity as measured by the ionization chamber in arbitrary units. All of the data have been corrected for the absorption of the window. If the x-ray intensity were expressed in number of quanta, the aluminum and bromine ordinates would be increased by a factor of approximately 1.57. The other curves would be affected only very slightly.

It is at once obvious that the energy of the mercury ions has a marked influence on the x-ray intensity. The fact that the intensity is zero or too small to measure at energies less than 300 kilovolts no doubt explains why this type of radiation has not been observed before. Somewhat similar curves are found for the x-rays excited by alpha-particles.[5]

The curves seem to fall into three groups: aluminum—small intensity; silver, molybdenum and bromine—medium intensity; and, lead—large intensity. It is of interest to note that the radiation in the first group was apparently the K radiation, in the second group apparently the L radiation, and in the third group the M radiation. In particular, aluminum and bromine have very nearly the same effective wave-length for their K and L spectra, respectively. Hence the difference in intensity for these two elements indicates the difference in excitation probability for the K and L spectra.

AN ESTIMATE OF THE EFFICIENCY OF THE EXCITATION PROCESS

It is of interest to determine how many x-ray quanta are excited by a given number of mercury ions. It was not possible to determine this quantity accurately due to uncertainties as to the efficiency of the ionization chamber, the absorption of the radiation in the target, etc. The result should be regarded as a lower limit, since it was assumed that the ionization chamber absorbed the x-rays completely and that no x-rays were absorbed in the target. The calculation was made for the silver target, bombarded by 2.38 million volt ions so as to produce 2600 volt x-rays. The result shows that at least one quantum is produced for every 2000 mercury ions striking the target. The results of Bothe and Fränz show that alpha-particles are of the order of 1000 times as efficient as the mercury ions.[5] It was also found that the 2.38 million volt ions produced about ten times as many x-rays as did 3800 volt electrons striking the same target (molybdenum). These electrons were used since they produced x-rays of approximately the same average hardness as did the beam of ions.

EVIDENCE FOR SOFTER RADIATION

The experimental results have shown that K, L and M radiations were excited in various targets. Still softer radiation should also be excited. For example, the L radiation of aluminum should have been excited as well as the K radiation. The absorption of the window makes it

impossible to observe such soft radiation with the ionization chamber. However such radiation should give rise to a noticeable photoelectric effect.

To investigate this possibility, the electrometer was connected to the brass grid which supports the mica window (Fig. 1). The remaining parts of the collector including the target were made 45 volts positive. When the target was bombarded by 2.38 million volt ions, a current indicating positive charges reaching the grid was observed. This current was about one-third of that to the target. The current seems too large to be due entirely to scattered ions, especially since it was nearly the same for an aluminum target as for a lead target. It is much more probable that the greater part of this current was due to photoelectrons ejected by very soft x-rays. If the observed effect were all due to photoelectrons the results would indicate about ten photoelectrons per mercury ion (over the whole solid angle), and of course many more x-ray quanta.

Another indication of the presence of very soft radiation was obtained when the ions were allowed to fall on an ordinary Eastman Kodak film. An intense blackening was produced after 30 seconds exposure to a current of 1×10^{-9} amperes of 2.38 million volt ions. It is not believed that the ions were able to penetrate the layer of gelatin which covers the emulsion in this type of film since the ions were found to be unable to penetrate the thinnest gold leaf available to the author (0.05 cm air equivalent). Hence the blackening must have been due to radiation excited by the ions, rather than to the ions themselves.

Discussion of the Results

The results obtained indicate that electrons have been ejected from the inner atomic shells as a result of mercury ion impacts. It seems probable that the process of excitation is somewhat as follows. Since the mercury ions have very large kinetic energies, the nuclei of the ion and the atom which it strikes sometimes approach very closely, and thus form essentially a molecule. Calculations show that the approach is in some cases so close that, for example, in the case of lead the M shells of the two atoms overlap. Hence, for a time, some of the M electrons are as near one nucleus as the other. When the molecule breaks up, it is possible that the M electrons will not be properly divided between the two nuclei, but that one nucleus will have one or more empty M levels. Hence M radiation must occur. It is obvious that either the target atom or the mercury atom might be excited. Similar considerations apply to the L and K shells of lighter atoms.

It is possible to calculate the minimum energy that a mercury ion must have in order to approach another atom closely enough to form such a quasi-molecule. The radius of the electron shells is given approximately by the Bohr theory. The distance of closest approach for a given energy is obtained by assuming a Coulomb repulsion between the two nuclei and taking into account the screening action of the electrons. From these considerations one readily obtains the following relation:

$$Z_1Z_2/x = V/300e(1+m_1/m_2),$$

where Z_1 and Z_2 are the effective atomic numbers of mercury and the target atom, m_1 and m_2 the respective masses, x the distance of closest approach (for a head-on collision), and V the energy of the mercury ion expressed in volts. To test the proposed theory, one may substitute for V the value of the experimental threshold of the excitation curve (Fig. 3) for each case, and for x the distance of approach which causes overlapping of the electron shells. A value for the effective atomic number may then be calculated. If the value proves to be of the right order of magnitude, the theory proposed will have been shown to be a possible explanation of the results.

Since there are two atomic numbers Z_1 and Z_2, the case of mercury ions striking lead atoms may be considered, where Z_1 and Z_2 can be assumed equal. The resulting value for Z_1 can then be used as the effective atomic number for mercury in the other cases. The distance x for this case is 1.53×10^{-9} cm. The threshold of the lead excitation curve (Fig. 3) gives the value 400,000 volts for V. The resulting value for Z_1 and Z_2 is 46.3, which seems quite reasonable since the effective atomic number varies from 1 at great distances of separation to 54 at the closest

approach. If the calculated value is considered too high, it may be decreased by requiring that the two nuclei approach more closely in order to cause excitation, or by assuming that the true threshold is somewhat lower than that observed experimentally.

In the case of molybdenum, the distance x proves to be 1.22×10^{-9} cm. For Z_1 the value 51 may be taken. A value larger than 46.3 is chosen because the two nuclei approach more closely in this case. Using 700,000 volts for the threshold, one obtains for Z_2 a value of 37, which is too high, since the maximum value is 32. However, if it is assumed that the two nuclei must approach to a distance of 1.0×10^{-9} cm, and that the true threshold is 600,000 volts, the value of Z_2 becomes 26, which is quite reasonable.

In the case of the aluminum K radiation, if the threshold is taken as 500,000 volts, Z_2 becomes 9.2. Since the maximum value of Z_2 is 11, the calculated value is not unreasonable.

In view of the agreement between the experimental results and the theoretical calculations, it seems possible that the theory is essentially correct. It would seem that either the true thresholds are somewhat lower than the experimental ones, or that the two nuclei must approach somewhat more closely than originally postulated. This difference is of the order of 20 percent at most.

The author takes pleasure in expressing his gratitude to Professor Ernest O. Lawrence, who suggested this problem and directed the work on it, for his constant interest and many helpful suggestions. The author is also greatly indebted to Mr. David H. Sloan for assistance in connection with the production of the high speed ions.

The Halogen Molecules and Their Spectra. *J–J*-Like Coupling. Molecular Ionization Potentials

ROBERT S. MULLIKEN, *Ryerson Physical Laboratory, University of Chicago*

(Received June 19, 1934)

The relations between molecular and atomic ionization potentials are discussed, and rules are formulated, differing for non-bonding, bonding, and anti-bonding electrons. Comparisons are made between ionization potential values predicted by these rules and observed values for N_2, CO, X_2, HX (X = halogen). Rather good agreement is found. Electron configurations of these molecules and O_2 are discussed. The low-energy states of the halogen ions X_2^+ and $(XY)^+$ are discussed, and some of their properties are predicted. With this as a background, low-energy excited states of X_2 and XY are discussed. Many new low-energy states are predicted (Tables III and IV), some giving halogen atoms both in unexcited electron configurations on dissociation, others giving one atom with an excited electron. The foregoing predictions are used to give a reasonable interpretation of the observed absorption spectra of the XY and X_2 molecules, extending into the vacuum ultraviolet. Suggestions are also made for interpreting observed fluorescence and emission spectra. The D level of I_2 is shown to be probably analogous to the $1s\sigma 2p\sigma$, $^1\Sigma^+_u$ state of H_2, with a wave function corresponding to $1^-(\sigma^2\pi^4)1^+(\pi^4)$. The vacuum ultraviolet bands of XY observed by Cordes and Sponer in the regions mainly λλ1600–1950 are of particular interest. The interpretation of an observed interval in these bands leads to the conclusion that the upper levels are in each case of the type $[X^+Y, {}^2\Pi_{i\frac{1}{2}}]\sigma^\times$ and $[X^+Y, {}^2\Pi_{i\frac{3}{2}}]\sigma^\times$, with Ω–s (J–J-like) coupling between the X^+Y core and the $\sigma^\times$ excited electron. Nearly Ω–s coupling is also present, according to the multiplet intervals, in the upper levels of the visible and infrared I_2, Br_2, ICl and IBr absorption bands. The possibility is discussed that part of the intensity in the continua associated with these bands belongs to an expected $^1\Pi \leftarrow {}^1\Sigma^+$ transition.

I. Molecular Electron Configurations and Ionization Potentials

1. Electron configurations of diatomic molecules

A few years ago the writer tentatively suggested a theoretical interpretation of the visible and near-visible absorption spectra of the halogen molecules,[1] which subsequent experimental[2,3] and theoretical[4] work has supported. The present paper deals mainly with a further development of this interpretation, including an extension to bands farther in the ultraviolet.

The theoretical treatment involves two aspects: (*a*), interpretation of electronic states in terms of electron configurations, and prediction of their properties; and (*b*), dissociation product correlations. The new development is chiefly in the former direction. We follow here mainly the Lennard-Jones procedure of assigning unshared electrons to atomic orbitals, shared electrons to molecular orbitals. In practice, the principal difficulty is in drawing the line properly between shared and unshared electrons. In border-line cases, it is useful to write down the electron configuration twice, with the doubtful electrons assigned in each of the two ways, then to study the implications of each, and perhaps to interpolate.

According to the writer's present judgment, the following represent the best formulations for the lowest-energy electron configurations of some typical diatomic molecules. Electrons inside the valence shell are omitted. In the case of the halogens (X, Y, with Y heavier than X and $n = 2, 3, 4, 5$ for F, Cl, Br, I), the atomic states which would result on dissociation are also given.

[1] R. S. Mulliken, Phys. Rev. **36**, 699, 1440 (1930); **37**, 1412 (1931); Rev. Mod. Phys. **4**, 17, 70 (1932). Cf. W. Weizel, *Bandenspektren*, W. Jevons, *Report on Band Spectra*, and Kayser and Konen, Handbuch der Spectroscopie, especially Vol. VII, Part 3 (1934), for numerous references on the halogen spectra, not given here.

[2] Visible and infrared bands of Br_2, I_2: W. G. Brown, Phys. Rev. **37**, 1007; **38**, 1179, 1187 (1931). For $U(r)$ curves cf. also R. S. Mulliken, Rev. Mod. Phys. **4**, 17 (1932), Fig. 42.

[3] Visible and infrared **ICl** bands: O. Darbyshire, Phys. Rev. **40**, 366 (1932); W. E. Curtis and J. Patkowski, Phil. Trans. Roy. Soc. **232**, 395 (1933); and especially W. G. Brown and G. E. Gibson, Phys. Rev. **40**, 529 (1932) and reference 4; cf. also O. K. Rice, J. Chem. Phys. **1**, 375 (1933); for intensity data, G. E. Gibson and H. C. Ramsperger, Phys. Rev. **30**, 603 (1927), also W. E. Curtis and O. Darbyshire, Trans. Faraday Soc. **27**, Part 2, p. 77, (1931). Also other papers cited by the foregoing writers. **IBr**, R. M. Badger and D. M. Yost, Phys. Rev. **37**, 1548 (1931); H. Cordes, Zeits. f. Physik **74**, 34 (1932); W. G. Brown, Phys. Rev. **42**, 355 (1932). $U(r)$ curves, cf. also reference 9.

[4] J. H. Van Vleck, Phys. Rev. **40**, 544 (1932), especially pp. 553–4: theory concerning I_2 and ICl; R. Schlapp, Phys. Rev. **39**, 806 (1932): band structures.

$$\mathbf{N_2}: \quad \cdots(s+s,\sigma_g)^2\ (s-s,\sigma_u)^2\quad (\pi+\pi,\pi_u)^4\quad (\sigma+\sigma,\sigma_g)^2,\ ^1\Sigma^+_g \Big\}, \tag{1}$$
$$\begin{matrix} [30] & 18.8 & (16.3) & 15.6 \\ \{>24.8\} & \{<24.8\} & \{>13.45\} & \{>14.1\} \end{matrix}$$

$$\mathbf{CO}: \quad \cdots(2s_O)^2(s_C+\sigma_O,\sigma)^2(\pi_O+\pi_C,\pi)^4(\sigma_O-s_C\pm\sigma_C,\sigma)^2,\ ^1\Sigma^+ \Big\}, \tag{2}$$
$$\begin{matrix} & 19.7 & 17.1 & 14.3 \\ \{32\} & \{\text{see text}\} & \{\text{see text}\} & \end{matrix}$$

$$\mathbf{O_2}: \quad \cdots(2s)^2(2s)^2(\sigma+\sigma,\sigma_g)^2(\pi+\pi,\pi_u)^4(\pi-\pi,\pi_g)^2,\ ^3\Sigma^-_g,\ ^1\Delta_g,\ ^1\Sigma^+_g \Big\}, \tag{3}$$
$$\{32\} \quad [18] \quad [16] \quad [11.5]$$

$$\mathbf{X_2}: \quad \cdots(\sigma+\sigma,\sigma_g)^2(np\pi)^4(np\pi)^4,\ ^1\Sigma^+_g \longleftrightarrow \text{two X}: \cdots(np)^5,\ ^2P_{1\frac{1}{2}} \Big\}, \tag{4}$$
$$\{>I^\circ_X\} \quad \{\text{near } I^*_X\}$$

$$\mathbf{XY}: \quad \cdots(\sigma_Y+\sigma_X,\sigma)^2\ (n_Yp\pi)^4\quad (n_Xp\pi)^4,\quad ^1\Sigma^+ \longleftrightarrow \text{Y}: (n_Yp)^5,\ ^2P_{1\frac{1}{2}} + \text{X}: (n_Xp)^5,\ ^2P_{1\frac{1}{2}} \Big\}, \tag{5}$$
$$\{>\text{I}^\circ_Y\} \quad \{\text{near } I^*_Y\}\{\text{near } I^*_X\}$$

$$\mathbf{HX}: \quad \cdots(\sigma_X+s_H,\sigma)^2\ (n_Xp\pi)^4,\quad ^1\Sigma^+ \longleftrightarrow \text{X}: (np)^5,\ ^2P_{1\frac{1}{2}} + \text{H}: 1s,\ ^2S \Big\} \tag{6}$$
$$\{>I^\circ_X\} \quad \{\text{near } I^*_X\}$$

Below each type of orbital is given a number or symbol indicating the ionization potential in volts for removing one electron. These apply to non-adiabatic ionization processes in which the distance between the nuclei is not changed (Franck-Condon maximum of probability). Hereafter we shall refer to such potentials as *vertical* ionization potentials, since they correspond to vertical lines on a diagram of potential energy curves. The numbers given in (1) to (6) are largely based on critical potential and spectrum data; values in parentheses or (more uncertain) brackets are, however, estimates, or else based on interpretations which are not certain or (π_g of O_2) averages. These are compared with *predicted* values given in curly braces { }; in regard to the latter, and the meaning of I^* and I°, cf. section 2, where are also given observational data on ionization potentials of the halogens (Table I).

Although the use of atomic orbitals for the π electrons in (4) gives without much doubt the best approximation, there is nevertheless undoubtedly an appreciable—possibly a strong—tendency toward an approximation (4*a*) using molecular orbitals:

$$\mathbf{X_2}: \cdots(\sigma+\sigma,\sigma_g)^2(\pi+\pi,\pi_u)^4(\pi-\pi,\pi_g)^4,\ ^1\Sigma^+_g. \tag{4a}$$
$$\{>I^\circ_X\} \quad \{>I^*_X\} \quad \{<I^*_X\}$$

In previous papers by the writer, the approximation (4*a*) has usually been used. A strong tendency toward (4*a*) would mean a considerable difference between the two ionization potentials π_u and π_g of (4*a*). Unfortunately no direct evidence on this point now exists, but it is likely that a continued study of the halogen spectra will give this.—Similar remarks apply to (5) and the corresponding (5*a*), but the tendency toward (5*a*) should be less than toward (4*a*).

XY:

$$\cdots(\sigma_Y+\sigma_X,\sigma)^2(\pi_Y+\pi_X,\pi)^4(\pi_X-\pi_Y,\pi)^4,\ ^1\Sigma^+. \tag{5a}$$

In the electron configurations (1) to (6), each parenthesis encloses a symbol which denotes a particular type of atomic or molecular orbital. These symbols are simplest for the homopolar molecules N_2, O_2, X_2. Here atomic orbitals are given by simple symbols such as $2s$, $np\sigma$, $np\pi$, and molecular orbitals by such symbols as $(s+s,\sigma_g)$ and $(\pi+\pi,\pi_u)$. Each of these is made up of an informal and particular part, such as $(s+s)$, $(\sigma+\sigma)$, $(\pi+\pi)$, these being abbreviations for $(2s+2s)$, $(np\sigma+np\sigma)$, $(np\pi+np\pi)$, and a *systematic*, internationally accepted, designation such as σ_g or π_u. The informal symbols are roughly descriptive of the individual forms of the orbitals, e.g. $(2s+2s)$ means a form which could be (somewhat roughly) approximated—as suggested by Hund—by forming the normal-

ized sum of two $2s$ atomic orbitals, one located on each of the atoms.

In earlier papers, the writer and others have used various other symbols for molecular orbitals, such as $2s\sigma$, $\sigma_g 2s$, $z\sigma_g$ for $(2s + 2s, \sigma_g)$; $2s\sigma'$, $\sigma_u 2s$, $y\sigma_u$ for $(2s - 2s, \sigma_u)$, $2p\pi$, $\pi_u 2p$, $w\pi_u$ for $(2p\pi + 2p\pi, \pi_u)$. The present informal symbols are introduced here for purposes of maximum momentary clearness and convenience. They could be improved by elaboration, e.g. $(s+s, \sigma_g)$ of N_2 could be written more accurately as $[a(2s + 2s) + b(2p\sigma + 2p\sigma), \sigma_g]$, where a and b are not known exactly, but $a > b$.

For the heteropolar molecules, we again have systematic symbols $(\sigma, \pi, \cdots)$ and informal symbols. Here relations are less symmetrical and more involved than in homopolar molecules. A form such as $(\sigma_O - s_C \pm \sigma_C)$ is intended to mean a molecular orbital whose form could be approximated by taking some linear combination of $2p\sigma$ of oxygen, $2s$ and $2p\sigma$ of carbon. In such a molecular symbol the atomic symbol which is written first (here $2p\sigma_O$) is supposed to be most prominent in the linear combination. Similarly, in $(\pi_O + \pi_C, \pi)$ of CO, $2p\pi_O$ is supposed to have the greater weight, in this case probably by a factor of two or three.

As for the occurrence of simple *atomic* orbitals in heteropolar molecules, we find examples of these above in $2s_O$ of CO and in $n_X p\pi$ and $n_Y p\pi$ of XY in (5). It should be noted that in heteropolar molecules one can go by continuous steps from molecular to atomic orbitals. Really, $(2s_O)$ in CO must contain a *little* admixture of $(2s_C)$ and might be written $(2s_O + 2s_C)$, while $n_Y p\pi$ and $n_X p\pi$ of XY can be written $(n_Y p\pi + n_X p\pi)$ and $(n_X p\pi - n_Y p\pi)$ as in $(5a)$. Since, however, the proportion of the second-named constituent is undoubtedly small in the cases mentioned, the use of pure atomic orbitals is sensible as giving a simple good approximation.

Molecular orbitals of types $(\alpha+\alpha)$ and $(\alpha+\beta)$, or $(\alpha-\alpha)$ and $(\alpha-\beta)$, are, respectively, bonding or anti-bonding. Polar forces also enter, in the cases of heteropolar molecules. The effect of atomic orbitals is non-bonding, i.e., neutral.

2. Molecular and atomic ionization potentials

The *vertical ionization potentials* (cf. immediately following (6)) of molecules may be expected to behave as follows:[5] non-bonding orbitals, roughly the same potential as for the atom alone; bonding orbitals, larger ionization potential than for the atomic orbitals in terms of which they may be approximated, e.g. $(\pi+\pi, \pi_u)$ larger than $np\pi$ in (1)–(6) above; anti-bonding orbitals, lower potential than the related atomic orbitals.

The basis for these rules is fairly obvious. Non-bonding orbitals are affected only indirectly by the entrance of an atom into a molecule, although these indirect effects may sometimes be very appreciable for non-bonding electrons in the outer shell of an atom (cf. $np\pi$ of the HX molecules, Table I). Bonding molecular orbitals are of a type which must differ from corresponding atomic orbitals in such a way as to stabilize the resulting molecule, making its energy lower than that of the separate atoms. This can hardly be the case in homopolar or nearly homopolar molecules unless the electrons which occupy them (bonding electrons) have a considerably higher ionization potential than the corresponding electrons in the atoms before union. Similarly, anti-bonding molecular orbitals are by definition of such a nature than their occupation by electrons tends to cause the molecule to fall apart; they may have lower ionization potentials than the corresponding atomic orbitals. A well-known example is that of the $(\pi-\pi)$ orbital of NO, whose ionization potential is much less than that of any orbital of unexcited N or O. The preceding considerations have often been used in earlier papers. They will, however, now be made more precise.

In applying the foregoing rules, we should not in general compare the observed molecular ionization potential directly with the ordinary minimum ionization potential of the atom. In the first place, the vertical molecular ionization potential may need correction: (a) the energy of the neutral molecule may need to be corrected, if the given molecular electron configuration yields more than one state (example, O_2); for most molecules, however (closed-shell $^1\Sigma^+$ states), there is no such correction; (b) the energy of the positive molecule-ion may similarly need correction; e.g., in the $^2\Pi$ ions of the halogen

[5] Cf. also the relations between atomic and molecular ionization potentials discussed by J. Savard, J. de Phys. et le Rad. [VII] **4**, 650 (1933); **5**, 27 (1934).

molecules, one should take the average energy of $^2\Pi_{\frac{1}{2}}$ and $^2\Pi_{\frac{3}{2}}$.

More notable, the atomic ionization potential nearly always needs correction; the proper potential is one corresponding to the removal of an electron from a "*valence state*" of the *atom*,[6] of valence, say, V_n, giving a valence state of the *positive ion* of valence V_{n+1} or V_{n-1}. Tables of such valence state ionization potentials of atoms are given in another paper.[6] An atomic valence state V_n is appropriate when an atom uses n valence electrons in forming the molecule; in the atom's valence state V_n, these are unpaired.

Removal of a non-bonding electron from the molecule corresponds to removing a non-valence electron from one atom, thus leaving an additional unpaired electron in the atom-ion; in the neutral atom, this was paired with the electron now removed. Thus there are $n+1$ unpaired electrons in the atom-ion, and one sees on due consideration that the proper atomic ionization potential is one corresponding to formation of an ion in a valence state V_{n+1}.[6] The corresponding valence ionization potential will be designated I^* (cf. (4), (5) and (4*a*) above).

Removal of a bonding electron from a molecule usually corresponds to removal of one of the valence electrons from the atom; hence for an atom in a valence state V_n, the atom-ion should be taken in a valence state V_{n-1}. Such an ionization potential will here be designated I° (cf. (4), (5) and (4*a*)). In some cases, e.g., a p^3, V_3 atom, as N in N_2, I° is somewhat different for $p\pi$ than for $p\sigma$ (cf. Ref. 6, Table II).

When electrons in bonding orbitals of type $(a+a)$ are accompanied by anti-bonding electrons of type $(a-a)$, the situation is more or less altered, however. In case there is a complete shell of both of the molecular orbital types $(a+a)$ and $(a-a)$, as e.g., $(s+s)^2(s-s)^2$ in (1) above, or $(\pi+\pi)^4(\pi-\pi)^4$ in (4*a*), we should always consider the alternative mode of description using two closed shells of non-bonding atomic orbitals, as, e.g., $(2s)^2(2s)^2$ instead of $(s+s)^2(s-s)^2$ in (1), or $(np\pi)^4(np\pi)^4$ as in (4) instead of (4*a*). The second mode of description shows clearly that the proper comparison atomic ionization potential in such a case is of the type I^*, and this applies to both the bonding and the anti-bonding molecular orbitals, if we use these for the electron configuration (example, cf. (4*a*)).

In a case like that of O_2 (cf. (3) above), where bonding electrons of type $(a+a)$ are accompanied by a lesser number of anti-bonding electrons of type $(a-a)$, the situation is more complicated. Here there are several ways of ionizing the molecule, corresponding part to I^* and part to I° of the atom. In cases like $(\sigma+\sigma)$ and $(\pi+\pi)$ of N_2 and $(\sigma+\sigma)$ of X_2, however, where anti-bonding electrons $(\sigma-\sigma)$ and $(\pi-\pi)$ are lacking, the proper atomic comparison potential is definitely I°.

The observed vertical ionization potentials of diatomic molecules (either directly observed or obtained by correcting observed non-vertical,—adiabatic,—potentials to verticality) are in good accord with the rules stated above. For N_2, the comparison is given in (1) above; for Cl_2, Br_2, and I_2, in Table I.

For heteropolar molecules, comparisons are often more difficult, since one often has orbitals intermediate between bonding and non-bonding, and other complications. For the $(\pi_O+\pi_C)$ orbital of CO, for example, we should expect $I > \frac{1}{2}(I^\circ_O + I^\circ_C)$ if π_O and π_C were equally represented in $(\pi_O+\pi_C)$, but $I=I^*_O$ for pure π_O. The actual case is believed to be intermediate. Now $\frac{1}{2}(I^\circ_O + I^\circ_C)$ is about 14 volts, while I^*_O is 14.73 volts.[6] The observed $I=17.1$ volts is reasonably consistent with our expectations. Similarly for the CO orbital called $(s_C+\sigma_O)$, we expect $I>\{\frac{1}{2}[I^*_C(s)+I^*_O(p)]=16.8\}$ for equal representation of s_C and σ_O, and $I=I^*_C(s)=18.8$ volts for pure s_C; the observed is 19.7 volts. An added complication in some cases (*e.g.*, N_2, CO) is $s-p$ hybridization.

In most of the molecules HX and XY the binding is more nearly homopolar than heteropolar. A good atomic comparison potential for the σ bonding orbital in such molecules appears to be $\frac{1}{2}(I^\circ_X+I_H)$ or $\frac{1}{2}(I^\circ_Y+I^\circ_X)$; this becomes I°_X, as it should, for $X=Y$. The same simple comparison potential may perhaps be best even for more heteropolar molecules, since otherwise we have various complications, e.g., if we give extra weight to the I of the more negative atom, we ought perhaps to take the latter as a negative

[6] Cf. paper by R. S. Mulliken on electronegativities, Section C and Table IV; to appear in J. Chem. Phys., Oct. or Nov., 1934.

TABLE I. *Vertical ionization and excitation potentials I and E (volts)*[a].

Ionization Process	*Molecule*	*Predicted I*[b]	*Obs. I*[c, d]
HX : $\sigma^2\pi^4, {}^1\Sigma^+ \rightarrow \sigma^2\pi^3, {}^2\Pi$, corresponding to X : $p^5, V_1 \rightarrow p^6, V_2 : I^\circ_X$	HF	18.23	———
	HCl	13.66	13.75 +0.04
	HBr	12.43	13.25 +(0.16)
	HI	11.16	12.75 +(0.33)
HX : $\sigma^2\pi^4 \rightarrow \sigma\pi^4, {}^2\Sigma^+$, corresponding to X : $p^5, V_1 \rightarrow p^6, V_0 : I^\circ_X$ or to H($1s$, V_1)$\rightarrow$H$^+$, $V_0 : I_H$. Predicted I from ave. of I°_X and I_H.	HF	>17.35	———
	HCl	>14.69	17.45
	HBr	>13.99	———
	HI	>13.23	———
XY : $\sigma^2\pi_Y^4\pi_X^4, {}^1\Sigma^+ \rightarrow \sigma^2\pi_Y^4\pi_X^3, {}^2\Pi$, corresponding to X : $p^5, V_1 \rightarrow p^6, V_2 : I^\circ_X$	BrCl	12.43 (π_{Br}) 13.66 (π_{Cl})	——— ———
	IBr	11.16 (π_I) 12.43 (π_{Br})	——— ———
XY : $\sigma^2\pi^4\pi^4 \rightarrow \sigma^2\pi_Y^2\pi_X^4, {}^2\Pi$ Y : $p^5, V_1 \rightarrow p^6, V_2 : I^\circ_Y$	ICl	11.16 (π_I) 13.66 (π_{Cl})	——— ———
XY : $\sigma^2\pi^4\pi^4 \rightarrow \sigma\pi^4\pi^4, {}^2\Sigma^+$, corresponding to Y or X : $p^5, V_1 \rightarrow p^6, V_0 : I^\circ_Y$ or I°_X Predicted I from ave. of I°_Y and I°_X.	BrCl	>15.14	———
	IBr	>13.68	———
	ICl	>14.38	———
$X_2 : \sigma^2\pi^4\pi^4, {}^1\Sigma^+_g \rightarrow \sigma^2\pi^4\pi^3, {}^2\Pi_{g,u}$, corresponding to X : $p^5, V_1 \rightarrow p^6, V_2 : I^\circ_X$	F_2	18.23(*ave.* $^2\Pi_g$, $^2\Pi_u$)	———
	Cl_2	13.66 "	13.2(+0.04) : $^2\Pi_g$
	Br_2	12.43 "	12.8(+0.16) : $^2\Pi_g$
	I_2	11.16 "	10.0(+0.33) : $^2\Pi_g$
$X_2 : \sigma^2\pi^4\pi^4 \rightarrow \sigma\pi^4\pi^4, {}^2\Sigma^+_g$, corresponding to X : $p^5, V_1 \rightarrow p^6, V_0 : I^\circ_X$	F_2	>21.17	———
	Cl_2	>15.84	———
	Br_2	>14.44	———
	I_2	>12.93	(14.2?)[f]
Excitation Process	*Molecule*	*Obs. E*[e]	*Term Value*[f]
XY or $X_2 : \sigma^2\pi^4\pi^4 \rightarrow \sigma^2\pi^4\pi^3\sigma^*, \Pi_{1,0,1,2}$ (mean) (cf. section 7)	BrCl	3.17	(9.3) $= \sigma^*$
	IBr	2.25	(8.9)
	ICl	2.41	(8.8)
	F_2	4.24	(14.0)
	Cl_2	3.7	9.5
	Br_2	2.88	10.1
	I_2	2.10	8.2
Same, except $\sigma^\times$ (cf. section 6)	BrCl	7.46	(4.97) $= \sigma^\times$
	IBr	6.67	(4.49)
	ICl	6.90	(4.26)
	I_2	(7.4)	(2.9)
XY or $X_2 : \sigma^2\pi^4\pi^4 \rightarrow \sigma\pi^4\pi^4\sigma^*, {}^{1,3}\Sigma^+$ (mean) (cf. section 9)	I_2	(6.1)	(14.3) $= \sigma$
	ICl	[8.0][f] ←	[16.8] $= \sigma$

Notes for Table I: (a) A "vertical" ionization potential corresponds to a process in which ionization is accomplished without change in the distance between nuclei. (b) Cf. section 2 of text; and reference 6 for numerical data on I^* and I°. The predicted I values here refer, in the case that the molecular ion is in a $^2\Pi$ state, to the mean of the $^2\Pi_{\frac{1}{2}}$ and $^2\Pi_{\frac{3}{2}}$ substates. (c) Directly observed I values for production of $^2\Pi$ molecular ions of course belong to $^2\Pi_{\frac{1}{2}}$; following each directly observed I is the correction needed (*estimated*, if in parentheses) to bring it up to the mean $(^2\Pi_{\frac{1}{2}}+{}^2\Pi_{\frac{3}{2}})/2$ and thus make it comparable with the predicted I; for example, in the case of HBr, the observed I is 13.25, the estimated correction 0.16. Corrections for lack of verticality of observed I's have not been made (because probably negligible compared with the error of measuring I) except in the case of the σ ionization potential of HCl (17.45 volts), where the correction (0.33 volts) has been included. In the cases of Cl_2, Br_2 and I_2, it should be noted that the observed potentials doubtless correspond to production of a $^2\Pi_g$ ion, and should for this reason be less than the predicted values, which refer to the average of $^2\Pi_g$ and $^2\Pi_u$. (d) The observed I values for π ionization of HX are averages of closely agreeing electron impact values by Knipping (Zeits. f. Physik **7**, 328 (1931)), and Mackay (Phys. Rev. **24**, 319 (1924)); it should be noted that Mackay's I measurements have in nearly all cases proved unusually reliable. The I values for X_2 are also by Mackay; also note that Mohler and Foote get 10.1 volts for I_2 (Phys. Rev. **21**, 382 (1923)), while Hogness and Harkness (Phys. Rev. **32**, 784

(1928)) get evidence that the I_2 ionization potential is less than that of the I atom. The σ potential for HCl is from the $I = 13.75$ for HCl, combined with spectroscopic data on HCl^+. (e) For $\pi \rightarrow \sigma^*$ the mean excitation potentials E are based on the observed maximum (λ_{max}, cf. Table IIB) of continuous absorption (process $^3\Pi_{0^+} \leftarrow {}^1\Sigma^+$), minus an estimated correction to reduce this to the desired value, i.e., to the mean E for $^3\Pi_1$ and $^1\Pi$ of $\sigma^2\pi^4\pi^3\sigma^*$. For $\pi \rightarrow \sigma^X$, the E values for XY are accurate, from data of Cordes and Sponer;[9] the value for I_2 assumes the λ1750 bands[10] to be analogous to the longer-wave $\pi \rightarrow \sigma^X$ bands of XY. For $\sigma \rightarrow \sigma^*$, we have only the approximate vertical $E = 6.5$ volts for $\cdots\sigma^*$, $^1\Sigma^+_u$ of I_2 (cf. reference 13). The mean E of $^1\Sigma^+$ and $^3\Sigma^+$ is here estimated as 6.1 volts. (f) The values for σ^* and σ^X were obtained by subtracting E values from π_X I values. Corrected experimental I values were used for X_2 ($^2\Pi_g$, mean, *viz.*, 13.2, 13.0, 10.3 for Cl_2, Br_2, I_2), predicted values for XY. The σ^X term values thus obtained for XY appear to be too large, which indicates that the predicted I values for XY are too large (cf. section 6). The term value for σ of I_2 is obtained by adding $(6.1) = (\sigma \rightarrow \sigma^*)$ to the term value 8.2 of σ^* as obtained above. The E for ICl is based on an estimated σ and semi-observed σ^* term value.

ion, in the field of a positive ion. Such considerations would affect somewhat the discussion of CO above, but the existence of multiple bonding there can allow some orbitals to be one-sided without making the molecule as a whole polar.

In the cases of HCl, HBr, HI (cf. Table I), the observed (probably nearly vertical) and predicted ionization potentials agree well for HCl, but in going from HCl to HI, the observed π potentials do not decrease as fast as expected. The non-bonding $np\pi$ electrons are unexpectedly difficult to ionize. Possibly the $np\pi$ orbitals have appreciable bonding power in HI, containing an appreciable contribution from $2p\pi$ of H. On the other hand, the strong tendency toward H^+Cl^- character in HCl might be expected to lessen the ionization potential of $3p\pi$ there, because of the shielding effect of the extra Cl electron.

II. The Halogen Molecules and Their Spectra

3. Halogen ions XY^+

We turn now to a more detailed consideration of the halogens. Having described the normal states in (4) and (5), we may consider next the low-energy states of the ions X_2^+ and $(XY)^+$, as a step toward understanding excited states of the neutral halogens. Taking ICl as an example of the XY type, the lowest-energy state of $(ICl)^+$ should be obtained by removing one iodine $5p\pi$ electron from (5), leaving

I^+Cl:

$$\cdots(3p\sigma_{Cl} + 5p\sigma_I, \sigma)^2(3p\pi_{Cl})^4(5p\pi_I)^3, {}^2\Pi_{1\frac{1}{2}, \frac{1}{2}}. \quad (7)$$

The $^2\Pi$ should be inverted, with a doublet interval roughly equal to the spin-orbit coupling coefficient a of an I^+ atom,[7] since it is determined by the group $(5p\pi)^3$ of I^+ (but see end of next paragraph). Although a is not known for I^+ (or Br^+), it can be estimated using the fact that a for the normal state of F^+ is 21 percent larger than for that of F, and for Cl^+ 13 percent larger than for Cl. We may estimate a for I^+ as about 10 percent greater than for I, where $a = (\frac{2}{3})(^2P_{\frac{3}{2}} - {}^2P_{1\frac{1}{2}}) = (\frac{2}{3})(0.94)$ volts; this gives $a = 0.69$ volts as the estimated width of $^2\Pi$ for I^+Cl in (7). Of course one does not expect to find exactly this value, since the $5p\pi$ orbitals of I^+ are appreciably affected by the presence of the ICl bond (cf. next paragraph), and by a tendency toward validity of (5a), which would cause some mixing in of $3p\pi$ of Cl and a consequent lowering of a. Evidence supporting these predictions as to ICl^+ is found in the interpretation of the vacuum ultraviolet spectrum of ICl given in section 6.

Since Cl is more electronegative than I, the neutral molecule ICl is expected to show polarity corresponding to a partial realization of the formulation I^+Cl^-; this is expressed in (5) in the fact that in the bonding orbital $(3p\sigma_{Cl} + 5p\sigma_I)$, the $3p\sigma_{Cl}$ constituent predominates. In the normal state of $(ICl)^+$, the $5p\pi$ ionization of the I atom should tend to attract electrons toward the latter, and so probably strongly reverse the polarity of the I—Cl bond, making it $(\sigma_I + \sigma_{Cl}, \sigma)^2$. Hence, although the ionization is primarily in the I atom, so that the normal state of the molecule may be fairly well characterized as I^+Cl, nevertheless the ionization must be partly at the expense of the Cl. A consequence of this is that the estimate of the width of the $^2\Pi$ of (7), given above as somewhat less than a of I^+, should be somewhat further reduced. An additional complication which may affect the $^2\Pi$ width is the existence of a marked tendency toward case c (atom-like) coupling,[1] which would allow only Ω, but not Λ and S, to be good quantum numbers.

[7] Cf. R. S. Mulliken, Rev. Mod. Phys. **4**, 34–39 (1932).

On dissociation, both components of the $^2\Pi$ of (7) should give $I^+(^3P_2) + Cl(^2P_{1\frac{1}{2}})$, as can be shown from the usual rules.[1] The energy of dissociation D could be calculated exactly from the known D of ICl (2.14 volts to give I, $^2P_{1\frac{1}{2}}$ + Cl, $^2P_{1\frac{1}{2}}$), if we knew the I value for ICl to give $^2\Pi_{1\frac{1}{2}}$ of I^+Cl and of the I atom to give $I^+(^3P_2)$. The predicted approximate value of the former (cf. Table I), and the estimated value of the latter,[6] are, respectively, (11.16−0.33=) 10.83, and 10.55, volts. Supposing these correct, D of I^+Cl would be 1.87 volts and 1.18 volts for the $^2\Pi_{1\frac{1}{2}}$ and the $^2\Pi_{\frac{1}{2}}$ levels, respectively. The values of r_e for these levels would probably not differ radically from that of neutral ICl, since the $(\sigma_{Cl}+\sigma_I)^2$ bond in I^+Cl is not radically different from that in ICl.

If we denote the electron configuration of the normal state of $(ICl)^+$ briefly by $\sigma^2\pi^4\pi^3$ (cf. (7)), the existence of many excited states of fairly low energy, with configurations $\sigma^2\pi^3\pi^4$, $\sigma\pi^4\pi^4$, $\sigma^2\pi^4\pi^2\sigma^*$, $\sigma^2\pi^3\pi^3\sigma^*$, etc., can be predicted, where σ^* is of the anti-bonding type $(5p\sigma_I - 3p\sigma_{Cl})$. Of these probably most are repulsive states, i.e., states with no minimum or practically none in their $U(r)$ curves.

For example, the inverted $^2\Pi$ state $\sigma^2\pi^3\pi^4$, obtainable by removing a $3p\pi$ Cl electron from (5), should be about 2.8 volts above the $^2\Pi_{1\frac{1}{2}}$ normal state of $(ICl)^+$, according to Table I. [I=11.16 volts predicted for production of $\sigma^2\pi^4\pi^3$, $^2\Pi$ (mean), 13.66 volts for $\sigma^2\pi^3\pi^4$, $^2\Pi$ (mean); or 10.82 and 13.62, for $^2\Pi_{1\frac{1}{2}}$ ions. This, of course, refers to vertical processes of ionization.] The separation $^2\Pi_{\frac{1}{2}} - {}^2\Pi_{1\frac{1}{2}}$ in this state should be about equal to a of Cl^+, or 0.08 volt.[7] If this state on dissociation gives $^3P_2$ of I^+ plus $^2P_{1\frac{1}{2}}$ of Cl, as is theoretically possible, then it should probably be unstable, since the energy 2.8 volts required for its vertical excitation considerably exceeds the estimated D of unexcited ICl. If, however, the $U(r)$ has a minimum, this should probably be at an r_e value not radically different from that of unexcited $(ICl)^+$ and ICl, since the $(\sigma+\sigma)^2$ bond still remains.

A third state of considerable interest, although in all probability repulsive, is $\sigma\pi^4\pi^4$, $^2\Sigma^+$. The vertical excitation potential for this should be in excess of 5 volts, according to Table I (probably as much as 6 volts). Certain other excited states of lower energy, besides the $^2\Pi$ above discussed, should, however, exist. According to Table I, only about 2.3 volts is required for the vertical excitation process $\sigma^2\pi^4\pi^4$, $^1\Sigma^+ \rightarrow \sigma^2\pi^4\pi^3\sigma^*$, $^{1,3}\Pi$ (mean) in neutral ICl. Hence in $(ICl)^+$ the group of states belonging to $\sigma^2\pi^4\pi^2\sigma^*$ may be expected to be about 2.3 volts above $\sigma^2\pi^4\pi^3$, $^2\Pi$ (mean). The states of $\sigma^2\pi^3\pi^3\sigma^*$ should come near 5.1 volts.

No bands attributed to $(ICl)^+$ are yet known, but according to the foregoing it is possible that visible bands may exist, corresponding to transitions from states of $\sigma^2\pi^4\pi^3$ or $\sigma^2\pi^4\pi^2\sigma^*$ to the normal state. It may be, however, that the excited states mentioned are all unstable and can give no emission bands.

Two of the excited states of $(ICl)^+$ just mentioned may be written as:

$$\left.\begin{array}{l}(ICl)^+: \\ \cdots(3p\sigma + 5p\sigma, \sigma)^2(3p\pi_{Cl})^3(5p\pi_I)^4, {}^2\Pi_{1\frac{1}{2},\frac{1}{2}}, \\ \text{and} \qquad \cdots(\sigma+\sigma)(\pi_{Cl})^4(\pi_I)^4, {}^2\Sigma^+\end{array}\right\}. \quad (8)$$

4. Halogen ions X_2^+

Halogen ions of the types $(XY)^+$ and X_2^+ should differ considerably in some respects. Taking I_2 as an example, we find that three low-energy states of I_2^+ analogous to the states (7) and (8) of $(ICl)^+$ can be obtained by removal of one electron. They are:

$$\cdots(5p\sigma + 5p\sigma, \sigma_g)^2(5p\pi)^4(5p\pi)^3, {}^2\Pi_{g1\frac{1}{2},\frac{1}{2}}, \quad (9)$$

$$\cdots(\quad\quad)^2(\quad)^4(\quad)^3, {}^2\Pi_{u1\frac{1}{2},\frac{1}{2}}, \quad (10)$$

$$\cdots(\quad\quad)(\quad)^4(\quad)^4, {}^2\Sigma^+_g. \quad (11)$$

Starting from the formulation (4) for I_2, one might at first expect for I_2^+ to find two $^2\Pi$ states, $\cdots(5p\pi)^4(5p\pi)^3$ and $\cdots(5p\pi)^3(5p\pi)^4$, with equal energy. Actually, however, the vacancy in the $(5p\pi)^4$ shell jumps back and forth between the two atoms with considerable speed, so that the formulation $(5p\pi)^{3\frac{1}{2}}(5p\pi)^{3\frac{1}{2}}$ might give a better description. This exchange of the vacancy corresponds to a quantum-mechanical resonance between $\pi^4\pi^3$ and $\pi^3\pi^4$, and we get two states, $^2\Pi_g$ and $^2\Pi_u$, both of type $\pi^{3\frac{1}{2}}\pi^{3\frac{1}{2}}$, although for systematic reasons we use the designation $\pi^4\pi^3$ for both (cf. (9) and (10)). Both should be inverted and each should have a doublet separation about equal to a of the I^+ or I atom, i.e., about 0.7 volts (cf. discussion of I^+Cl in section

3). The energy difference between the $^2\Pi_g$ and the $^2\Pi_u$ should probably not be large, since the atomic groups $(5p\pi)^4$ and $(5p\pi)^3$ are far apart and do not overlap much. Possibly the interaction is so small that the doublets overlap, giving the energy order $^2\Pi_{1/2g}$, $^2\Pi_{1/2u}$, $^2\Pi_{3/2g}$, $^2\Pi_{3/2u}$.

That the $^2\Pi_g$ is the lower can be readily seen by using molecular orbitals for the $5p\pi$ electrons (cf. 4*a*). Then, to get the actual case, we interpolate between the case using molecular orbitals and the other ideal case (4), in which we have precisely zero interaction so that $^2\Pi_g$ and $^2\Pi_u$ are equal in energy. Starting from $\sigma_g^2\pi_u^4\pi_g^4$ as in (4*a*), one can remove either one π_g to get $^2\Pi_g$, or one π_u to get $^2\Pi_u$. Since π_g is the more easily ionized, $^2\Pi_g$ is the lower in energy.

The two low $^2\Pi$ levels should probably have about the same r_e as neutral I_2, since the bond (σ_g^2) remains unchanged. If the two levels differ much in energy, however, the lower one should have somewhat the smaller, the upper one somewhat the larger, r_e.

The observed ionization potentials of Cl_2, Br_2, I_2 (cf. Table I) are on the whole somewhat lower than the values predicted on the assumption that the $np\pi$ electrons are non-bonding; this is what would be expected if the $^2\Pi_u$ and $^2\Pi_g$ states of X_2^+ differ appreciably in energy, the former being then produced at a lower ionization potential than if their energies were equal.

Both of the low $^2\Pi$ states of I_2^+ should give unexcited $I + I^+$ on dissociation ($^2P_{1/2} + {}^3P_2$). If I values were known accurately for I and for I_2, and the $^2\Pi_u$, $^2\Pi_g$ separation in I_2^+ were known, the D values of these states could be calculated from the known D of I_2. On the basis of the considerations given above and the data in Table I, it seems likely that the D's of the $^2\Pi_{1/2u}$ and $^2\Pi_{3/2u}$ are of the same order of magnitude as for neutral I_2, while those of the $^2\Pi_g$ are less but still large enough to give stability.

More than two volts, probably about 4 volts, measured vertically (cf. Table I), above the $^2\Pi_g$ normal state of I_2^+ should come the $\sigma_g\pi^4\pi^4$, $^2\Sigma^+_g$ state. This state, which should give $^2P_{1/2} + {}^3P_2$ (or $^3P_1$) on dissociation, is very likely of the repulsive type. Other low-energy states of I_2^+, some of which may be stable, should exist with the configuration $\sigma_g^2 5p\pi^3 5p\pi^3(5p\sigma - 5p\sigma,\ \sigma_u)$; this should give nine electronic states.

Visible I_2^+ bands corresponding to transitions connecting some of the excited states mentioned with the ground state may exist, but have not yet been definitely found. Certain emission bands of I_2, Br_2 and Cl_2 may, however, prove to be due to I_2^+, Br_2^+ and Cl_2^+, although further work on them is needed.[8] The analyses of these bands are incomplete, but in the case of Br_2 there appear to be two systems with a common lower state having $\omega_e'' = 362$; the upper levels have ω_e' about 193 and 153. If these bands are really Br_2^+, the ω_e'' value 362 is reasonable for the $^2\Pi_g$ (normal) state of the latter. For neutral Br_2, ω_e is 324. The somewhat higher value for Br_2^+ would indicate that the strength of the bond is somewhat increased by the net action of the seven π electrons, corresponding to an appreciable tendency from (4) toward (4*a*).

5. Excited states of halogens XY and X_2

The excited states of ICl and I_2 (examples of XY and X_2) may be thought of as obtained by adding one electron in an "*excited orbital*" to any of the various states of the ions $(ICl)^+$ and I_2^+. Each excited orbital has an ionization potential (term value) which is smaller than that of any unexcited orbital, i.e., orbital present in the unexcited molecule. Most of the excited orbitals are related to *excited atomic* orbitals and should have term values not over 3 or 4 volts. There is, however, one excited orbital with an ionization potential of the same order of magnitude as the ordinary ionization potential of the molecule. This is the important anti-bonding σ orbital $(5p\sigma_I - 3p\sigma_{Cl},\ \sigma)$ of ICl or $(5p\sigma - 5p\sigma,\ \sigma_u)$ of I_2, complementary to the bonding orbital $(3p\sigma_{Cl} + 5p\sigma_I)$ or $(5p\sigma + 5p\sigma,\ \sigma_g)$. It will be convenient to call this σ^* or σ^*_u.

The lowest excited states of ICl or I_2 are obtained by adding σ^* to the normal state (7) or (9) of $(ICl)^+$ or I_2^+:[1]

$$\text{ICl: } \sigma^2\pi_{Cl}{}^4\pi_I{}^3\sigma^*,\ {}^{1,3}\Pi;\quad I_2\text{: } \sigma_g{}^2\pi^4\pi^3\sigma^*{}_u,\ {}^{1,3}\Pi_u. \quad (12)$$

Transitions from the normal state of ICl or I_2 (cf. (4) and (5)) to the $^3\Pi_{0^+}$ and $^3\Pi_1$ levels of (12) give the well-known visible and infrared

[8] Br_2 and Cl_2: Y. Uchida and Y. Ota, Jap. J. Phys. **5**, 53, 59 (1928); I_2 (weak group near λ2700): G. Cario and O. Oldenberg, Zeits. f. Physik **31**, 914 (1925); also the visible Geissler tube emission spectra of I_2 may perhaps be in part I_2^+ bands.

absorption bands of ICl and I_2; analogous statements apply for XY and X_2.[1]

Above the $^{1,3}\Pi$ of ICl given by (12) there should be another $^{1,3}\Pi$; and a little above the $^{1,3}\Pi_u$ of I_2 there should be a $^{1,3}\Pi_g$:

$$\text{ICl: } \sigma^2\pi_{Cl}{}^3\pi_I{}^4\sigma^*,\ ^{1,3}\Pi; \quad I_2\text{: } \sigma_g{}^2\pi^4\pi^3\sigma^*{}_u,\ ^{1,3}\Pi_g. \quad (13)$$

These states are those obtained by adding σ^* to the low $^2\Pi$ excited state of $(ICl)^+$,—cf. (8),—or $\sigma^*{}_u$ to the low $^2\Pi_u$ of $I_2{}^+$. The center of gravity of the $^{1,3}\Pi$ of (13) for ICl should then be about 2.5 volts above that of (12), this interval being that between the two $^2\Pi$'s in $(ICl)^+$, as estimated in Table I. The interval from $^{1,3}\Pi_u$ of (12) to $^{1,3}\Pi_g$ of (13) for I_2 is probably less than 1 volt, like the estimated interval between the low $^2\Pi_g$ and $^2\Pi_u$ of $I_2{}^+$ (cf. section 4).

Still higher in energy should be the states obtained by adding σ^* to the $^2\Sigma^+$ of (8) or (11);

$$\text{ICl: } \sigma\pi^4\pi^4\sigma^*,\ ^{1,3}\Sigma^+; \quad I_2\text{: } \sigma_g\pi^4\pi^4\sigma^*{}_u,\ ^{1,3}\Sigma^+{}_u. \quad (14)$$

Transitions to these states from the normal state should occur in the cases of both ICl and I_2. These, as well as transitions involving the states of (12) and (13), will be fully discussed in sections 9–10 below.

Numerous additional excited states (cf. Tables III, IV) are obtainable by adding a σ^* electron to one of the following several states of $(ICl)^+$ or corresponding $I_2{}^+$ states: $\sigma^2\pi^4\pi^2\sigma^*$, $\sigma^2\pi^3\pi^3\sigma^*$, $\sigma^2\pi^2\pi^4\sigma^*$, $\sigma\pi^4\pi^3\sigma^*$, $\sigma\pi^3\pi^4\sigma^*$, $\pi^4\pi^4\sigma^*$.

Infinitely many additional excited states are obtainable by adding an electron in an excited orbital other than σ^* to any of the states of $(ICl)^+$ or $I_2{}^+$. We shall consider only the lowest-energy excited states of this category, namely, those obtainable by using the normal $^2\Pi$ state of ICl^+, or the normal $^2\Pi_g$ or low-energy $^2\Pi_u$ of $I_2{}^+$, and adding an electron in the most firmly bound type of excited orbital other than σ^*.

All of the outer-electron orbitals involved in (4)–(5) and (7)–(14) are, or correspond on dissociation to, unexcited halogen atom orbitals, and have ionization potentials of the order of 10 volts or more. The stages of excitation with which we are now concerned, however, involve an excited orbital one unit greater in principal quantum number in the halogen atom, and therefore much larger in size and with an ionization potential of only 3 or 4 volts.

For our purposes it is not necessary to inquire further into the exact nature of the next-most-firmly-bound-after-σ^* orbital. It is sufficient that it is probably a σ orbital of large size and weak bonding power. Let us call it $\sigma^\times$. We shall be especially interested in the states:

$$\left.\begin{aligned} &XY\text{: } \sigma^2\pi_Y{}^4\pi_X{}^3\sigma^\times,\ \Pi_{1,\,0,\,1,\,2} \\ &X_2\text{: } \sigma_g{}^2\pi^4\pi^3\sigma^\times,\ \Pi_{(1,\,0,\,1,\,2)g,\,u} \end{aligned}\right\}. \quad (15)$$

6. Ω–s (J–J-like) coupling in halogen molecules: vacuum ultraviolet bands

In the states (15), the coupling between the $\sigma^\times$ excited electron and the XY^+ or $X_2{}^+$ core should be weak. The situation should strongly resemble that in the excited states of the rare gas,—or halogen,—atoms; in other words, the coupling should be of a J–J-like type similar to that between *e.g.* the $3p^5$, $^2P_{1\frac{1}{2}}$ or $3p^5$, $^2P_{\frac{1}{2}}$ core of ionized argon and a $4s$ electron. Comparison with the rare gases indicates coupling practically completely of the J–J-like type for the states (15) of all halogen molecules except F_2 and perhaps ClF and Cl_2. Even in the states (12) and (13) a strong J–J tendency would also be expected.

For J–J-like coupling, the Π states in (15) would not be definitely either singlet or triplet, but would have the combining properties of both. They could most accurately be described as follows:

$$XY\text{: } \{[\sigma^2\pi_Y{}^4\pi_X{}^3,\ ^2\Pi_{1\frac{1}{2}}]\sigma^\times\}_{2,\,1} \text{ and } \{[\sigma^2\pi_Y{}^4\pi_X{}^3,\ ^2\Pi_{\frac{1}{2}}]\sigma^\times\}_{0,\,1}, \quad (16)$$

$$X_2\text{: } \{[\sigma_g{}^2\pi^3\pi^4,\ ^2\Pi_{u\,1\frac{1}{2}}]\sigma^\times{}_g\}_{2,\,1\,u} \text{ and } \{[\sigma_g{}^2\pi^3\pi^4,\ ^2\Pi_{u\frac{1}{2}}]\sigma^\times{}_g\}_{0,\,1\,u}. \quad (17)$$

In (16) and (17), we have a core with good quantum numbers S_c, Λ_c, Σ_c, Ω_c. To the magnetic axis defined by Ω_c is weakly coupled the spin s_{ez} of the $\sigma^\times$ excited electron, with quantum number $\sigma_{ez}=\pm\frac{1}{2}$, giving a resulting $\Omega=\Omega_c\pm\frac{1}{2}$. In this type of coupling, which may be designated Ω–s coupling, the molecule as a whole has $\Lambda(=\Lambda_c)$ and Ω as good quantum numbers, but it has no quantum number S. [A more complicated type of coupling, in which Λ might no longer be a good quantum number, would occur if the excited electron had $\lambda>0$, e.g., if it were π or δ.

It may also be pointed out that Ω–s coupling depends on the existence of a strong Λ_c–Σ_c coupling within the core, which is of course impossible unless $\Lambda > 0$.] Selection rules for a transition between two states both having Ω–s coupling may be summarized as follows: transitions within the core are the same as if the excited electron were absent ($\Delta\Lambda_c$, $\Delta\Omega_c = 0$, ± 1 with $\Delta\Omega_c = \Delta\Lambda_c$), while $\Delta\Omega = 0$, ± 1; in practice, because Ω–s coupling, which depends on strong spin-orbit coupling in the core, may be expected often to be modified by a marked tendency toward atomic spin-orbit (case c) coupling,[1] $\Lambda_c = \Lambda$ is likely to be not entirely well-defined, so that the rules $\Delta\Lambda = 0$, ± 1 and $\Delta\Lambda = \Delta\Omega_c$ are not strict. Transitions from an ordinary (case b or a) state to a state with Ω–s coupling should be limited only by $\Delta\Lambda = 0$, ± 1, $\Delta\Omega = 0$, ± 1, with no $\Delta\Omega = \Delta\Lambda$ restriction.

In the case of X_2 in (17), the σ^x is assumed to be $\sigma^x{}_g$; this then requires a $^2\Pi_u$ core to give $_u$ total states. There would also be similar states of X_2, of lower energy, with $^2\Pi_g$ core, but the total states would then be $_g$, and transitions to them from the $^1\Sigma^+{}_g$ normal state of X_2 would be contrary to the $g \longleftrightarrow u$ selection rule. That the lowest excited σ^x orbital is $\sigma^x{}_g$ is indicated by analogy with the cases of He_2 and H_2 (cf. Ref. 7, pp. 59–64). In He_2, the lowest σ^x is $2s\sigma_g$, which is weakly bonding and is much larger than the ($^2\Sigma^+{}_u$) He_2^+ core, closely resembling a $2s$ united-atom orbital; the $2s\sigma_g$ in He_2 is the first of a Rydberg series of atom-like molecular orbitals. By analogy, the lowest excited σ^x in X_2 is probably a weakly bonding type $(n+1)s\sigma_g$, where $n = 2, \cdots 5$ for F, $\cdots$I. Following the analogy to He_2, the next σ^x orbitals should be $(n+1?)p\sigma_u$, $(n+1)p\pi_u$, $(n+1)d\sigma_g$, etc. It seems likely that the $^2\Pi_u$ core plus $(n+1)s\sigma_g$ is lower in energy than $^2\Pi_g$ plus $p\sigma_u$. The nature of the σ^x orbitals in the XY type is more difficult to predict, but presumably they are large and atom-like, at any rate.

In (16), if the coupling of σ^x to the $(XY)^+$ core is very weak, the two components $\Omega = 0$ and 1 derived from $^2\Pi_{\frac{1}{2}}$ of $(XY)^+$ by the coupling of Ω of the core with s of σ^x, should be close together, and should be separated by approximately the interval $a = {}^2\Pi_{\frac{1}{2}} - {}^2\Pi_{1\frac{1}{2}}$ of $(XY)^+$ (cf. section 3) from the two components $\Omega = 2$ and 1 derived from $^2\Pi_{1\frac{1}{2}}$. Transitions from the $^1\Sigma^+$ normal state of XY should occur to both the $\Omega = 1$ levels with about equal intensity, and to the 0^+ level.

Since the σ^x orbital should presumably have little bonding power, the molecular constants (ω_e and r_e) should not differ greatly for the excited levels of (13) from those of the normal state of $(XY)^+$. The latter in turn should not be radically different (cf. section 3), from the constants of the normal state of neutral XY, if expressions (5) and (7), using atomic (nonbonding) orbitals for the π electrons are good approximations, as we believe.

Now Cordes and Sponer have found in the ultraviolet between λ1600 and λ2000, for each of the molecules ICl, IBr and BrCl, a pair of absorption band systems which agree in all respects with what we should expect for transitions to the states (16). In each case the two systems are almost alike in intensity, appearance, and in ω_e', and in the fact that ω_e' is 12–18 percent greater than ω_e'' (ω_e'' refers of course to the normal state of the molecule).

The upper levels of the two systems are tentatively classed by Cordes and Sponer as the $^3\Pi_1$ and $^3\Pi_0$ components of a $^3\Pi$. The observed intervals $\Delta\nu$ between the (0,0) bands of the two systems of each molecule (cf. Table IIA) are, however, larger than one could reasonably expect for a normal interval $^3\Pi_0 - {}^3\Pi_1$. For an ordinary triplet, one expects $^3\Pi_0 - {}^3\Pi_1 \approx {}^3\Pi_1 - {}^3\Pi_2 \approx \frac{1}{2}A$, where A is the spin-orbit ($\Lambda - \Sigma$) coupling coefficient.[7] To account for a $^3\Pi$ excited state of XY at the level observed, no reasonable electron configuration but one of the type $\sigma^2\pi^4\pi^3\sigma$ seems open. For such a $^3\Pi$, A would be determined by the group π^3, and if the π orbitals in π^3 are essentially atomic $np\pi$, as has been shown in section 3 to be entirely probable, then A should be nearly the same as a for np of the corresponding atom ($a = 2(^2P_{\frac{1}{2}} - {}^2P_{1\frac{1}{2}})/3$ for a halogen atom np^5, ^2P). In short, for a state $\sigma^2\pi_Y{}^4\pi_X{}^3$, $^3\Pi$ of XY, A should be about equal to a of atom X, and $^3\Pi_0 - {}^3\Pi_1$ should be half this, or about one-third of $(^2P_{\frac{1}{2}} - {}^2P_{1\frac{1}{2}})$. More precisely, something between a of X and of X^+ might be expected. On this basis, we should predict $^3\Pi_0 - {}^3\Pi_1$ to be about 2700 in the cases of ICl and IBr, assuming that it is an I atom π electron which is excited, and about 1300 for BrCl assuming a Br π electron

TABLE IIA. *Multiplet intervals.*

Molecule[a]	*Predicted*[b]		*Observed* $\Delta\nu$(volts)[c]
	Λ–Σ *coupling*	Ω–s(*J–J-like*) *coupling*	
XY or X_2	$\pi_Y^4\pi_X^3\sigma$: $^1\Pi$; $^3\Pi_{0,1,2}$	$[(\cdots\pi_Y^4\pi_X^3, {}^2\Pi_{\frac{1}{2}})]\sigma$: $_{1,0}$ $[(\cdots\pi_Y^4\pi_X^3, {}^2\Pi_{1\frac{1}{2}})]\sigma$: $_{1,2}$	
	$^3\Pi_0-{}^3\Pi_1={}^3\Pi_1-{}^3\Pi_2$ $\approx \frac{1}{2}a_{X^+}$ or $\frac{1}{2}a_X$	$(^2\Pi_{\frac{1}{2}}\sigma)\Pi_{1,0}-(^2\Pi_{1\frac{1}{2}}\sigma)\Pi_{1,2}\approx a_{X^+}$ or a_X	
ICl (*uv*)	$\frac{1}{2}a_{I^+}=(0.344)$: $\frac{1}{2}a_I=0.312$	$a_{I^+}=(0.688)$; $a_I=0.625$	$0.582=\Pi_{1,0^+}-\Pi_1$
IBr (*uv*)	same as ICl	same as ICl	0.576 "
BrCl (*uv*)	$\frac{1}{2}a_{Br^+}=(0.168)$; $\frac{1}{2}a_{Br}=0.152$	$a_{Br^+}=(0.336)$; $a_{Br}=0.303$	0.276 "
ICl (*vis*)	as ICl above	as ICl above	$0.44=\Pi_{0^+}-\Pi_1$
IBr (*vis*)	as ICl	as ICl	0.50 "
I_2 (*vis*)	as ICl	as ICl	$0.68\pm0.05=\Pi_{0^+}-\Pi_1$
Br_2 (*vis*)	as BrCl	as BrCl	0.27 "

Notes for Table IIA. (a) Here "*uv*" refers to the upper levels of the ultraviolet absorption bands near λ1800, "*vis*" to the well-known visible and infrared bands. (b) Values of a for Br and I from np^5, ^2P : $a=2(^2P_{\frac{1}{2}}-{}^2P_{1\frac{1}{2}})/3$; for Br^+ and I^+ estimated (cf. section 3). (c) Data for visible bands are from Brown (Ref. 3, under IBr); for ultraviolet bands from Ref. 9. The values given refer to the interval between the *potential minima* of $^3\Pi_{0^+}$ and $^3\Pi_1$. This should give satisfactory results provided $^3\Pi_{0^+}$ and $^3\Pi_1$ have about equal r_e and ω_e values, as is the case in the ultraviolet bands and very probably also in the visible, infrared bands (cf. Brown[3]). The $\Delta\nu$ values for the latter bands are, however, less certain than for the former, for experimental reasons (cf. Brown[3]) and also because of the fact that the $^3\Pi_{0^+}$ dissociates differently than the $^3\Pi_1$ and other components ($^1\Pi$, $^3\Pi_{0^-}$, $^3\Pi_2$). This latter fact should tend to produce a relative distortion of the U(r) curve of $^3\Pi_{0^+}$. In the case of I_2 an independent, but probably less reliable value, of $\Delta\nu$ (6060 cm^{-1} = 0.75 volt) is obtained by taking the difference between the ν value of the intensity maximum of the $^3\Pi_{0^+}\leftarrow{}^1\Sigma^+_g$ continuum (λ5060) and that of the $^3\Pi_1\leftarrow{}^1\Sigma^+_g$ continuum (λ7320, Brown[3]).

excited (cf. Table II). The observed $\Delta\nu$ values, however, are 4713 for ICl, 4668 for IBr, and 2238 for BrCl, all much larger than expected for an ordinary $^3\Pi_0-{}^3\Pi_1$.

If, however, (cf. (16)), we interpret the lower-frequency system in each pair as having the upper electron level $\{[X^+Y, {}^2\Pi_{\frac{1}{2}}]\sigma^x\}_1$, and the higher-frequency system as having $\{[X^+Y, {}^2\Pi_{\frac{1}{2}}]\sigma^x\}_{0^+,1}$, with the components $\Omega=0^+$ and 1 too close together to be resolved with the dispersion used, then the observed $\Delta\nu$'s agree rather well with what we should expect. The predicted $\Delta\nu$'s (somewhat less than a of X^+) are now about 5400 for ICl and IBr, and about 2600 for BrCl. The observed values are 86 percent (BrCl) or 87 percent (ICl, IBr) as large as the predicted. The discrepancy of some 13 percent can be attributed to various influences which tend to modify the atomic or ionic a when the atom or ion enters a molecule (cf. section 3).

Particularly striking is the close agreement between the $\Delta\nu$ values of ICl and IBr. This supports the idea that it is essentially an I atom π electron which is excited in both cases, and that the use of atomic orbitals for the π electrons in halogen molecules of the type XY, as in (5) and (7), is a good approximation. The $\Delta\nu$ of BrCl likewise agrees with the idea that it is the Br whose π electron is excited.

At somewhat shorter wave-lengths than the bands here discussed are others,[9] apparently similar, which may be attributable to a more highly excited σ^x.

Accompanying the bands under discussion there is continuous absorption, increasing toward shorter wave-lengths. This has been attributed to dissociation and predissociation processes[9] resulting from the (expected) presence of repulsive potential energy curves of the molecule. Plenty of such curves are to be found among the states discussed in section 9; in particular, if Table IV should happen to be nearly correct, the $\sigma^2\pi^3\pi^3\sigma^{*2}$, $^3\Sigma^+$ and $^3\Delta_{1,2}$ states might cause predissociation of our $\sigma^2\pi^4\pi^3\sigma^x$, Π states.

Certain strong I_2 absorption bands,[10] near λ1750, with ω_e' and ω_e'' apparently about equal,

[9] Vacuum and near λ2000 ultraviolet absorption of Cl_2, Br_2, ICl, IBr, BrCl: H. Cordes and H. Sponer, Zeits. f. Physik **63**, 334 (1930); **79**, 170 (1932).

[10] Vacuum ultraviolet I_2 bands: H. Sponer and W. W. Watson, Zeits. f. Physik **56**, 1841 (1929).

are presumably similar to the lower-frequency systems of ICl, IBr, and BrCl bands just discussed. If this interpretation is correct, the corresponding higher-frequency I_2 system should appear near λ1615. Sponer and Watson state[10] that strong absorption occurs in the region from λ1600–λ1500, but was observed only qualitatively because of the failure of the continuous source there. Later, Cordes and Sponer at the end of their 1932 paper[9] indicate briefly that the relations in I_2 have been further studied, and are indeed similar to those in ICl and the rest. The analogous bands of Br_2 and Cl_2 probably lie below λ1600.

It is of interest to inquire why the ω_e' values are larger than the ω_e'' in the XY bands ($\omega_e'/\omega_e'' = 1.12$ in the ICl bands, 1.15 in IBr, 1.18 in BrCl). A reasonable explanation would be that the σ^x orbital has an appreciable bonding power. Other factors, however, such as bonding action of the group $\pi^4\pi^3$ of X^+Y, or changes in heteropolar forces, may also contribute.

Another point of interest is the term value (ionization energy) of σ^x. If the predicted ionization potentials of ICl, IBr, BrCl in Table I should be correct (11.16, 11.16, and 12.43 volts, respectively, for removal of π_X to give *mean* of $^2\Pi_{1\frac{1}{2}}$ and $^2\Pi_{\frac{1}{2}}$), then the σ^x term values (cf. Table I) are, respectively, 4.26, 4.49, and 4.97 volts. These are of the right order of magnitude, but decidedly higher than we expect if σ^x is essentially an atomic orbital. This may be due partly to bonding properties of σ^x suggested above, or it may also be that the predicted I values of ICl, IBr, BrCl used above are somewhat (perhaps about 1 volt) larger than the actual values.

In the I_2 bands near λ1750, ω_e' and ω_e'' appear to be about equal. This difference as compared with the XY bands may be due to the necessity of having the I_2^+ core in the (somewhat excited) form $^2\Pi_u$ in order to satisfy the $g \longleftrightarrow u$ selection rule (cf. (17)). The $^2\Pi_u$ core should have a somewhat larger r_e and smaller ω_e than neutral I_2 if the $^2\Pi_u - {}^2\Pi_g$ interval is appreciable (cf. section 4). This tendency, counterbalanced by a mild bonding effect of the $\sigma^x{}_g$ orbital, might well produce a resultant state with r_e and ω_e about the same as for the normal state of I_2.

7. Ω–*s* coupling in halogen molecules: infrared, visible bands

The preceding explanation of the $\Delta\nu$'s in the vacuum ultraviolet XY bands receives strong support from the $\Delta\nu$ data on the Π upper levels of the infrared and visible band-systems of XY and X_2. These upper levels have been interpreted[1, 2] as a $^3\Pi_1$ (infrared bands, mostly) and a $^3\Pi_{0^+}$ (visible bands) belonging to an upper electron configuration $\sigma^2\pi^4\pi^3\sigma^*$ (cf. (11)), except that the formulation $\pi_Y{}^4\pi_X{}^3\sigma^*$ for molecules XY has not heretofore been clearly stated. The electron configuration here is exactly like that attributed to the upper levels of the vacuum ultraviolet bands (cf. (16), (17)) except that we have σ^* instead of σ^x.

As will be seen from the $\Delta\nu$ data in Table IIA, the interval $\Pi_{0^+} - \Pi_1$ in I_2 and Br_2 corresponds well to Ω–*s* coupling as in the ultraviolet bands. In IBr and especially ICl, the $\Delta\nu$ values are smaller than in the ultraviolet bands, suggesting that the coupling departs appreciably from the Ω–*s* type. It seems likely that Ω–*s* coupling is incomplete also in Br_2 and I_2, and that their relatively large $\Delta\nu$'s are partly a result of a strong tendency toward case *c*.[1]

It will be of great interest to look for the $^3\Pi_1 \leftarrow {}^1\Sigma^+$ bands of Cl_2, in order to determine the $\Delta\nu(^3\Pi_{0^+} - {}^3\Pi_1)$ and thus see whether Ω–*s* coupling still persists. Data on BrCl, ClF, and F_2 would of course also be of interest.

The preceding results lead to the prediction that a $^3\Pi_2$ should in each case be close below the $^3\Pi_1$, and a $^1\Pi$ close above the $^3\Pi_0$, especially in I_2. The question of the existence of transitions to the $^1\Pi$ will be discussed in the next section.

Ω–*s* coupling, of course, means that the Π upper levels, although for convenience we shall continue to designate them as $^3\Pi_1$, $^3\Pi_{0^+}$, $^1\Pi$, etc., are really not definitely either singlet or triplet. Further, the case *c* tendency makes even the classification as Π levels not quite sharp.

With nearly Ω–*s* coupling, we expect $^3\Pi_1 \leftarrow {}^1\Sigma^+$ and the predicted $^1\Pi \leftarrow {}^1\Sigma^+$ should have about equal intensity, $^3\Pi_1 \leftarrow {}^1\Sigma^+$ getting relatively weaker, however, in the lighter halogens if these should tend strongly away from Ω–*s* toward Λ–Σ coupling. The observed, on the whole very weak, $^3\Pi_1 \leftarrow {}^1\Sigma^+$ transitions in the heavier halo-

gens may then probably be assumed equal to the $^1\Pi \leftarrow {}^1\Sigma^+$ in intensity, and so may probably be taken approximately as a true measure of the natural intensity of the transition from the normal electron configuration $\sigma^2\pi^4\pi^4$ to the excited configuration $\sigma^2\pi^4\pi^3\sigma^*$.

The much greater strength of the $^3\Pi_{0^+} \leftarrow {}^1\Sigma^+$ transitions must be accounted for in some other way, as will be shown in a moment. Van Vleck has suggested that these transitions probably get their intensity mainly because $^3\Pi_{0^+}$($^3\Pi_{0^+u}$ in X_2) steals from a higher-energy $^1\Sigma^+$($^1\Sigma^+_u$ in X_2) which combines very strongly with the $^1\Sigma^+$ ($^1\Sigma^+_g$ in X_2) normal state. Such stealing, corresponding to mutual perturbation and partial mixing of wave functions of $^3\Pi_{0^+u}$ and $^1\Sigma^+_u$ (in X_2), could readily occur in view of the Ω–s type of coupling in the $^3\Pi_{0^+}$, both states being of type 0^+_u. In the case of I_2, Van Vleck tentatively identifies the $^1\Sigma^+_u$ state in question as the "D" state, and the $^1\Sigma^+_u \leftarrow {}^1\Sigma^+_g$ as the well-known and extensive band-system near λ2000. As we shall see in section 9, this is very reasonable. The reader may wonder why we *must* attribute the $^3\Pi_{0^+u} \leftarrow {}^1\Sigma^+_g$ intensity mainly to perturbation by another state. This is simply because, with Ω–s coupling in the Π states, we could not otherwise account for the great difference in intensity between $^3\Pi_1 \leftarrow {}^1\Sigma^+$ and $^3\Pi_{0^+} \leftarrow {}^1\Sigma^+$. If both were unperturbed, the former should be about twice as intense as the latter. Since perturbations are not likely to decrease, but only to increase, a low intensity, we conclude that the intensity of $^3\Pi_{0^+} \leftarrow {}^1\Sigma^+$ must probably have been increased by a perturbing influence.

As Van Vleck has pointed out, the abnormally high intensity of the $^3\Pi_{0^+u} \leftarrow {}^1\Sigma^+_g$ might be due to a strong perturbation either of the $^3\Pi_{0^+u}$ or of the $^1\Sigma^+_g$, or of both; he concluded, however, that it is essentially only perturbation of the $^3\Pi_{0^+u}$ which is responsible for the high intensity. We are now in a position to reconsider the matter, in view of our increased understanding of the halogen molecules (cf. results and predictions summarized in Table III, and discussed in section 10).

It seems probable that the normal state $\sigma^2\pi^4\pi^4$, $^1\Sigma^+_g$ of I_2 is strongly perturbed by the predicted $\sigma^2\pi^3\pi^4\sigma^*$, $^3\Pi_{0^+g}$, which should have Ω–s coupling and probably is located about 3 volts above the normal state (cf. Table III and section 10). Now the $\sigma^2\pi_u{}^3\pi_g{}^4\sigma^*$, $^3\Pi_{0^+g}$ may well combine strongly with the $\sigma^2\pi_u{}^4\pi_g{}^3\sigma^*$, $^3\Pi_{0^+u}$ (cf. the very strong combination of $\sigma^2\pi_u{}^4\pi_g{}^2$, $^3\Sigma^-_g$ with $\sigma^2\pi_u{}^3\pi_g{}^3$, $^3\Sigma^-_u$ in O_2,—the Schumann-Runge bands), hence strong perturbation of $^1\Sigma^+_g$ by $^3\Pi_{0^+g}$ should enable the former to combine readily with $^3\Pi_{0^+u}$; but need not much strengthen $^3\Pi_{1u} \leftarrow {}^1\Sigma^+_g$, since $^3\Pi_{0^+g}$ may combine only weakly with $^3\Pi_{1u}$ (cf. discussion of selection rules following (17)). It seems likely that this perturbation of $^1\Sigma^+_g$ by $^3\Pi_{0^+g}$ may be the main reason for the strong combination of $^1\Sigma^+_g$ with $^3\Pi_{0^+u}$, rather than perturbation of the $^3\Pi_{0^+u}$ by $^1\Sigma^+_u$. In general, of course, the intensity of perturbation of a state A by a state B depends on $H_{AB}/(H_B - H_A)$. Now $H_B - H_A$ is decidedly smaller for the $^1\Sigma^+_g$ and $^3\Pi_{0^+g}$ than for $^3\Pi_{0^+u}$ and $^1\Sigma^+_u$, and it seems probable also that H_{AB} is larger; arguments for this will be given below. The foregoing discussion applies, of course, to homopolar molecules X_2, but somewhat similar considerations apply to XY molecules.

However this may be, a difficulty is the surprisingly low intensity of the $^3\Pi_1 \leftarrow {}^1\Sigma^+$ transitions, which suggests that these would be forbidden but for some weak perturbing influence, whereas the assumed electron configurations, which appear almost inevitable in our theory, would incline us (for Ω–s coupling) to expect a strong transition. This weakness may be attributable simply to smallness of overlapping of the π and σ^* orbitals of initial and final state wave functions, but the matter appears to deserve further study (cf. also Van Vleck[4]).

The increasing intensity of $^3\Pi_{0^+} \leftarrow {}^1\Sigma^+$ in the order Cl_2, Br_2, I_2 (cf. Table IIB) has formerly been attributed to the usual increase in probability of an intersystem combination with increasing atomic weight (tendency toward J–J-like, i.e., Ω–s, coupling). Under ordinary circumstances (coupling still nearly L–S-like) the intensity of singlet-triplet, as compared with singlet-singlet, combinations is about proportional to $(\delta\nu/\Delta\nu)^2$, where $\delta\nu$ is the width of the triplet (proportional to a) and $\Delta\nu$ is the interval between the triplet and corresponding singlet (cf. $^3\Pi$ and $^1\Pi$ in our case). Qualitatively, the observed intensities agree with this. Since, however, the coupling has been shown to be nearly

TABLE IIB. *Intensity data on* $\sigma^2\pi^4\pi^3\sigma^*$, $^3\Pi \leftarrow \sigma^2\pi^4\pi^4$, $^1\Sigma^+$ *bands.*

Ω of $^3\Pi$		F_2	Cl_2	Br_2	I_2	ICl	IBr
0^+	$\lambda_{conv.}$	—	4785	5106	4991	(5481)	(5450)
	$\lambda_{max.}$	2900	3300	4100	5060, 5575	4700	4950
	$\nu_{\frac{1}{2}max.}$	41,500	33,100	26,400	20,800	24,100	—
	$\nu_{max.}$	34,500	30,300	24,400	19,800	21,300	—
	$\nu_{\frac{1}{2}max.}$	29,500	27,800	20,000	17,200	19,600	—
	$k_{max.}$	0.542	6.8	16.6	93.7	8.7	—
	$[P/e]$ in A	0.026	0.067	0.13	0.26	0.083	—
1	$\lambda_{conv.}$	—	—	6291	8039	5758	6820
	$\lambda_{max.}$	—	—	—	7320	[near $\lambda_{conv.}$]	[near $\lambda_{conv.}$]
	$k_{max.}$	—	—	(much?) less than 0^+; stronger (×5?) than for 1 of I_2	very much less than for 0^+	<10% as strong as 0^+	Ratio to 0^+ nearly like ICl

Notes for Table IIB. $\lambda_{conv.}$ = λ of convergence limit of vibrational levels (data from references 2, 3); this is given for comparison with $\lambda_{max.}$ = λ of maximum absorption, which is usually, but not always, in the continuum above the convergence limit. $0^+ = {}^3\Pi_{0^+}$, $1 = {}^3\Pi_1$. $\lambda_{\frac{1}{2}max.}$ = two λ values at which k has fallen to one-half of $k_{max.}$; k = absorption coefficient defined by $I = I_0 e^{-kl}$, where l = path in cm; I, I_0 = light intensity; k values here recalculated to basis of ideal vapor at 0°C and 760 mm pressure. Data on $\lambda_{max.}$, $\lambda_{\frac{1}{2}max.}$, and $k_{max.}$ are based on: F_2, v. Wartenberg et al.[12]; Cl_2, v. Halban and Siedentopf and Gibson, Bayliss and Rice[11]; Br_2 $^3\Pi_{0^+}$, Ribaud[11]; Br_2 $^3\Pi_1$, private communication from W. G. Brown (also cf. reference 2); I_2 $^3\Pi_{0^+}$, K. Vogt and J. Königsberger, Zeits. f. Physik **13**, 294 (1923)[11]; I_2 $^3\Pi_1$, W. G. Brown[2]; ICl $^3\Pi_{0^+}$, G. E. Gibson and H. C. Ramsperger, Phys. Rev. **30**, 603 (1927); ICl $^3\Pi_1$, interpretation of Brown and Gibson[2], according to which $\lambda_{max.}$ is near $\lambda_{conv.}$ for $^3\Pi_1$ and, if so, $k_{max.}$ of $^3\Pi_1$ is so small as to be obscured by the curve of k against λ sloping upward to $k_{max.}$ of $^3\Pi_{0^+}$ (cf. Fig. 2 of Gibson and Ramsperger); IBr, cf. reference 3, especially Brown. P = effective electric moment of electronic transition, P/e = corresponding effective amplitude of a vibrating electron. The P/e values have been calculated from $P/e = 0.0619 \times 10^{-8} (\int k_\nu d\nu/\nu)^{\frac{1}{2}}$, using as an approximation for $\int k_\nu d\nu/\nu$ the expression $k_{max.}\Delta\nu/\nu_{mean}$, where $\Delta\nu$ is the interval between the two positions $\nu_{\frac{1}{2}max.}$, and ν_{mean} is their mean; the approximation is a good one if, as here, the $k-\nu$ graph is approximately triangular in shape.

The k given above for I_2 is based on low-pressure data of Vogt and Königsberger (t = 48°C, vapor density 2.54×10^{-5} g/cc), since these authors find that Beer's law fails for vapor densities above 4×10^{-5} in I_2; data for higher densities give much lower k values. Conceivably, however, there is some hidden source of error in the low-pressure data, since the failure of Beer's law occurs at the same pressure and to the same extent in the region of discrete bands as in the continuum. Work of Plumley, however (Phys. Rev. **45**, 678 (1934)) tends to support the high ratio of k for I_2 as compared with Br_2 (the high-pressure data of V. and K. would give a much lower ratio). The data used for k of Br_2 (p = 66 mm Hg) are in the region of validity of Beer's law, according to Ribaud and V. and K. Presumably this is true also of Cl_2 and F_2.

The low-pressure data of V. and K. on I_2 show a secondary maximum of k in I_2 at about λ5575. At higher pressures, this shifts somewhat and finally disappears, leaving only a wave and a shoulder in the k–λ curve.

In regard to the $^3\Pi_1 \leftarrow {}^1\Sigma^+$ infrared bands of Br_2 and I_2, Dr. W. G. Brown states (private communication) that these are stronger at 200 mm pressure in Br_2 than at 760 mm pressure in (hot) I_2, for the same path-length. Also he states that the continuum of these bands in Br_2, at high pressures, blots out the visible bands, while an analogous phenomenon does not occur in I_2. (This, of course, can be partly accounted for because the visible bands are weaker in Br_2 than in I_2.)

Ω–s, modified by a case c tendency, the foregoing relations do not apply, and the observed increase in intensity with atomic weight must probably be attributed to other causes (variation in perturbation index $H_{AB}/(H_B - H_A)$, itself probably due, however, largely to the increase in case c tendency, hence in H_{AB}, with atomic weight (cf. fourth following paragraph)).

It is instructive to express the intensities of the various $^3\Pi_{0^+} \leftarrow {}^1\Sigma^+$ transitions in terms of amplitude of vibration P/e of corresponding electric moment P (e = electronic charge). For Cl_2, Gibson, Bayliss and Rice[11] obtain for P/e the value 0.016×10^{-8} cm, but there appears to have been an error in the calculation. For, using the simple relation $P/e = 0.0619 \times 10^{-8} (\int k_\nu d\nu/\nu)^{\frac{1}{2}}$, one gets $P/e = 0.067 \times 10^{-8}$ cm = 0.067A for Cl_2, in disagreement with their result. Values for the other halogens calculated using the above formula range from 0.026A for F_2 to 0.26A for I_2 (cf. Table IIB). As a comparison, the value 0.50A

[11] For absorption intensity data on I_2, Br_2, Cl_2, cf. International Critical Tables, Vol. V, p. 269; Cl_2, also G. E. Gibson, N. S. Bayliss and O. K. Rice, Phys. Rev. **44**, 188, 193 (1933).

TABLE III. *Predicted electronic states of I_2.*

Est. mean vertical energy[a]	*Elec. Config.* in terms of molecular orbitals; numbers of σ_g	π_u	π_g	σ_u	*Electron States*[b] Parity	Case *a* or *b* or Ω–*s* type	Case *c* type	*Dissociation*[c] Products	Energy (volts)	*Elec. Config.* in terms of atomic orbitals Atom A	Atom B
12	0	4	4	2	*g*	$^1\Sigma^+$	0^+	*ex*		$5p\sigma^2\,5p\pi^4$	$5p\pi^4$
8.8	1	3	4	2	*u*	$^{1,3}\Pi$	$1,0^-,0^+,1,2$	*ex*		$\sigma^2\pi^4$	$\sigma\pi^3$
8.1	1	4	3	2	*g*	$^{1,3}\Pi$	,,	*ex*			
7.3	2	3	4	$\sigma^\times_g$ and others	*u*	Π	,,	*ex*		$\sigma\pi^4$	$\sigma\pi^3\,6s$
6.1	1	4	4	1	*u*	$^1\Sigma^+$	0^+	*ex*		$\sigma^2\pi^4$	π^4
						$^3\Sigma^+$	1	*bb**		$\sigma\pi^4$	$\sigma\pi^4$
							0^-	*bb*			
5.6	2	2	4	2	*g*	$^1\Sigma^+,\,^1\Delta,\,^3\Sigma^-$	$0^+,\,2,0^+,1$	*ex*			
4.9	2	3	3	2	*u*	$^1\Sigma^+$	0^+	*ex*		$\sigma^2\pi^4$	$\sigma^2\pi^3$
						$^1\Delta$	2	*ex*			
						$^3\Sigma^-$	0^+	*ex*			
							1	*ex**	8.28		
						$^3\Sigma^+$	$0^-,1$	*ab*		$\sigma^2\pi^3$	$\sigma^2\pi^3$
						$^3\Delta$	1,2	*ab*			
							3	*aa*†			
						$^1\Sigma^-$	0^-	*aa*			
4.2	2	4	2	2	*g*	$^1\Sigma^+$	0^+	*bb*	3.42		
						$^1\Delta,\,^3\Sigma^-$	$2,1,0^+$	*ab*			
2.8	2	3	4	1	*g*	$^1\Pi$	1	*ab*		$\sigma^2\pi^3$	$\sigma\pi^4$
						$^3\Pi$	0^-	*ab*†			
							$0^+,1,2$	*aa*			
2.1	2	4	3	1	*u*	$^1\Pi$	1	*aa*			
						$^3\Pi$	0^+	*ab*†	2.48		
							$0^-,1,2$	*aa*			
0.0	2	4	4	0	*g*	$^1\Sigma^+$	0^+	*aa*	1.54	$\sigma\pi^4$	$\sigma\pi^4$

General notes for Table III. The electron configuration of each electron state is expressed at the left of the table wholly in terms of *molecular orbitals* for the ten outer electrons (cf. (4a) in section 1; and note that by σ_u is meant σ^*_u of section 5 (cf. (12)), except in one case where $\sigma^\times_u$ of (15) is meant). Of course it is to be understood that such "pure electron configurations" have only an approximate meaning (cf. section 1) and that the actual states involve mixtures of these but usually with one configuration predominant. At the right of Table III the best pure electron configurations in terms wholly of *atomic orbitals* are given for the same electron states; it will be noticed that part of these belong to I+I, part to $I^+ + I^-$. *Mixed* electron configuration descriptions using molecular orbitals for shared (σ) and atomic orbitals for nearly unshared (π) electrons, such as have been used for the most part in this paper, and constitute probably the best pure electron configuration approximations, can be readily written by taking the σ parts of the electron configuration of any state from the left of the table, the π parts from the right. The electron states listed in Table III include *all* states derivable by combining two iodine atomic electron configurations containing ten $5p$ electrons between them, *viz.*, $I(p^5)+I(p^5)$ and $I^-(p^6)+I^+(p^4)$. Exactly analogous tabulations would of course hold for Br_2, Cl_2 and F_2. It should be noted that the case *a* or *b* or Ω–*s* type classification of electron states has a well-defined meaning only for fairly small r values, while the case *c* classification is applicable for large r values, and is important for dissociation product correlations.

The forms of the $U(r)$ curves of the various states listed in Table III can be roughly predicted from the vertical excitation energy given in the first column, combined with the predicted dissociation energies given in the "dissociation" column, together with a consideration of the nature of the σ orbitals present. The bonding type σ_g tends to make the minimum, if any, of the $U(r)$ curve come at relatively small r values, the anti-bonding type σ^*_u to make it come at large r values. The π types should also have some effect, π_u and π_g being, respectively, a little bonding and anti-bonding.

Special notes for Table III.[a] These estimates are based on assumed mean excitation potentials of 2.1 volts for $\pi_u \rightarrow \sigma_u$, 6.1 volts for $\sigma_g \rightarrow \sigma_u$, and 0.7 volt for $\pi_g \rightarrow \pi_u$. The value 2.1 is based on data on the visible bands, 6.1 on the rough value

6.5 volts for $\sigma_g\pi_u{}^4\pi_g{}^4\sigma_u$, $^1\Sigma^+{}_u \leftarrow \sigma^2\pi^4\pi^4$, $^1\Sigma^+{}_g$, assuming that the D level of I_2 may be identified as this $^1\Sigma^+{}_u$ (cf. E values in Table I); the value 0.7 is a guess. The value 7.3 for $\pi_u \rightarrow \sigma^\times{}_g$ is based on the observed value $\sim$ 7.05 volts for the process (λ1750) here tentatively identified as $\sigma^2\pi^3\pi^4\sigma^\times{}_g$, $^3\Pi_{1u} \leftarrow \sigma^2\pi^4\pi^4$, $^1\Sigma^+{}_g$. It should be especially noted that the estimates given refer to *vertical* excitation energies; in the case of all states which are not repulsive, the minimum excitation energy, to minimum of $U(r)$ curve, must be less.—One should of course not place too much reliance on these energy estimates. [b]The electron states associated with each electron configuration are given in their probable order of energy, as indicated by theoretical considerations and by experimental data on molecules with similar configurations. Innumerable other excited states of I_2 must exist, derivable from I+I, I^++I^-, I^{++}+I^{--} etc. with one or more atomic electrons excited out of their normal orbits. [c] Under "dissociation products," *aa* means *a*+*a*, and so on, where *a* means $I(5p^5, {}^2P_{1\frac{1}{2}})$ and *b* means $I(5p^5, {}^2P_{\frac{1}{2}})$; *ex* means one atom, at least, with an excited electron, or else $I^+(p^4)+I^-(p^6)$. The three cases marked with a dagger are "unique states" (cf. reference 1, p. 1445) which practically *must* dissociate in the manner indicated. In the other cases marked *aa*, *ab*, or *bb*, there is always a possibility (except in cases where the correlation is experimentally known) that the state may tend strongly to dissociate into products with more energy than those predicted by the strict case *c* rules, which assume that no crossing of $U(r)$ curves of states of identical case *c* type can take place (cf. reference 1, pp. 1449–50 and reference 4, p. 567 in regard to reasons why such tendencies may exist; and Brown and Gibson[3] and Brown[3] for an example of such a case in ICl and IBr). The predicted dissociation correlations given in the table may, of course, also be subject to partial alteration if, as is highly probable, the energy order of some of the levels is different from that estimated. The dissociation correlations marked* in the table require the crossing of two $U(r)$ curves of the same case *c* type (1_u), contrary to the strict rules; this *may* be incorrect, but the two states thus marked are so unlike in electron configurations that the occurrence of an effective crossing seems probable.

obtained by Stueckelberg[12] for the very intense Schumann ultraviolet O_2 band-system (mostly continuum) may be noted. This value 0.50 is also obtained very simply by using the above formula, thus checking Stueckelberg's result.

The above expression for P/e is obtained as follows. One readily finds that the absorption probability coefficient B for a frequency ν is given by $Bd\nu = (c/hn)(k,d\nu/\nu)$, where n = molecules/cc, k = absorption coefficient. For the total probability connected with a given electron transition, we may take $\int Bd\nu = (c/hn)(\int k,d\nu/\nu)$. The associated electric moment P is given by $P^2 = (3h^2/8\pi^3)\int Bd\nu$. From these relations, putting in numerical values, if k corresponds to gas at 0°C, 760 mm, one gets the above expression for P/e.

The notably large P/e value for I_2 means a really strong transition and so implies a very strong perturbation of $^3\Pi_{0^+u}$ by its presumed interaction with the $^1\Sigma^+{}_u$ above it, or of $^1\Sigma^+{}_g$ by the $^3\Pi_{0^+g}$ above it. In the former case, the $^3\Pi_{0^+u}$ should be pushed down, enough to make the interval up from $^3\Pi_{1u}$ to $^3\Pi_{0^+u}$ abnormally small; in the latter case the $^1\Sigma^+{}_g$ should be pushed down, but the position of the $^3\Pi_{0^+u}$ left unaffected. Actually the $^3\Pi_{0^+u} - {}^3\Pi_{1u}$ interval is a trifle larger, if anything, than we should expect even for ideal Ω–s coupling. This may then be taken as evidence that, as was suggested above, it is mainly the $^1\Sigma^+{}_g$, rather than the $^3\Pi_{0^+u}$, which is perturbed.

The strong mutual perturbation of $^1\Sigma^+{}_g$ and $^3\Pi_{0^+g}$ inferred above can be understood in terms of the recognized strong tendency toward case *c* coupling[1] in the halogens, especially I_2. In case *c*, Λ is no longer a good quantum number, and the pure $^1\Sigma^+{}_g$ and $^3\Pi_{0^+g}$ wave functions tend to become more or less mixed, both being of the case *c* type $0^+{}_g$. Such mixing is especially to be expected since the two $0^+{}_g$ states in question are the only ones derived from the union of two $^2P_{1\frac{1}{2}}$ X atoms (cf. Table III).

A peculiarity of the absorption curve of k against λ for I_2, as measured by Vogt and Königsberger, is the appearance, but only at very low vapor densities, of a secondary maximum of intensity at longer wave-lengths than the chief maximum, in the midst of the discrete bands (cf. Table IIB, and its notes). Further investigation may be desirable, especially since an unexplained failure of Beer's law beginning at low vapor densities has been found (Table IIB, notes). It may also be worth noting that the $k-\lambda$ curve of Br_2, like that of I_2, but unlike those of the lighter halogens, is broader on the long-λ than on the short-λ side of k_{max}. (cf. data on $\nu_{\frac{1}{2}max}$. in Table IIB). A possible explanation would be that the perturbing effect of $^3\Pi_{0^+g}$ on $^1\Sigma^+{}_g$ is greater for larger r values, where their $U(r)$ curves approach each other; this would tend to increase the intensity of the longer-λ

[12] E. C. G. Stueckelberg, Phys. Rev. **44**, 234 (1933).

regions of absorption, especially if absorption from excited states ($v''=1$, 2) is important, as in I_2.

From the data on the infrared, visible bands and their correlated continua, excitation energy data are available (cf. Table I), from which we can get approximate term values for the σ^* orbital in the various molecules. The σ^* vertical term value proves to be about 9 volts in all cases (cf. Table I), but is somewhat uncertain because of the uncertainty in the I values of XY noted at the end of section 6. More definite are the excitation energies E for $\sigma^2\pi^4\pi^4 \rightarrow \sigma^2\pi^4\pi^3\sigma^*$, which show indications of interesting regularities. According to the discussion in earlier sections, the π orbital which is here excited is probably approximately an I atom π orbital in I_2, ICl, IBr, a Br atom π orbital in Br_2 and BrCl, and so on, while the σ^* excited orbital is predominantly (cf. section 5) σ_I in I_2, IBr, and ICl, σ_{Br} in Br_2 and BrCl. In harmony with these ideas, the E values for I_2, IBr, ICl are nearly alike, as are those of Br_2 and BrCl; but in each series, the E values increase as the second atom in the molecule gets lighter, as we might expect.

8. Absorption $^1\Pi \leftarrow {}^1\Sigma^+$ related to the visible and infrared bands?

As we have seen in section 7, the existence of nearly Ω–s coupling in the heavier halogen molecules requires that the transition $^1\Pi \leftarrow {}^1\Sigma^+$ should occur with approximately the same intensity as, or slightly greater intensity than, the $^3\Pi_1 \leftarrow {}^1\Sigma^+$, and also indicates that the $^1\Pi$ level should lie, at small r values, close above $^3\Pi_{0^+}$. According to the usual rules,[12a] the $^1\Pi$ $U(r)$ curve should give $^2P_{1\frac{1}{2}}+{}^2P_{1\frac{1}{2}}$ on dissociation, and would then be repulsive in character, or at most would have a very shallow minimum, for all the molecules XY and X_2 heavier than Cl_2 (cf. $U(r)$ curves of known states of these molecules[2, 3]). The absorption $^1\Pi \leftarrow {}^1\Sigma^+$ would then be continuous, and would be superposed on the continuum associated with $^3\Pi_{0^+} \leftarrow {}^1\Sigma^+$. Being much weaker than the latter, it would not appreciably affect the appearance of the observed absorption curves. This is in agreement with observation: nothing about the observed continua of F_2, Cl_2, Br_2, or ICl (cf. Table IIB) gives any indication of compositeness; the secondary maximum in the I_2 absorption curve at long wave-lengths, noted in section 7, can hardly be attributed to $^1\Pi \leftarrow {}^1\Sigma^+$, because it occurs at too long λ (and is too intense, if the present ideas are correct).

In the case of Cl_2, Gibson, Bayliss, and Rice have measured the absorption curve with great care, and found that its form could be calculated quantum-mechanically using for the upper level a $U(r)$ curve which can be joined on rather well to the known lower part of the $^3\Pi_{0^+u}$ curve of Cl_2, as determined from the discrete bands. Nevertheless, the observed curve is a little higher than the $^3\Pi_{0^+u}$ Morse curve, and might, so far as its form is concerned, equally well belong to the expected $^1\Pi_u$, which would then probably have a shallow minimum, and should then give rise to a few weak discrete absorption bands. If Cl_2 has nearly Ω–s coupling, the fact that $^3\Pi_{0^+} \leftarrow {}^1\Sigma^+$, but not yet $^3\Pi_1 \leftarrow {}^1\Sigma^+$, bands have been found, would indicate that $^1\Pi \leftarrow {}^1\Sigma^+$ must be relatively weak and that the observed continuum is mainly $^3\Pi_{0^+} \leftarrow {}^1\Sigma^+$. Systematic comparison of the absorption curves for the Cl_2, Br_2, and I_2 continua supports this. In this connection, it may, however, be noted that $^3\Pi_1 \leftarrow {}^1\Sigma^+$, according to Brown (Table IIB), is considerably stronger in Br_2 than in I_2.

On the whole, it seems probable that the

[12a] The first report on the F_2 absorption spectrum appears to be that given by H. G. Gale and G. S. Monk (Phys. Rev. **29**, 211A, 1927), who state briefly that absorption occurs from about λ4100, using tubes from 7 mm to 3 cm long at 1 atm. Their (unpublished) photographs show the maximum of absorption to be near λ2900. Later T. R. Hogness (unpublished private communication) investigated the F_2 absorption up to several atmospheres pressure and 200° or 300°C in a 3 m tube and found evidence of discrete bands (apparently diffuse) near λ4500. H. von Wartenberg, G. Sprenger and I. Taylor [Göttinger Nachr. 1930, p. 119, and Bodenstein-Festband, p. 61 (Ergänzungsband of the Zeits. f. physik. Chemie, Leipzig, 1931)], measured the absorption coefficient of F_2 in the ultraviolet, finding the maximum absorption at λ2900, with k as noted above in Table IIB. [Their citation of previous work on I_2 seems inaccurate; they use the higher-pressure k for I_2 (cf. reference 11).] The absorption spectrum of F_2 has also been studied by G. E. Gibson and W. G. Brown and by R. Grinfeld and F. A. Jenkins (unpublished, private communications.)

Gale and Monk have also reported a continuous or nearly continuous emission spectrum in the ultraviolet, with two maxima, near λ2600 and λ2800. Examination of their plates (unpublished details) suggests a resemblance to the ultraviolet I_2 semi-continuous emission bands. Gale and Monk (l.c. and Astrophys. J. **69**, 77 (1929)) have also reported and analyzed a $^1\Sigma \rightarrow {}^1\Pi$ (either $^1\Sigma^+_u \rightarrow {}^1\Pi_g$ or $^1\Sigma^-_g \rightarrow {}^1\Pi_u$) system of F_2 emission bands. W. G. Brown (private communication) considers that these bands really comprise two or three systems. No obvious interpretation of the $^1\Sigma$ and $^1\Pi$ levels in terms of electron configurations (cf. Table III for I_2) is at hand.

observed ultraviolet continuum is still mainly $^3\Pi_{0^+} \leftarrow {}^1\Sigma^+$ even in F_2, although it seems somewhat remarkable that in so light a molecule as F_2, such an intersystem transition should exceed the corresponding $^1\Pi \leftarrow {}^1\Sigma^+$ in intensity. A considerable persistence of tendency toward case *c* coupling is needed to account for this. Further investigation of the Cl_2 and F_2 absorption spectra will be of great interest in this connection.

In connection with the foregoing discussion, Dr. W. G. Brown has called the writer's attention to a further point which may be pertinent. Thermodynamic data on Br_2 and HBr[12b] indicate, according to Brown, that Br_2 has a low-energy excited level or levels, even lower than the low predicted $^3\Pi_{2u}$. Brown suggests that possibly the $^1\Pi_u$ is *lower* than the $^3\Pi_{1u}$ and $^3\Pi_{2u}$, giving far infrared bands. This, however, seems improbable, but the data in question nevertheless demand explanation.

9. The *D* level of I_2 and its analogues

Several investigators have studied an extensive set of I_2 absorption bands in the region surrounding λ2000.[13] It now appears very probable that these bands belong to a single upper electronic level,[14] called the *D* level. The *D* state, since it does not dissociate into two $5p$, ^2P atoms, probably gives the next lowest possible pair of dissociation products, *viz.*, one unexcited atom ($5p^5$, $^2P_{1\frac{1}{2}}$) and one excited atom[10, 13] ($5p^46s$, $^4P_{2\frac{1}{2}}$, with nearly *J*–*J* coupling). Van Vleck[4] has suggested that the *D* level may be a $^1\Sigma^+_u$. Several reasons can be advanced to support this suggestion.

In the first place, $^1\Sigma^+_u$ is a type of level which cannot dissociate into two $5p^5$, ^2P atoms. According to the ordinary Wigner-Witmer rules, $^2P+{}^2P$ gives no $^1\Sigma^+_u$ states. We cannot, however, rely entirely on these rules for I_2 but must use the modified rules appropriate to case *c*; in case *c*, $^1\Sigma^+_u$ is 0^+_u. According to these rules,[1] only one 0^+_u state can result from $^2P+{}^2P$, and this is already known, it being the familiar low-energy $^3\Pi_{0^+u}$ state. Hence if the *D* level is $^1\Sigma^+_u$, or any other 0^+_u, it cannot dissociate into two ^2P atoms.

We can now go further and tentatively identify the *D* state as the $\sigma_g\pi^4\pi^4\sigma^*_u$, $^1\Sigma^+_u$ given in (14) of section 5. According to the approximate $U(r)$ curve given by Curtis and Evans,[13] the vertical excitation energy of the *D* state is about 6.5 volts, while the *minimum* of its $U(r)$ is perhaps about 5.15 volts up.[14]

The *D* state is remarkable in that it has a very low ω_e ($\sim$100 as compared with 215 for the ground state),[14] and doubtless a correspondingly large r_e, yet has a dissociation energy larger than that of the ground state. The same peculiarities (wide flat $U(r)$ curve with large r_e and large *D*) are found in the $1s\sigma 2p\sigma$, $^1\Sigma^+_u$ state of H_2 and in analogous states of Li_2, Na_2, etc.[15] This similarity, taken together with other reasons already noted, renders the argument for $\sigma_g\pi^4\pi^4\sigma^*_u$, $^1\Sigma^+_u$ very strong.

If we omit the closed shells of non-bonding electrons $\pi^4\pi^4$ in I_2, we have, for both H_2 and (cf. Table III) for I_2:

$$\left\{\begin{array}{l}\text{Normal states: } \sigma_g^2,\ ^1\Sigma^+_g \\ \text{Peculiar } ^1\Sigma^+_u \text{ and repulsive } ^3\Sigma^+_u \text{ state:} \\ \qquad\qquad \sigma_g\sigma_u,\ ^{1,\,3}\Sigma^+_u \\ \text{Also, } \sigma_u^2,\ ^1\Sigma^+_g,\end{array}\right\}, \quad (18)$$

where σ_g, $\sigma_u = (1s\sigma \pm 1s\sigma)$ in the case of H_2, $(5p\sigma \pm 5p\sigma)$ in that of I_2.

In H_2 the vertical interval from the $^1\Sigma^+_g$ normal state ($r = r_e$) to the $^1\Sigma^+_u$ state is about 12 volts, in I_2 about 6.5 volts according to the present interpretation of the *D* state. In H_2 the explanation of the shape of the $U(r)$ curve of the $^1\Sigma^+_u$ has been given by Hund, Kemble and others, and is well known: two neutral H atoms each with a $1s$ electron may give either the $^1\Sigma^+_g$ attractive or the $^3\Sigma^+_u$ repulsive state (Heitler-London); two *ions* $H^+ + H^-(1s^2, {}^1S)$ tend to give the $^1\Sigma^+_u$ state or a second $^1\Sigma^+_g$ (cf. (18)). It is the essentially ionic character of the $^1\Sigma^+_u$ which causes its $U(r)$ curve at moderately large r

[12b] W. G. Brown, J. Am. Chem. Soc. **54**, 2394 (1932); A. R. Gordon and C. Barnes, J. Chem. Phys. **1**, 692 (1933).

[13] Cf. W. E. Curtis and S. F. Evans, Proc. Roy. Soc. **A141**, 603 (1933), for a survey of the I_2 spectrum, with references to earlier work; also reference 10, Fig. 2, p. 610 shows an approximate $U(r)$ curve for the *D* state.

[14] D. T. Warren, Phys. Rev. **45**, 561 (1934), and private communications.

[15] Cf. e.g., R. S. Mulliken, Rev. Mod. Phys. **4**, 16 and 46 (1932).

values to resemble in shape that of two ions $H^+ + H^-$, while the presence of the anti-bonding electron σ^*_u causes the curve to reach a minimum at large r_e.

The $^1\Sigma^+_u$ state of H_2 in (18) does not actually give two ions on dissociation, because to do so its $U(r)$ curve would have to cross several other $^1\Sigma^+_u$ curves derived from one normal plus one excited atom; actually it avoids such crossings and dissociates to give an atom in a 2-quantum state. For the D state of I_2, an analogous explanation may well be accepted. Several workers[13] have suggested previously that it dissociates to $I^+ + I^-$, and this seems quite possible, but more probably it really dissociates to neutral atoms, one normal and one excited. The energy required to excite $2(5p^5, {}^2P_{1\frac{1}{2}})$ to produce $p^5, {}^2P_{1\frac{1}{2}} + p^4s, {}^4P_{2\frac{1}{2}}$ is 6.74 volts, to produce $I^- + I^+(p^4, {}^3P_2)$ is about 7.3 volts.[6]

With these points tentatively decided, we can predict that I_2 has a $^3\Sigma^+_u$ state, like H_2, with a $U(r)$ curve lying somewhat below that of the $^1\Sigma^+_u$ for small r values, but probably giving two $np^5, {}^2P$ atoms on dissociation, like the normal state of the molecule. [There is a possibility, however, that the 1_u (case c) component of this $^3\Sigma^+_u$, in order to avoid crossing another 1_u curve (cf. Table III), gives $p^5, {}^2P + p^4s, {}^4P$ instead of $2(p^5, {}^2P)$ on dissociation.] Transitions from the normal state of I_2 to this $^3\Sigma^+_u$ state should give rise to a continuum [or possibly to discrete bands] in the ultraviolet with maximum intensity perhaps near λ2200. Strong absorption, apparently continuous, beginning at λ3700 or sooner, and increasing toward a maximum at λ2200 or below, is present in I_2 (also at shorter wave-lengths in Br_2) according to Coehn and Stuckardt.* Other authors, however, have reported only discrete bands in this region for I_2, but have reported continuous absorption for Br_2 and Cl_2.[9]

No absorption to a level analogous to the D $^1\Sigma^+_u$ level of I_2 has been found in Br_2 or Cl_2, although the spectrum has been investigated down to λ1560 (equivalent to 7.9 volts).[9] This probably means that the D levels of these molecules lie (vertically) higher than 8 volts above the normal level. This is not unreasonable, at least for Cl_2, since the interval between the normal state and the D state would be expected to increase with decreasing atomic number. Continuous absorption, attributable presumably to transitions to $\sigma_g\sigma_u, {}^3\Sigma^+_u$ and some of the other highly repulsive $U(r)$ curves that the theory demands (cf. Table III) is present in this region, especially in Br_2, increasing in intensity toward shorter wave-lengths. In the case of Br_2, this might have obscured weak $D \leftarrow {}^1\Sigma^+_g$ bands which one would be inclined to expect near λ1600 or even at greater wave-lengths.

If the foregoing interpretation of the D level of I_2 is correct, we have a means of determining approximately the I (term value) of the orbital $(5p\sigma + 5p\sigma,\ \sigma_g)$ of I_2: cf. Table I, next-to-last line, together with footnote f and last sentence of footnote e. The rough value $I = 14.3$ volts so obtained is in satisfactory agreement with that predicted in Table I ($I > 12.93$).

Taking $I = 14.3$ for the bonding σ_g orbital of I_2, we can estimate I for the bonding σ orbital $(3p\sigma_{Cl} + 5p\sigma_I)$ of ICl (cf. next to last paragraph of section 2). This should be considerably larger than for σ_g of I_2, because the orbital is composed predominantly of $3p\sigma_{Cl}$; 16.8 volts seems a reasonable estimate for it. Subtracting from this the estimated term value of $\sigma^* = (5p\sigma_I - 3p\sigma_{Cl})$ as given in Table I, we get 8.0 volts for $\sigma \rightarrow \sigma^*$ in ICl, the energy required to excite normal ICl to the state $\sigma\pi^4\pi^4\sigma^*$ (mean of $^3\Sigma^+$ and $^1\Sigma^+$) analogous to that of I_2 in (18). We then estimate 7.5 and 8.5 volts as the respective vertical excitation potentials of the $^3\Sigma^+$ and $^1\Sigma^+$. While these estimates are of course uncertain, they at least give a possible reason why no bands having an upper level analogous to D of I_2 have yet been observed in ICl: they indicate that these bands should lie at shorter wave-lengths than the bands discussed in section 5, while the reverse is true in I_2. Similar relations are predicted in BrCl and IBr.

The probable predissociation observed by Cordes and Sponer in the states $\sigma^2\pi^4\pi^3\sigma^{\times}$ of ICl, IBr, and BrCl discussed in section 6 may now perhaps be attributed to crossing of their $U(r)$ curves by the $\pi^4\pi^4\sigma^*, {}^3\Sigma^+$ curve, or else by repulsive curves of the $^3\Sigma^+$ (or $^3\Delta$) states of the configuration $\sigma^2\pi^3\pi^3\sigma^{*2}$ (cf. Table IV).

* Absorption of HI, HBr, I_2, Br_2, Cl_2 to λ2200, A. Coehn and K. Stuckardt, Zeits. f. physik. Chemie **91**, 737 (1916).

TABLE IV. *Predicted electronic states of ICl.*

Est. mean vert. energy[a]	*Elec. Confign.* in terms of molecular orbitals; numbers of σ	π	π	σ^*	*Electron States* Case *a*, *b*, or Ω–*s* type	Case *c* type	*Dissociation*[c] products	energy	*Elec. Confign.* (atomic orbitals) Cl	I
16	0	4	4	2	$^1\Sigma^+$	0^+	*ex*		$3p\pi^4$	$5p\sigma^2\,5p\pi^4$
12.9	1	3	4	2	$^1,^3\Pi$	$1,0^-,0^+,1,2$	*ex*		$\sigma\pi^3$	$\sigma^2\pi^4$
10.4	1	4	3	2	$^1,^3\Pi$	"	*ex*		$\sigma^2\pi^4$	$\sigma\pi^3$
9.8	2	2	4	2	$^1\Sigma^+, ^1\Delta, ^3\Sigma^-$	$0^+,2,1,0^+$	*ex*		$\sigma^2\pi^2$	$\sigma^2\pi^4$
8.0	1	4	4	1	$^1\Sigma^+$	0^+	*ex*		$\sigma^2\pi^4$	π^4
					$^3\Sigma^+$	1 0^-	*bb** *bb**		$\sigma\pi^4$	$\sigma\pi^4$
7.2	2	3	3	2	$^1\Sigma^+$ $^1\Delta$ $^3\Sigma^-$ $^3\Sigma^+$ $^3\Delta$ $^1\Sigma^-$	0^+ 2 0^+ 1 $1,0^-$ 1,2 3 0^-	*ex* *ex* *ex* *ex* *ba** *ba** *aa*† *aa***	3.08	$\sigma^2\pi^3$	$\sigma^2\pi^3$
6.90	2	4	3	$\sigma^\times$	Π	0^- $1,0^+,1,2$	*ex* *ex**	8.88	$\sigma\pi^4$	$\sigma\pi^3\,6s$
4.9	2	3	4	1	$^1\Pi$ $^3\Pi$	1 0^- 0^+ 1,2	*ab* *ab*** *bb* *aa*, *ab*	3.19	$\sigma^2\pi^3$	$\sigma\pi^4$
4.8	2	4	2	2	$^1\Sigma^+$ $^1\Delta$ $^3\Sigma^-$	0^+ 2 $1,0^+$	*aa**** *aa* *ab*, *ba*		$\sigma^2\pi^4$	$\sigma^2\pi^2$
2.4	2	4	3	1	$^1\Pi$ $^3\Pi$	1 0^+ $0^-,1,2$	*aa* *ab**** *aa*	2.25	$\sigma\pi^4$	$\sigma^2\pi^3$
0.00	2	4	4	0	$^1\Sigma^+$	0^+	*aa*	2.14	$\sigma\pi^4$	$\sigma\pi^4$

Notes for Table IV (*cf. also Table III notes*). [a] Cf. note *a* of Table III. Estimated mean energies based on: $\pi_I \rightarrow \sigma^*$, 2.4 volts, from visible bands (cf. Table I); $\pi_{Cl} \rightarrow \pi_I$, 2.5 volts, from difference between I^*_{Cl} and I^*_I (cf. Table I); $\sigma \rightarrow \sigma^*$, 8.0 volts, rough (cf. Table I, and its note **f**); $\pi_I \rightarrow \sigma^\times$, from vacuum ultraviolet bands. [c] *aa*, *ab*, *ba*, *bb* mean $^2P_{1\frac{1}{2}}+^2P_{1\frac{1}{2}}$, $^2P_{1\frac{1}{2}}(I)+^2P_{\frac{1}{2}}(Cl)$, $^2P_{\frac{1}{2}}(I)+^2P_{1\frac{1}{2}}(Cl)$, $^2P_{\frac{1}{2}}+^2P_{\frac{1}{2}}$. The one "unique state" is marked with a dagger. Cf. Table III, footnote *c* in regard to uncertainties in dissociation products. These are greater here than for I_2, because of the loss of the $_g$, $_u$, classification.

10. Ultraviolet fluorescence and emission spectra of I_2

When I_2 absorbs light in the region of the $D \leftarrow {}^1\Sigma^+_g$ bands, a complicated fluorescence spectrum is obtained, which has been studied by McLennan, Oldenberg and others.[13] The short wave-length end of this is a series of sharp lines (or narrow groups of lines) representing transitions from the initial rotational and vibrational level (or levels) of the D state produced by the absorption act to various levels of the $^1\Sigma^+_g$ normal state of the molecule. At longer wave-lengths are numerous diffuse bands. This part of the fluorescence spectrum is independent of the exciting wave-length over a wide range of the latter. Oldenberg[13] suggests that it results from the occurrence of two (or more) sets of transitions in succession, the first from the D_u level to vibrational levels of an unknown electron level, say X_g, slightly below D, the second from X_g vibrational levels to a lower electron state Y_u. There might of course be more than one X_g or Y_u. The transitions $D_u \rightarrow X_g$ might be in the infrared, Oldenberg suggests.

The emission spectrum of iodine[13, 16] at low pressures shows part of the fluorescence bands. At high pressures additional sets of bands appear, some of which are also developed in fluorescence under high pressures of foreign gas. Some F_2, Br_2 and Cl_2 emission bands are also known,[16, 12] and deserve further investigation.

No attempt will be made here to offer a detailed explanation of the fluorescence and emission spectra of the halogens. One finds, however, on applying the method of electron configurations, that the I_2 molecule must possess a surprisingly large number of hitherto unknown low-energy states, some $_g$ and some $_u$, theoretically derivable by bringing together two $5p^5$, ^2P I atoms or $I^+(5p^4)+I^-(5p^6, {}^1S)$. These are given, with rough estimates of their energy, in Table III. Most of the lower-energy ones among these states should be of repulsive type, giving two $5p^5$, ^2P I atoms on dissociation. Two groups of states, however, one $_u$ and one $_g$, estimated to lie in the energy range 5–6 volts, and having wave functions of nearly ionic character (I^+I^-), must dissociate to give an excited I atom (or I^++I^-), and must be stable states, although all should have the minima of their $U(r)$ curves at very large r values. One of these predicted states is of type $^1\Sigma^+_g$ and its estimated position is right for the postulated level X_g. This and some of the other predicted states offer promising possibilities for explaining the various observed I_2 emission bands. It should, however, be pointed out that while the *existence* of the states listed in Table III is inescapable according to the theory, the estimates of their energies given there are to a considerable extent only enlightened guesswork. It should also be emphasized that the energy estimates given refer to *vertical* excitation energies; the course of the $U(r)$ curves is not estimated except insofar as this is determined from the vertical energy together with the dissociation products (cf. Table III, notes, second paragraph). It may also be well to mention that, from about 7 volts up, there should appear innumerable additional electronic states derivable from atoms or ions in which one or more electrons are in excited orbits.

Among the as yet unknown excited states of I_2 predicted in Table III, the $^3\Pi_g$ and $^1\Pi_g$ states given by (13) are of considerable interest. As we have seen in section 5, they should lie only a little above, or perhaps in part overlapping, the $^{1,3}\Pi_u$ states of (12), whose $^3\Pi_{0^+u}$ and $^3\Pi_{1u}$ are the upper levels of the known visible and infrared absorption bands. Like the $^{3,1}\Pi_u$, they should show Ω–s coupling, so that the triplet, singlet labels are really not apt. The case c dissociation rules[1] make it probable that the $^3\Pi_{2g}$, $^3\Pi_{1g}$, and $^3\Pi_{0^+g}$ dissociate into unexcited atoms (both $^2P_{\frac{3}{2}}$) and so are repulsive, but show that the $^3\Pi_{0^-g}$ and $^1\Pi_g$ must give one excited atom on dissociation, so that the $U(r)$ curve of $^3\Pi_{0^-g}$, and of $^1\Pi_g$, may have a shallow minimum. Absorption transitions to these states $^{3,1}\Pi_g$ are of course forbidden by the $g\longleftrightarrow u$ selection rule. Emission transitions from the D_u state to the $^1\Pi_g$ should occur; also, to the $^3\Pi_{1g}$ and $^3\Pi_{0^+g}$. Transitions to the last-named should be strong if the strong mutual perturbation between it and the normal state, suggested in section 7, exists.

11. Middle ultraviolet absorption continua of ICl, IBr, BrCl; fluorescence of IBr

Just as in I_2, so in ICl there should exist a large number of hitherto unknown or little known low-energy excited states, most of them unstable (repulsive) because dissociating to $I(5p^5, {}^2P)+Cl(3p^5, {}^2P)$. Others, higher up, should be stable, because giving a strongly excited atom on dissociation. The predicted states theoretically derivable by bringing together $I(p^5, {}^2P)+Cl(p^5, {}^2P)$, $I^+(p^4)+Cl^-(p^6, {}^1S)$, or $I^-(p^6, {}^1S)+Cl^+(p^4)$ are shown, with rough estimates of their energies, in Table IV. Of especial interest are the $\sigma^2\pi_{Cl}{}^3\pi_I{}^4\sigma^*$, $^3\Pi$ and $^1\Pi$. These (cf. (13)) are analogous to the $^{1,3}\Pi_g$ of I_2 just discussed. They differ from the latter in two important respects: (1) absorption transitions to them from the normal state of the molecule are now to be expected, since there is no longer any $g\longleftrightarrow u$ selection rule; (2) the interval between the $^{1,3}\Pi$ of (12) and the $^{1,3}\Pi$ of (13) should probably (see below) be very considerably larger than the corresponding interval for I_2 ($^{1,3}\Pi_g$

[16] R. J. Strutt and A. Fowler, Proc. Roy. Soc. **A86**, 105 (1911): excitation of Cl_2, Br_2, and especially I_2 emission bands in active nitrogen. This interesting work, containing extensive data and an excellent photograph of the I_2 band spectrum, seems to be generally overlooked. Cf. also reference 8 ($X_2{}^+$? or perhaps X_2 emission bands).

$-{}^{1,3}\Pi_u$) and, as a result, the $^{1,3}\Pi$ of (13) should be entirely repulsive for ICl, so that the absorption spectrum for transitions to them from the normal state should be continuous. Also, (3), since the $^{1,3}\Pi$ of (13) correspond to excitation of a Cl π electron, the multiplet width should correspond to that of the Cl atom, instead of to that of the I atom as in (12); as a result of this, the coupling should tend more toward the Λ–Σ rather than the Ω–s type.

The energy interval $\Delta\Pi$ between $^{1,3}\Pi$ of (12) and of (13) would be expected to be approximately equal to the interval $(\Delta\Pi)^+$ between the two low-energy $^2\Pi$ states of the molecule-ion (cf. (7), (8) for ICl, (9), (10) for I_2), since (12) and (13) are, respectively, obtainable by the addition of a σ^* electron to (7) or (9) and (8) or (10), respectively. As we have seen in section 4, $(\Delta\Pi)^+$ is probably not large for I_2, while for ICl it should be approximately equal to the difference between the π_{Cl} and π_I ionization of type I^*, namely, 2.5 volts (cf. Table I).

As we have seen in the last paragraph of section 8, the ICl transitions $^{1,3}\Pi \leftarrow {}^1\Sigma^+$ to the $^{1,3}\Pi$ of (12) consist of bands accompanied by a continuum, whose maximum is at about λ4700. In the analogous cases of IBr, BrCl, the maximum of the continuum is at λ4950, λ3750, respectively. It seems safe in these cases to take the continuum-maxima as giving roughly the mean vertical excitation energy of the $^{1,3}\Pi$ of (12). Now there is in the ultraviolet spectrum of each of the above three molecules, according to Cordes and Sponer,[9,3] one (and only one) additional strong continuum in the region between the above-mentioned continua and λ2000. The second continuum has its maximum at λ2400 for ICl, λ4050 for IBr, λ2150 for BrCl.

It seems very reasonable to identify the second continuum in each case as corresponding to transitions from the normal state of the molecule to the predicted higher-energy $^{1,3}\Pi$ given by (13). According to our discussion in a preceding paragraph, the frequency interval between the maxima of the two continua may then be called $\Delta\Pi$ and should be roughly equal to the interval $(\Delta\Pi)^+$ of the molecule-ion. In Table V, the $\Delta\Pi$ and estimated $(\Delta\Pi)^+$ are compared. The agreement is good enough, in view of the necessary neglect of various modifying factors, theoretical as well as perhaps also experimental, to give strong support to our explanation of the second continua.

TABLE V. *Frequency intervals (volts).*

	$\Delta\Pi$(obsd.)	$(\Delta\Pi)^+$(est.)
ICl	2.52	2.50
IBr	0.55	1.27
BrCl	2.45	1.23

Note: The $(\Delta\Pi)^+$ values are obtained by taking $I^*_Y - I^*_X$ from Table I. The $\Delta\Pi$ for BrCl is based on an observed maximum at λ3700 or 3800 for BrCl dissolved in CCl_4 and on a second maximum at λ2150 in the vapor.

A reasonable interpretation can now be given for the $U(r)$ curve of 0^+ type which was found, by Brown and Gibson[3] in ICl and by Brown[3] in IBr, to cross the $U(r)$ curve of the $^3\Pi_{0^+}$ state belonging to the lower-energy $^{1,3}\Pi$ group. This second 0^+ curve (cf. also discussion by Cordes and Sponer[9]) may reasonably be identified as belonging to the $^3\Pi_{0^+}$ component of the higher-energy $^{1,3}\Pi$ group,—in agreement with the suggestions of Brown and Gibson and of Brown that this 0^+ curve might be the cause of the λ2400 continuum in ICl and of the λ4050 continuum in IBr.

An analogous explanation should apply to the similar 0^+ curve of IBr, reported by Brown (cf. Van Vleck,[4] footnote 23).

If Table IV for ICl is approximately correct in regard to the energies of various states, a group of states ($^1\Sigma^+$, $^1\Delta$, $^3\Sigma^-$) belonging to $\sigma^2\pi_{Cl}{}^4\Pi_I{}^2\sigma^{*2}$ should exist at about the same energy as the $\sigma^2\pi^3\pi^4\sigma^*$, $^{1,3}\Pi$ just discussed; and transitions to the $^1\Sigma^+$ and the $^3\Sigma^-$ from the normal state of ICl should occur. These might contribute to the λ2400 continuum of ICl. It seems likely, however, that this contribution is relative very weak since transition to $\sigma^2\pi^4\pi^2\sigma^{*2}$ from $\sigma^2\pi^4\pi^4$ (normal state) would mean a two-electron jump.

No other low-energy levels of ICl are predicted in Table IV below the neighborhood of $\sigma^2\pi^4\pi^3\sigma^\times$ (upper level of the bands discussed in section 6). Further discussion of the predicted levels of I_2 and ICl in Tables III and IV, and of analogous but energetically different levels in the other halogens, is unnecessary. From the electron configurations and states, their esti-

mated energies, selection rules, likely weakness of many not-forbidden transitions (especially, perhaps, two-electron jumps), etc., readers can draw their own conclusions.

The ultraviolet fluorescence spectrum of I_2 which follows excitation to the D electron level has already been discussed. No similar spectrum has been found in any of the other halogens X_2 or XY, except in IBr.[17] The IBr fluorescence resembles that of I_2, except that it does not follow excitation to the D state of IBr, which is not yet known (cf. end of section 9), but presumably (cf. Cordes[3]) to energy levels belonging to $\sigma^2\pi^4\pi^3\sigma^\times$, II (cf. section 6).

[17] F. W. Loomis and A. J. Allen, Phys. Rev. **33**, 639 (1929) obtained IBr and I_2 fluorescence by λ1849 excitation, but obtained none in Br_2, ICl, or BrCl.

OCTOBER 1, 1934 PHYSICAL REVIEW VOLUME 46

Rotational and Vibrational Structure of the Fourth Positive Bands of Carbon Monoxide

D. N. READ, *Palmer Physical Laboratory, Princeton University*

(Received August 4, 1934)

The rotational structure of twelve of the fourth positive bands of CO ($A\,^1\Pi - X\,^1\Sigma$) has been measured and analyzed. The analyses of two bands are given. The values obtained for the rotational constants of the normal state are $B_0 = 1.9170$ cm^{-1}, $\alpha = 0.01738$ cm^{-1}. This is in disagreement with the result of infrared band measurements, which give $B_0 = 1.84$. The data obtained on the excited $A\,^1\Pi$ state are in complete agreement with the results of Angstrom ($B\,^1\Sigma - A\,^1\Pi$) band studies. The higher value of B_0 for the normal state is verified by measurement of the 0−0 band of the ultraviolet system $B\,^1\Sigma - X\,^1\Sigma$. The recently reported predissociation of the B state is also observed in this band. New measurements are given of the fourth positive band heads below 2270A. A formula is given to represent all the known band heads, and from this a formula for band origins is obtained.

INTRODUCTION

THE carbon monoxide spectrum is one of the most exhaustively studied of all molecular spectra. Nevertheless, no rotational analyses have been reported of bands involving the normal state of the molecule. Most of these lie in the far ultraviolet region.

The most important of the ultraviolet band systems is the fourth positive ($A\,^1\Pi - X\,^1\Sigma$). About 140 band heads have been identified, extending from about 1300 to 2600A. The upper state of this system is the lower state of the well-known Angstrom band system ($B\,^1\Sigma - A\,^1\Pi$). The vibrational analysis is given by Birge,[1] and more recent band head measurements have been reported by Headrick and Fox,[2] and by Estey.[3] The object of this paper is to report rotational analyses of a number of these bands, and more accurate band head measurements.

[1] Birge, Phys. Rev. **28**, 1157 (1926).
[2] Headrick and Fox, Phys. Rev. **35**, 1033 (1930).
[3] Estey, Phys. Rev. **35**, 309 (1930).

EXPERIMENTAL

The present work is based on a spectrogram taken by Professor H. D. Smyth with the two-meter vacuum spectrograph at Massachusetts Institute of Technology.[4] The source used was a hollow cathode discharge in flowing CO_2. The original object was to search for CO_2 emission bands, but none were found in this region.

The plate covers the region from 0 to about 2475A with a dispersion of 4.2A/mm. It shows about 65 heads of the fourth positive system of CO. Many of the bands are quite intense and well resolved except in the immediate neighborhood of the heads. There are also present on the plate a number of the first negative bands of CO^+, six of the ultraviolet bands of CO reported by Hopfield and Birge,[5] and atomic lines due to C, O, N, and Ni.

The measurements of the plate were converted to wave-lengths by use of a dispersion table for

[4] Compton and Boyce, Rev. Sci. Inst. **5**, 218 (1934).
[5] Hopfield and Birge, Phys. Rev. **29**, 922 (1927).

TABLE I. *1–1 band, 1560.133A.*

J	R(J)	Q(J)	P(J)	R(J) −Q(J)	Q(J+1) −P(J+1)	R(J) −Q(J+1)	Q(J) −P(J+1)
0							
1							
2							
3							
4	(64097.11H)						
5							
6			64056.7		22.3		
7	64095.5	64070.6	048.3	24.9	24.8	30.8	30.7
8	093.1	064.7	039.9	28.4	28.5	34.0	34.1
9		059.1a	030.6		31.4		38.2
10	086.2		020.9				
11	082.1		64009.8		38.0	45.7	
12		036.4	63998.4b		40.4		49.1
13		027.7	987.3c		44.2		53.3
14	066.6	018.6	974.4	48.0	47.1	57.9	57.0
15	059.1a	64008.7	961.6	50.4	50.6	60.7	60.9
16	052.3	63998.4b	947.8	53.9	53.6	65.0	64.7
17		987.3c	933.7		56.7		68.5
18	035.3	975.5	918.8	59.8	59.9	72.0	72.1
19	026.6	963.3	903.4	63.3	62.8	76.4	75.9
20	016.2	950.2	887.4	66.0	65.8	79.8	79.6
21	64005.2	936.4	870.6	68.8	69.2	82.9	83.3
22	63993.8	922.3	853.1	71.5	71.9	87.0	87.4
23	982.4	906.8	834.9	75.6	75.6	90.7	90.7
24	969.2	891.7	816.1	77.5	78.3	94.4	95.2
25	954.6	874.8	796.5	79.8	83.0	95.8	99.0
26	944.5	858.8	775.8	85.7	87.4	103.7	105.4
27	928.7	840.8	753.4	87.9	87.0	106.5	105.6
28	913.5	822.2	735.2	91.3	89.8	111.2	109.7
29	897.7	802.3	712.5	95.4	94.1	113.6	112.3
30	881.4	784.1	690.0	97.3	96.7	118.0	117.4
31	863.9	763.4	666.7	100.5	99.6	121.2	120.3
32	845.6	742.7	643.1	102.9	103.1	124.6	124.8
33	827.9	721.0	617.9	106.9	105.0	130.0	128.1
34	808.3	697.9	592.9	110.4	110.6	130.6	130.8
35	788.4	677.7	567.1	110.7	112.3	135.7	137.3
36	767.9	652.7	540.4	115.2	115.6	139.4	139.8
37	746.5	628.5	512.9	118.0	118.8	142.5	143.3
38	724.6	604.0	485.2	120.6	122.5	146.0	147.9
39	701.9	578.6	456.1	123.3		149.9	
40		552.0					
41		524.7					
42		497.1					
43		468.4					

H. Position of head calculated from other lines of the band. The head is obscured on the plate.
a, b, c Blends of two lines.

TABLE II. *4–10 band, 1990.890A.*

J	R(J)	Q(J)	P(J)	R(J) −Q(J)	Q(J+1) −P(J+1)	R(J) −Q(J+1)	Q(J) −P(J+1)
0							
1					6.0		
2		50216.4a	50210.4f		8.7		10.2
3		214.9	206.2		12.4		14.6
4		212.7b	200.3g		15.0		17.3
5	50228.8H	210.4f	195.4	18.4	17.8	21.6	21.0
6	228.8H	207.2	189.4	21.6	20.8	25.0	24.2
7	228.3	203.8c	183.0	24.5	24.1	28.0	27.6
8		200.3g	176.2		27.3		31.6
9	226.4	196.0	168.7	30.4	30.9	35.3	35.8
10	224.6	191.1	160.2h	33.5	33.3	38.8	38.6
11	222.0	185.8	152.5i	36.2	36.1	41.8	41.7
12	219.3	180.2d	144.1j	39.1	39.2	45.5	45.6
13	216.4a	173.8e	134.6	42.6	42.3	49.2	48.9
14	212.7b	167.2	124.9	45.5	45.3	52.5	52.3
15	207.9	160.2h	114.9	47.7	48.2	55.4	55.9
16	203.8c	152.5i	104.3	51.3	50.9	59.7	59.3
17	198.8	144.1j	093.2	54.7	54.1	63.0	62.4
18	193.2	135.8	081.7	57.4	57.2	66.3	66.1
19	186.8	126.9	069.7	59.9	60.0	69.5	69.6
20	180.2d	117.3	057.3	62.9	63.2	72.8	73.1
21	173.8e	107.4	044.2	66.4	66.3	76.8	76.7
22		097.0	030.7		69.6		80.2
23	158.0	086.4	016.8	71.6	72.2	83.6	84.0
24	149.5	074.6	50002.4	74.9	75.0	86.8	86.9
25	140.6	062.7	49987.7	77.9	77.9	90.4	90.4
26	131.1	050.2	972.3	80.9	81.0	93.8	93.9
27	121.2	037.3	956.3	83.9			97.3
28	110.7		940.0		86.8	100.6	
29	099.8	50010.1	923.3	89.7	89.7	104.0	104.0
30	088.6	49995.8	906.1	92.8	93.0	107.6	107.8
31	076.4	981.0	888.0	95.4		110.9	
32		965.5					
33		949.7					
34		933.6					
35		916.3					
36		898.8					
37		880.9					

a, b, c etc. Blends of two lines.

the spectrograph. A graphical correction was applied to these results, using Edlén's[6] measurements of the C, O and N lines as standards. This amounted at most to 0.01A.

ROTATIONAL ANALYSIS

The rotational structure of twelve of the fourth positive bands has been measured and analyzed. The bands chosen include all values of the lower vibrational quantum number from 1 to 10. The structure consists of single *P*, *Q* and *R* branches, to be expected from a $^1\Pi \rightarrow {}^1\Sigma$ transition, the *R* branches forming the heads. The *P* and *Q* branches are about equally strong, and the *R* branch considerably weaker in the region where the lines are well resolved. In most bands, from 50 to 100 lines can be identified. In the neighborhood of the origins and heads, which are quite close together, the structure is practically unresolved.

The analyses of two of the bands are given in Tables I and II, together with the combination differences

$$R(J)-Q(J)=Q(J+1)-P(J+1)$$

and

$$R(J)-Q(J+1)=Q(J)-P(J+1), \qquad (1)$$

which give the separations of the rotational levels of the upper and lower states, respectively. These equalities are strictly valid only if the Λ-type doubling of the $^1\Pi$ state is negligible. From studies of the Angstrom bands[7, 8, 9] this is known to be the case for the *A* state of CO, except where the state is perturbed. Actually the equations are satisfied to within about 0.5 cm^{-1} in most cases where lines are not blended except in these perturbed regions.

Since the band lines are not traced with certainty to *J* values lower than about 10, there

[6] Edlén, Zeits. f. Physik **85**, 85 (1933).

[7] Hulthén, Ann. d. Physik **71**, 41 (1923).
[8] Johnson and Asundi, Proc. Roy. Soc. **A123**, 560 (1929).
[9] Rosenthal and Jenkins, Proc. Nat. Acad. Sci. **15**, 896 (1929).

might be some question about the assignment of quantum numbers. The quantum numbers have been assigned in every case so as to make the combination differences for the upper state agree with those for the lower state of the Angstrom band which involves the same vibration level. All the lines near the origins of the Angstrom bands are resolved, and the numbering is certain. With the quantum numbers as assigned, the combination differences (Eq. (1)) also satisfy the condition that when plotted as a function of J they should extrapolate to 0 at $J=-1$.

It is well known that perturbations are observed in the lines of the Angstrom bands. These have been studied by Rosenthal and Jenkins,[9] and found to be due to the A state. Since this is the upper state of the fourth positive system, the same perturbations should be observed in these bands. The quantum numbers of the displaced lines are easily predicted from the data of Rosenthal and Jenkins. The appropriate displacements are observed in all cases. This is shown, for instance, by the inequality of the combination differences in Table I in the neighborhood of $J=25$, and their deviations from a smooth curve. The displaced lines are $R(25)$, $Q(24)$ and $P(27)$. The measurements are not sufficiently accurate to make a careful study of the perturbations, such as Rosenthal and Jenkins have given.

Rotational Constants

The rotation function is assumed to be

$$F(J)=B_v J(J+1) \tag{2}$$

and accordingly the combination differences are given by

$$\Delta F(J)=F(J+1)-F(J)=2B(J+1). \tag{3}$$

This simple form of rotation function seems adequate to represent the data up to about $J=25$. Beyond this point the perturbations of the upper state cause considerable displacements of the band lines, obscuring the effect of higher power terms in the rotation functions.

The values of B_v'' for the twelve bands are determined by fitting Eq. (3) to the combination differences, up to about $J=25$, by the method of least squares. The results are given in Table III. The values of B_v'' are assumed to be related by the equation

$$B_v''=B_0''-\alpha''v''. \tag{4}$$

Table III. *Rotational constants of lower state.*

Band	B_v(obs.)	B_v(calc.)	O−C
1–1	1.8981		−0.0015
4–1	1.9001	1.8996	+0.0005
7–1	1.9012		+0.0016
2–2	1.8819	1.8822	−0.0003
1–3	1.8634	1.8649	−0.0015
3–4	1.8492	1.8475	+0.0017
3–5	1.8287	1.8301	−0.0014
1–6	1.8130	1.8127	+0.0003
3–7	1.7953	1.7954	−0.0001
3–8	1.7775	1.7780	−0.0005
3–9	1.7610	1.7606	+0.0004
4–10	1.7433	1.7432	+0.0001

The constants of this equation are evaluated by least squares. The results are: $B_0''=1.9170$, $\alpha''=0.01738$ cm^{-1}. The values of B_v'' calculated from Eq. (4) with these constants are also given in Table III. The residuals are seen to be less than 0.002 in all cases.

The other constants of the normal state of the molecule which follow immediately are:

$I_0=1.443\times10^{-39}$ g cm^2 $\quad r_0=1.130\times10^{-8}$ cm
$I_e=1.436$ " " $\quad r_e=1.127$ " " .

Table IV gives the values of B_v' determined from the present data, compared with their values calculated in the same way from the Angstrom band data. The agreement proves the

Table IV. *Rotational constants of upper state.*

Band	B_v(obs.)	B_v from Angstrom bands
1–1	1.5724	
1–3	1.5706	1.5716
1–6	1.5720	
2–2	1.5502	1.5519
3–4	1.5300	
3–5	1.5280	
3–7	1.5282	1.5297
3–8	1.5276	
3–9	1.5284	
4–1	1.5043	
4–10	1.5047	
7–1	1.4344	

consistency of the analysis and the quantum-number assignments.

Comparison with Other Data

Asundi[10] has analyzed some of the fourth positive bands of high vibrational quantum number which could be photographed with a 21-ft. grating in air. He obtained $B_{18}''=1.60$, $\alpha''=0.023$. Eq. (4) gives by extrapolation $B_{18}''=1.604$, in good agreement with Asundi's value. His value of α'', however, is somewhat too high.

Snow and Rideal[11] have observed the $1\leftarrow 0$, $2\leftarrow 0$, and $3\leftarrow 0$ vibration-rotation bands of CO in the infrared absorption spectrum. The $1\leftarrow 0$ band was well resolved, and they obtained from the separation of the lines $B_0=1.84$. This is in considerable disagreement with the value obtained in the present work, 1.917. Their methods and results have been studied carefully in the hope of finding some explanation of the discrepancy, but none has been found.

Ultraviolet Bands of Hopfield and Birge

In view of this disagreement between the infrared results and the present ones, it is interesting to have independent evidence from other electronic bands. There appear on the plate six of the ultraviolet CO bands reported by Hopfield and Birge.[5] They are:

Transition	λ	ν
B−X 0-0	1150.52	86917.3
" 0-1	1179.59	84775.2
" 0-2	1209.80	82658.3
C−X 0-0	1087.86	91923.6
" 0-1	1113.89	89775.9
E−X 0-0	1077.10	92841.9

All these bands appear similar in structure, consisting of P and R branches lying entirely on opposite sides of the origins. The line structure is very fine, and practically unresolved in most cases.

The B–X system connects the upper state of the Angstrom system with the lower state of the fourth positive. The present value of the rotational constants for the normal (X) state can therefore be used, together with the constants of the B state found from the Angstrom band analysis, to predict the structure of the bands of the B–X system. This prediction has been made for the 0−0 band ($B_0'=1.943$, $B_0''=1.917$), and compared with measurements of the R branch of this band, which is completely resolved on the plate in both the first and second orders. The prediction is accurate for the first 25 lines. Beyond this point there is a slight divergence due to higher power terms in the rotation functions. If the infrared value $B_0''=1.84$ were used instead of the present value, $B'-B''$ would be about four times as large, and an entirely different type of band would be expected.

A striking feature of this band is the sudden decrease in intensity of the lines of the R branch after $R(36)$. The behavior of the P branch is not observed, since it is obscured by atomic lines. This is the same effect as has recently been reported by Coster and Brons,[12] who observed it in the 0-1 Angstrom band. They interpret it as predissociation of the B state. The decrease in intensity in the present case is greater than they observed, amounting almost to complete termination of the structure, but otherwise the observations are identical.

Band Head Measurements and Vibrational Constants

New measurements have been made of the fourth positive band heads below 2270A. They are given in Table V. The intensity figures are taken from the paper of Headrick and Fox,[2] and represent densitometer measurements.

In order to represent these band heads together with those of longer wave-length measured by Estey,[3] it has been found necessary to use a slightly more complicated equation than is usually given. The equation is:

$$\nu_h(v', v'') = 64{,}756.3 + (1497.49v' - 17.1841v'^2) - (2155.61v'' - 13.2843v''^2 + 0.012v''^3) - 0.0804v'v''. \quad (5)$$

The O−C column of Table V is determined from this equation. Most of Estey's measurements show residuals of the same order of magnitude. A few of them, however, are not well represented either by his own equation or the present one.

[10] Asundi, Proc. Roy. Soc. **A124**, 277 (1929).
[11] Snow and Rideal, Proc. Roy. Soc. **A125**, 462 (1929).
[12] Coster and Brons, Nature **133**, 140 (1934); Physica **1**, 155 (1934).

TABLE V. *Band heads.*

λ	ν cm^{-1}	Int.	$v'-v''$	O−C	λ	ν cm^{-1}	Int.	$v'-v''$	O−C
2262.42	44200.4	0.1	5–14	−0.4	1712.19	58404.7	3.9	0–3	−4.0
2238.98	44663.3	0.1	4–13	+0.4	1705.16	58645.7	3.1	3–5	+0.2
2150.87	46492.8	0.3	4–12	+0.5	1704.30	58675.2	1.5	6–7	−1.5
2128.97	46971.1	0.3	3–11	0.0	1669.68	59891.8	3.9	1–3	+3.0
2107.88	47441.0	0.3	2–10	−0.3	1653.02	60495.5	6.0	0–2	−2.6
2090.58	47833.7	0.5	5–12	−0.5	1647.90	60683.4	4.0	3–4	+0.9
2068.35	48347.8	0.7	4–11	+0.3	1630.40	61334.6	6.9	2–3	+0.1
2047.00	48852.1	0.5	3–10	+0.1	1629.61	61364.4	2.0	5–5	−0.3
2035.00	49140.0	0.7	6–12	−1.7	1611.26	62063.3	3.1	4–4	+3.9
2026.44	49347.5	1.4	2–9	−0.4	1597.14	62611.8	6.9	0–1	−2.2
2012.52	49688.9	0.7	5–11	−0.6	1595.60	62672.4	1.6	6–5	−0.4
2006.56	49836.7	0.4	1–8	+1.5	1576.67	63425.0	7.1	2–2	+0.9
1990.89	50228.8	1.6	4–10	+0.4	(1560.14)	(64096.9)*	6.0	1–1	+2.7
1970.08	50759.3	2.8	3–9	+0.6	1559.47	64124.4	5.0	4–3	+1.7
1950.07	51280.2	2.6	2–8	−0.2	1542.34	64836.4	6.9	3–2	+1.0
1939.12	51569.9	0.5	5–10	−0.6	1527.52	65465.5	4.0	5–3	+0.1
1930.70	51794.8	3.0	1–7	+1.2	1525.75	65541.6	5.3	2–1	+1.6
1918.08	52135.4	1.4	4–9	+0.2	1509.66	66240.0	5.0	1–0	+3.4
1897.83	52691.6	4.0	3–8	+0.2	1493.60	66952.3	6.0	3–1	+0.7
1878.33	53238.9	6.1	2–7	−0.1	1477.48	67682.9	3.0	2–0	+0.4
1859.41	53780.4	4.8	1–6	+2.3	(1463.47)	(68330.8)*	6.0	4–1	+2.1
1841.47	54304.6	1.3	0–5	−4.3	1452.17	68862.5	4.9	6–2	−0.9
1829.81	54650.6	4.0	3–7	+0.6	1447.27	69095.4	1.0	3–0	+1.3
1825.38	54783.1	0.8	6–9	−2.0	1435.28	69672.9	6.4	5–1	+1.5
1810.82	55223.8	7.6	2–6	+0.3	1425.78	70137.2	4.7	7–2	−0.2
1804.74	55409.8	1.9	5–8	−0.3	1418.91	70476.6	1.0	4–0	+5.3
1792.38	55791.7	7.5	1–5	+2.9	1408.86	70979.6	4.8	6–1	−0.2
1774.90	56341.3	3.4	0–4	−4.3	1401.02	71376.5	2.5	8–2	−0.5
1747.20	57234.4	3.8	2–5	+0.1	1391.97	71813.8	0.5	5–0	−0.4
1743.12	57368.4	0.7	5–7	−0.5	1384.00	72254.2	2.7	7–1	+0.4
1729.25	57828.7	6.1	1–4	+3.0	1377.75	72582.3	1.5	9–2	+0.1
1723.79	58011.9	2.2	4–6	+0.5	1355.84	73755.0	0.4	10–2	+2.0

* Band heads obscured on the plate. Position calculated from the rotational analysis.

In Eq. (5), the coefficient of v''^2 is appreciably larger than the value 12.7 which is usually given. This is due in part to the use of a cubic term, though even if this term is neglected a value of about 13.10 seems necessary to represent the data.

By use of the B's and α's found in the rotational analysis, an equation may be found for the band origins.[13] It is:

$$\nu_0(v', v'') = 64{,}746.5 + (1498.36v' - 17.2505v'^2) - (2156.05v'' - 13.2600v''^2 + 0.012v''^3). \quad (6)$$

[13] Jevons, *Report on Band Spectra of Diatomic Molecules*, p. 54, *et seq.*

The fundamental vibration constants of the normal state may be found by writing this equation as a function of $(v+\frac{1}{2})$. They are:

$$\omega_e = 2169.32 \qquad \omega_e x_e = 13.2780 \qquad \omega_e y_e = 0.012.$$

For the A state, $T_e = 65{,}075.2$ cm^{-1}. It is believed that these values, as well as those derived from the rotational data, are somewhat more accurate than those previously obtained for the normal state of the CO molecule.

In conclusion, the author wishes to express his appreciation to Professor H. D. Smyth for suggesting and supervising this work.

The Fifty-Three Electron Spectra of Caesium and Barium: Cs III and Ba IV

SISTER M. AMBROSIA FITZGERALD AND R. A. SAWYER, *University of Michigan*

(Received August 3, 1934)

The separations of the lowest levels $5s^25p^5\ ^2P$ of the Cs III and Ba IV spectra have been predicted and observed. In the case of Cs III, the prediction was made from the s^2p^5p levels of Cs II by use of Shortley's equations. The separation as found is 13,870 cm^{-1} and several combinations of the terms with higher levels were located. The ^2P separation for Ba IV was estimated by the irregular doublet law and located from the data as 17,830 cm^{-1}. New data were obtained for caesium by use of the vacuum spark, for barium by the vacuum spark and the condensed discharge in helium. The more complete data for barium enabled the location of a group of terms which combine both with the $(s^2p^5)\ ^2P$ terms and also with a higher group of terms allowing the classification of about fifty lines in this spectrum.

INTRODUCTION

THE systems neutral iodine, singly ionized xenon, doubly ionized caesium and triply ionized barium are the first members of the isoelectronic sequence having fifty-three electrons outside of the nucleus. Although the spectrum of iodine I has been photographed from the ultraviolet, through the visible, into the infrared region, little advance has been made on the classification of the observed lines. The task of classifying the lines of this spectrum is particularly difficult. The multiplet separations of the levels are very large; consequently, lines belonging to the same series lie in widely separated regions of the spectrum. Turner[1] observed several pairs of lines in the violet which he attributed to the transitions to the normal state. Evans[2] and Deb[3] have attempted to classify the spectrum, but there is no agreement between the results of their work. The extrapolations made in this problem were based upon the results given by Evans. This was done for two reasons: it has been pointed out by Curtis[4] that of the one hundred sixty lines classified by Deb, sixty-four had been observed by Bloch[5] as spark lines; on the other hand, hyperfine structure data given by Tolansky[6] agree with assignments given by Evans. Although it is not entirely free from uncertainty, the scheme given by Evans is perhaps the most satisfactory that is available concerning the spectrum of neutral iodine. Classifications for the spectra of both neutral and singly ionized xenon have been given by Meggers, deBruin and Humphreys.[7] The separation of the low ^2P terms of xenon II may be computed from the known values of the low terms in the xenon I spectra by the use of equations given by Shortley,[8] which will be discussed later, and which express the values of the levels of a rare gas like spectrum in terms of several parameters, one of which is $\frac{3}{4}$ the doublet separation of the once more ionized atom. Thus Shortley predicted 10,500 cm^{-1} for the Xe II separation, while Meggers, deBruin and Humphreys had found 10,540 cm^{-1}. We were thus encouraged to use the data on Cs II of Olthoff and Sawyer[9] to predict the fundamental separation of Cs III. In Ba IV this could not be done since no classification of Ba III has been carried out, although a list of lines attributed to Ba III has been published by Kimura and Nakamura.[10]

EXPERIMENTAL

A condensed discharge in helium was used to excite the Ba IV spectrum. Data obtained from this source were duplicated by a vacuum spark between electrodes made of a barium-aluminum alloy. The vacuum spark was also used to excite the Cs III spectrum, the electrodes being

[1] L. A. Turner, Phys. Rev. **27**, 397 (1926).
[2] S. F. Evans, Proc. Roy. Soc. **A133**, 417 (1931).
[3] S. C. Deb, Proc. Roy. Soc. **A139**, 380 (1933).
[4] W. E. Curtis, Nature **131**, 398 (1933).
[5] Leon and Eugene Bloch, Ann. d. Physik **11**, 141 (1929).
[6] S. Tolansky, Proc. Roy. Soc. **A136**, 585 (1932).
[7] W. F. Meggers, T. L. deBruin, C. J. Humphreys, Bur. Stand. J. Research **3**, 731 (1929); W. F. Meggers, T. L. deBruin, Science **68**, 573 (1928); W. F. Meggers, T. L. deBruin, C. J. Humphreys, Bur. Stand. J. Research **6**, 287 (1931).
[8] G. H. Shortley, Phys. Rev. **44**, 666 (1933).
[9] J. Olthoff and R. A. Sawyer, Phys. Rev. **42**, 766 (1932).
[10] M. Kimura and G. Nakamura, Jap. J. Phys. **3**, 197 (1924).

aluminum cored with caesium alum. The ultraviolet region was photographed by a one meter vacuum spectrograph and the near violet by an E_2 Hilger quartz spectrograph.

Analysis of the Cs III and Ba IV Spectra

The normal state of the Cs III and Ba IV spectra is $5s^25p^5\ ^2P_{3/2,\ 1/2}$. If one of the $5s$ electrons is removed to a $5p$ orbit, the configuration becomes $5s5p^6$ yielding $^2S_{1/2}$. As one of the $5p$ electrons is removed from the system, it may pass into a $5d$, $6s$, $6p$, $6d$, $\cdots$ orbit. The resulting configurations and theoretical terms for Cs III and Ba IV are given in Table I.

In order to get some idea as to the region in which the transitions to the normal state might lie, extrapolations were made by means of a Moseley diagram. Since the configurations $5s^25p^5$ and $5s^25p^45d$ involve valence electrons of the same total quantum number 5, it would be expected that they should form a screening doublet and have parallel Moseley lines. The lines obtained from the available data on iodine I and Xe II are decidedly non-parallel and lead us to believe that there was some misassignment of terms in either or both of the iodine I and Xe II spectra. However, if the terms are real, even though wrongly assigned, a tentative prediction of the location of analogous transitions in Cs III and Ba IV may be made and gives for Cs III the region 114,000–139,000 cm^{-1} and for Ba IV, 144,000–178,000 cm^{-1}.

The search for Cs III doublets was aided by the prediction of the doublet separation by the use of Shortley's[8] equations which for low stages of ionization seem to give a better prediction than the irregular doublet law.

Shortley's equations for the s^2p^5p levels of a rare gas type spectrum are:

Upper levels

$$(2c) = -F_0+\zeta'+\tfrac{1}{2}\zeta+4G_2$$

$$(1c) = -F_0+\zeta'+\tfrac{1}{2}\zeta$$

$$(1d) = -F_0+\zeta'-\zeta$$

$$(0d) = -F_0+\zeta'-\zeta+2G_0$$

Lower levels

$$(3a) = -F_0-\tfrac{1}{2}\zeta'+\tfrac{1}{2}\zeta-F_2$$

$$\left.\begin{matrix}2a\\2b\end{matrix}\right\} = -F_0-\tfrac{1}{2}\zeta'-\tfrac{1}{4}\zeta+F_2+4G_2 \pm[(\tfrac{3}{4}\zeta+F_2)^2+(2F_2-4G_2)^2]^{\frac{1}{2}}$$

$$\left.\begin{matrix}1a\\1b\end{matrix}\right\} = -F_0-\tfrac{1}{2}\zeta'-\tfrac{1}{4}\zeta-\tfrac{1}{2}F_2 \pm[(\tfrac{3}{4}\zeta-\tfrac{1}{2}F_2)^2+20F^2]^{\frac{1}{2}}$$

$$(0a) = -F_0-\tfrac{1}{2}\zeta'+\tfrac{1}{2}\zeta-5F_2+4G_0.$$

The expression on the left-hand side of any one of the equations stands for the value of the level having j equal to the number which appears there. It is expressed in terms of parameters of which one is directly related to the ionic doublet

Table I. *Electron configurations and theoretical terms of the Cs III and Ba IV spectra.*

	Russell-Saunders			$j-j$			Number of levels
$5s^25p^4$	^3P	^1D	^1S	^3P	^1D	^1S	
$5s^25p^45d$	$^4F_{9/2\ 7/2\ 5/2\ 3/2}$ $^4D_{7/2\ 5/2\ 3/2\ 1/2}$ $^4P_{5/2\ 3/2\ 1/2}$ $^2F_{7/2\ 5/2}$ $^2D_{5/2\ 3/2}$ $^2P_{3/2\ 1/2}$	$^2G_{9/2\ 7/2}$ $^2F_{7/2\ 5/2}$ $^2D_{5/2\ 3/2}$ $^2P_{3/2\ 1/2}$ $^2S_{1/2}$	$^2D_{5/2\ 3/2}$	9/2 7/2 5/2 3/2 1/2 7/2 5/2 3/2 5/2 7/2 5/2 3/2 1/2 5/2 3/2 1/2 3/2	9/2 7/2 5/2 3/2 1/2 7/2 5/2 3/2 1/2	5/2 3/2	(28)
$5s^25p^46s$	$^4P_{5/2\ 3/2\ 1/2}$ $^2P_{3/2\ 1/2}$	$^2D_{5/2\ 3/2}$	$^2S_{1/2}$	5/2 3/2 1/2 1/2	5/2 3/2	1/2	(8)
$5s^25p^46p$	$^4D_{7/2\ 5/2\ 3/2\ 1/2}$ $^4P_{5/2\ 3/2\ 1/2}$ $^4S_{3/2}$ $^2D_{5/2\ 3/2}$ $^2P_{3/2\ 1/2}$ $^2S_{1/2}$	$^2F_{7/2\ 5/2}$ $^2P_{3/2\ 1/2}$ $^2D_{5/2\ 3/2}$	$^2P_{3/2\ 1/2}$	7/2 5/2 3/2 1/2 5/2 3/2 1/2 3/2 5/2 3/2 3/2 1/2 1/2	7/2 5/2 3/2 1/2 5/2 3/2	3/2 1/2	(21)

splitting $s^2p^5\,{}^2P$. By using the term values for Cs II as given by Olthoff and Sawyer,[9] it was found that for caesium

$$3/2\zeta' = 13{,}840,$$

which from the definition of the parameters is the $s^2p^5\,{}^2P$ separation. With this predicted separation as a guide, a search was made for doublets in the vacuum spark data for caesium. Several pairs of lines were found having $\Delta\nu = 13{,}870\ \text{cm}^{-1}$, a value in good agreement with the predicted one. See Table II. These pairs are believed to represent transitions from higher terms to the low $s^2p^5\,{}^2P$ of Cs III. The possible assignment of these higher levels will be discussed together with the treatment of the Ba IV spectrum.

TABLE II. *Possible resonance lines of Cs III.*

Int	ν	Int	ν	$\Delta\nu$
(3)	127779	(7)	113909	13870
(1)	136146	(1)	122262	13884
(2)	138458	(00)	124564	13894
(0)	145656	(1)	131770	13886
(4)	155041	(1)	141155	13886
(2)	167872	(0)	153988	13884
(2)	181759	(2)	167872	13887
(2)	182548	(0)	168659	13889
(0)	188789	(1)	174914	13875

The next problem was to find $\Delta\nu$ for Ba IV. By use of the Sommerfeld formula,

$$\Delta\nu = \frac{R\alpha^2(Z-s)^4}{n^3l(l-1)}$$

the values of s, the screening constant, were calculated for the first three members of the series. The results are shown in Table III. It has been observed that as we proceed through the members of an isoelectronic series, there is usually a progressive diminishing in the value of both s and Δs. Assuming that Δs from Cs III to Ba IV might be 0.75, the calculated value of s for Ba IV would be 26.47 and the corresponding $\Delta\nu$ would be 17,695 cm^{-1}. The search for recurring frequency differences in the ultraviolet data yielded a group of lines having frequency separations of 17,830 cm^{-1}. This difference occurred more often than any other and between some of the most intense lines. Finally, it yielded terms which combine both with the $s^2p^5\,{}^2P$ and with a higher group of terms. Lines in the near violet region led to the location of this upper group of terms. It seemed reasonable, therefore, to assume 17830 as the value of $\Delta\nu$ for Ba IV. On this assumption, the calculated value of s for Ba IV is 26.42 making the consecutive values of s as given in Table III.

TABLE III. *Values of $\Delta\nu$ and Δs for Ba IV.*

Spectrum	$\Delta\nu$	$Z-s$	Z	s	Δs
I I	7600	23.90	53	29.10	1.04
Xe II	10540	25.94	54	28.06	.84
Cs III	13870	27.78	55	27.22	.80
Ba IV	17830	29.58	56	26.42	

Analysis of the Barium Data

The location of four pairs of lines in the ultraviolet region having a frequency difference of 17,830 units was the starting point in the analysis of the barium data. The frequencies of the lines fixed the position of an intermediate group of terms with respect to the ground levels. The spacings between the members of this intermediate group led to the identification of lines in the near violet which were interpreted as being transitions from a higher group of levels to the intermediate ones. With the spacings of this upper group as a guide, more lines were found. These lines proved to be transitions from the higher levels to levels in the intermediate group which due to Δj selection could not be located by pairs of resonance lines. Once the position of one of these additional intermediate levels was determined, a transition from it to one of the ground states could be estimated and verified by the data. All of the intermediate levels which combine with neither of the lowest levels, or with only one of them, were located in this manner. The arrangement of the lines in a quadratic scheme is shown in Table IV. Some of the expected lines are missing and there are remarkable differences in intensities among the observed lines. Both of these facts are also true of the observed lines in Xe II. The authors of the Xe II paper suggest that the majority of the missing lines are possible quartet-doublet inter combinations which might be expected to be very weak. Similar reasoning would hold in

TABLE IV. *Classification of lines of Ba IV.*

j		1/2	5/2	7/2	3/2 or 1/2	7/2	1/2	5/2
	Relative term values	152963	154481	154631	156738	157656	157741	158170
3/2	0	152952 (5) −11	154493 (5) 12		156745 (2) 7		157731 (2) −10	158158 (2) −12
1/2	17830	135133 (5) 0			138918 (5) 10		139911 (2) 0	
5/2	196549			41918.0 (15) 0.0	39810.1 (15) 0.1	38893.4 (15) 0.4		
5/2	197504		43023.9 (20) 0.9		40765.2 (0) −0.8	39848.2 (10) 0.2		39332.9 (15) −1.1
7/2	197698		43218.5 (3) 1.5	43066.8 (2) −0.2		40041.8 (7) −0.2		39527.3 (1) −0.7
3/2	197711		43229.6 (6) −0.4					39542.1 (8) 1.1
3/2	198005	45042.0 (0) 0.0	43522.7 (10) −1.3		41266.9 (0) −0.1		40265.7 (4) 1.7	
5/2	198758		44277.2 (3) 0.2	44126.7 (0) −0.3		41100.7 (15) −1.3		40588.4 (5) 0.4
5/2	198889		44406.4 (1) −1.6	44258.8 (3) 0.8	42149.4 (8) −1.6			

j		5/2	7/2	5/2	5/2	3/2	5/2
	Relative term values	158444	158750	158998	163254	175431	175926
3/2	0	158453 (2) 9		158990 (2) −8	163265 (1) 11	175423 (2) −8	
1/2	17830					157607 (0) 5	
5/2	196549						
5/2	197504	39058.4 (20) −1.6	38751.7 (7) −2.3				
7/2	197698	39255.9 (10) 1.9	38946.9 (10) −1.1			22266.9 (2) 0.1	21772.3 (5) 0.3
3/2	197711					22278.1 (8) −1.9	21783.2 (2) −1.8
3/2	198005			39005.7 (5) −1.3	34750.6 (7) −0.4		
5/2	198758	40314.8 (4) 0.8		39761.0 (0) 1.0	35502.6 (5) −1.4	23327.3 (3) 0.3	22831.8 (8) −0.2
5/2	198889						

the case of Ba IV. The irregular intensities indicate that the perturbations between the levels is probably very great.

An attempt to assign the terms either of this spectrum or of that of Cs III to possible configurations does not seem to offer much promise of success. It may be said that since the ^1S and ^1D states of the next ion probably lie much higher than the ^3P, the terms found here are believed to be built on ^3P. In his extension of Houston's and Slater's multiplet relations, Goudsmit[11] has derived a set of expressions giving the change in positions of the energy levels of the configuration ^3P+s with change in electron coupling. Neither the assignments in iodine I nor in Xe II satisfy these expressions. This fact together with the non-parallelism of the Moseley diagram lines, mentioned above, leads to the belief the reassignments need to be made in the first members of this isoelectronic series.

Since the transition $5s^25p^5 \leftarrow 5s5p^6$ would have to follow the irregular doublet law, it should be possible to locate the level $5s5p^6\ ^2S_{1/2}$. Our data, however, yielded no levels that would form a sequence involving the level assigned to this configuration in Xe II. Because it seemed probable that $5s5p^6\ ^2S_{1/2}$ would lie nearest to the normal state, the levels 127,779 above the normal state in Cs III and 152,963 in Ba IV were thought to be $5s5p^6\ ^2S_{1/2}$. Extrapolating backwards from Cs III and Ba IV would place $5s5p^6\ ^2S_{1/2}$ at about 102,700 in Xe II. Meggers gives a level in Xe II at 102,798 which he has assigned to $5s^25p^46s\ ^2P$. Although the assignments in iodine I and Xe II are doubtful, the levels are probably real. Extrapolating from them led to the discovery of a set of levels for Ba IV which we believe are also real but assignments of which are sugject to considerable uncertainty. The terms near 156,000 are too closely grouped to belong wholly to any one configuration, but some of them are probably due to $5s^25p^45d$. The two highest of the even levels are separated from the remainder of the group by about 12,000 units. It may be that they are the beginning of the levels due to $5s^25p^46s$. The group of upper terms must come from the addition of a p electron to $5s^25p^4$. They too are very closely grouped. Some of them may be due to $5s^25p^46p$.

The classified lines of caesium are listed in Table V, and those of barium in Table VI.

[11] S. Goudsmit, Phys. Rev. **35**, 1325 (1930).

TABLE V. *Wave-length list of Cs III lines.*

Int.	λ vac.	ν vac.	Int.	λ vac.	ν vac.
0	529.7	188789	1	708.4	141155
2	547.8	182548	2	722.2	138458
2	550.2	181759	1	734.5	136146
1	571.7	174914	1	758.9	131770
0	592.9	168659	3	782.6	127779
2	595.7	167872	00	802.8	124564
4	645.0	155041	1	817.9	122262
0	649.4	153988	7	877.9	113909
0	686.5	145656			

TABLE VI. *Wave-length list of Ba IV lines.*

Int.	λ in air	ν vac.	Int.	λ in air	ν vac.
2 vac.	570.1	175423	15	2432.31	41100.7
1 "	612.5	163265	0	2452.43	40765.2
2 "	629.0	158990	5	2463.01	40588.4
2 "	631.1	158453	4	2479.78	40314.8
2 "	632.3	158158	4	2482.75	40265.7
2 "	634.0	157731	7	2496.64	40041.8
0 "	634.5	157607	10	2508.77	39848.2
2 "	638.0	156745	15	2512.17	39810.1
5 "	647.3	154493	0	2514.27	39761.0
5 "	653.8	152952	8	2528.19	39542.1
2 "	714.7	139911	1	2529.14	39527.3
5 "	719.9	138918	15	2541.62	39332.9
5 "	740.0	135133	10	2546.62	39255.9
0	2220.15	45042.0	20	2559.50	39058.4
1	2251.23	44406.4	5	2562.96	39005.7
3	2257.80	44277.2	10	2566.83	38946.9
3	2258.74	44258.8	15	2570.36	38893.4
0	2265.50	44126.7	2	2576.01	38808.1
10	2296.84	43522.7	7	2579.76	38751.7
6	2312.52	43229.6	5	2815 86	35502.6
3	2313.36	43218.5	7	2876.80	34750.6
2	2321.26	43066.8	3	4285.62	23327.3
20	2323.57	43023.9	8	4378.62	22831.8
8	2371.79	42149.4	8	4487.46	22278.1
15	2384.88	41918.0	2	4489.70	22266.9
0	2422.51	41266.9	2	4589.40	21783.2
			5	4591.72	21772.3

Nuclear Magnetic Moments from the Polarization of Resonance Radiation

Sodium, $3^2S_{1/2}-3^2P_{3/2,\ 1/2}$

LEWIS LARRICK, *University of Iowa*

(Received July 19, 1934)

The polarization of sodium D line resonance radiation excited by plane polarized light in a magnetic field parallel to the electric vector of the exciting light increases from 16.5 percent in zero field to almost 50 percent in a field of 300 gauss as a consequence of the Paschen-Back effect of the hyperfine structure. The experimental results are well fitted by a curve calculated with $A(3^2P_{3/2})=7.45\times10^{-4}$ cm^{-1} and $\tau(3^2P_{3/2})=1.64\times10^{-8}$ sec. These results are for a nuclear moment of $3/2(h/2\pi)$ which was at first thought to give too low zero field polarization (15.27 percent). The higher polarization is the effect of proximity of hyperfine levels in $3^2P_{3/2}$.

IT has long been known that a magnetic field applied parallel to the electric vector of plane polarized exciting light would increase the polarization of sodium D line resonance radiation. This change in polarization, due to the Paschen-Back effect of the hyperfine multiplet, is discussed in detail in the following paper of Ellett and Heydenburg on the λ3303A resonance radiation of sodium. The writer has calculated the Paschen-Back effect of the hyperfine multiplet which constitutes any $^2S_{1/2}-^2P_{3/2}$ line for a nuclear moment of one (in units of $h/2\pi$) but as it is now evident, from atomic beam measurements,[1] from intensities in the hyperfine structure pattern[2] of the D lines, and from alternation of intensities in the band spectrum[3] that the nuclear moment of sodium is 3/2 the discussion of results will be based on the Paschen-Back calculations for this value of the nuclear moment, kindly placed at the writer's disposal by the authors of the following paper.

EXPERIMENTAL PROCEDURE AND RESULTS

The resonance radiation was excited by light from a hydrogen-sodium discharge tube. The temperature of that portion of the tube from which the light was taken was kept just below the softening point of the glass (softening point of Pyrex is between 600°C and 700°C). Pure metallic sodium was distilled into the discharge from a side tube. The rate of distillation was so controlled that the discharge was faintly yellow just at the junction of the side tube and main discharge tube. The color of the rest of the discharge was the characteristic red of the hydrogen spectrum.

Any increase in the vapor pressure of sodium in the discharge would increase the intensity of resonance radiation up to a certain pressure, but ultimately would cause self-reversal in the source. This would decrease the polarization by decreasing the intensity ratio of D_2/D_1, since the effect of self-reversal on two lines of unequal intensity is greater for the line of greater intensity.

The exciting radiation was brought to a focus at the center of the resonance bulb. An Ahrens prism was placed between the lenses of the condenser to plane polarize the incident beam. The depth of focus of the lens system was sufficiently great that the beam of incident radiation showed no divergence over the region covered by the slit of the polariscope.

The resonance bulb was made of thin-walled Pyrex. Tubing of 1–1½ inches in diameter was sealed off and blown out to a spherical bulb about two inches in diameter. In order to reduce reflected light the walls of the bulb were flattened to a square. A side tube containing a small quantity of pure sodium was sealed to the bottom of the resonance bulb. The bulb was connected through a liquid air trap to a mercury diffusion pump run continuously.

After the system had been thoroughly evacuated sodium was distilled into the resonance lamp until a thin film of metal was formed over the top of the bulb.

The polarization was measured visually by the Cornu method. The Cornu polariscope consisted of a slit, a Wollaston double image prism,

[1] Rabi and Cohen, Phys. Rev. **43**, 582 (1933).
[2] C. M. Van Atta and L. P. Granath, Phys. Rev. **44**, 60 (1933); **44**, 935 (1933).
[3] J. Joffe, Phys. Rev. **45**, 468 (1934).

and an analyzing Nicol mounted in brass telescope tubing. The slit was carefully machined and adjusted so that the sides were parallel and about 4 mm apart. The distance between slit and Wollaston was adjusted until the two fields were separated by a very narrow black line when illuminated by a sodium light. If this adjustment is carefully made the black line disappears when the analyzing Nicol is rotated to the point of equal intensity of the two fields of vision. The vernier on the Nicol could be read accurately to 50 minutes of arc.

The slit of the polariscope was kept two millimeters from the walls of the resonance bulb. Stray light was either eliminated by slits or trapped. All slits were painted black with a lampblack-shellac solution.

The resonance lamp was heated to 115–120°C by an air stream from a non-magnetically wound electric heater placed three feet below the lamp. Experiments have shown that there is no variation of the zero field polarization for a temperature range of 85–120°C and that no appreciable depolarization sets in until the temperature of the resonance bulb is raised to 135°C.

The zero field polarization was measured by three observers, each making a large number of settings of the analyzing Nicol. Before measuring the polarization in any magnetic field readings were taken on the zero field polarization to insure that there was no depolarization from any cause.

The results are given in Table I. The probable errors were computed by the method of least squares, at least 16 observations being made in each field.

Discussion

Fig. 1 shows an attempt to fit the experimental results by means of the curve calculated for $I=1$.

Table I. *Percent polarization of sodium resonance radiation in various magnetic fields.*

H	$P_{D_1+D_2}$	Error
0	16.48	0.38
10	16.26	0.30
20	21.37	0.38
50	34.54	0.33
70	38.86	0.33
90	43.0	
170	45.7	
315	46.25	

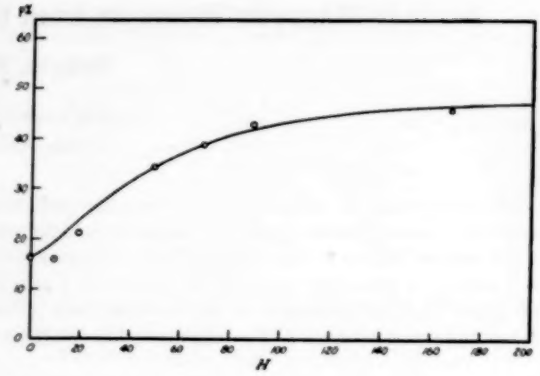

Fig. 1. Polarization as a function of magnetic field. Circles represent observations. Heavy curve computed with $I=1$, $A(3^2P_{3/2})=1.2\times10^{-3}$ cm^{-1}.

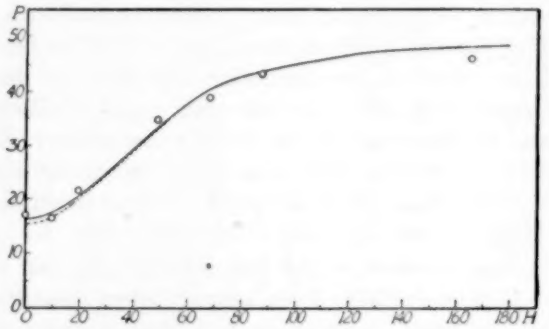

Fig. 2. Polarization as a function of magnetic field. Circles represent observations. Heavy curve computed with $I=3/2$, $A(3^2P_{3/2})=7.45\times10^{-4}$ cm^{-1}, $\tau=1.64\times10^{-8}$ sec. Broken curve computed neglecting effect of proximity of hyperfine levels.

The best fit is secured for A, the hyperfine multiplet separation constant, equal to 0.0012 cm^{-1}, but there is a significant deviation in the region of small fields, the curve at ten and twenty gauss coming well above the observed values. This calculated curve does not take into account the effect of finite breadth of levels,[4] and to do so will make the agreement even worse, as this effect operates to raise the polarization in weak fields so that the apparent agreement in zero field will be destroyed and the gap between calculated and observed values at ten and twenty gauss increased.

With a nuclear moment of 3/2 the situation is quite different. The calculation neglecting the

[4] G. Breit, Rev. Mod. Phys. **5**, 117 (1933).

effect of finite breadth of levels gives too low a zero field polarization (15.27 percent), but on taking into account the finite breadth of levels using $\tau = 1.64 \times 10^{-8}$ sec. the zero field polarization comes out 16.25 percent in fair agreement with the observed value. The heavy curve in Fig. 2 is computed for a nuclear moment of 3/2 with $A = 7.45 \times 10^{-4}$ cm^{-1}, $\tau = 1.64 \times 10^{-8}$ sec.[5]

[5] R. Minkowski, Zeits. f. Physik **36**, 839 (1926).

OCTOBER 1, 1934 PHYSICAL REVIEW VOLUME 46

Nuclear Magnetic Moments from the Polarization of Resonance Radiation

Sodium, $3^2S_{1/2} - 4^2P_{3/2,\ 1/2}$

A. ELLETT AND N. P. HEYDENBURG, *University of Iowa*

(Received July 19, 1934)

The polarization of sodium $3^2S_{1/2} - 4^2P_{1/2,\ 3/2}$ (λ3303A) resonance radiation excited by unpolarized light has been measured as a function of the intensity of a magnetic field applied parallel to the direction of the incident light beam. Detailed Paschen-Back effect calculations have been carried out for the hyperfine multiplet which constitutes a $^2S_{1/2} - ^2P_{3/2}$ transition for a nuclear moment of $3/2(h/2\pi)$. From the fitting of the observed polarization field strength curves we find the hyperfine structure separation constant for $4^2P_{3/2}$ to be $1.87 \pm 0.05 \times 10^{-4}$ cm^{-1}. The polarization field strength curve shows very clearly the effect of proximity of hyperfine levels in $4^2P_{3/2}$.

IN many cases the splitting of atomic energy levels due to nuclear spin is on a scale so small that the resolution of the hyperfine components of a spectral line is difficult or impossible. The splitting of the $3^2S_{1/2}$ level of sodium has been observed by Schüler[1] and measured by L. Granath and C. M. Van Atta,[2] who also obtained values for the hyperfine separation in $3^2P_{1/2,\ 3/2}$. The separation of the hyperfine levels making up the $4^2P_{3/2}$ and higher states is too small to be resolvable. However, the effect of a magnetic field upon the polarization of resonance radiation affords an indirect means of measuring these separations. The method has the advantage that it is not limited by the resolving power attainable with interference spectroscopes, nor by Doppler breadth. In fact it is only necessary that the separations to be measured should be of the order of magnitude of the natural breadth of the spectral line in question. The existence of structure on a scale smaller than this is not to be expected for one could scarcely recognize levels as distinct unless separated by an amount comparable with their own indefiniteness. That the dependence of the polarization of resonance radiation upon the intensity of an applied magnetic field should afford a means of measuring separations in hyperfine multiplets is due to the fact that such multiplets undergo a Paschen-Back effect. Intensities in the Paschen-Back effect are functions of a single variable, $g(J)(eH/4\pi mcA)$ where A is the separation constant of the hyperfine multiplet. From this, as we shall see, it follows that the polarization of resonance radiation is a function of H and A only through the ratio H/A, and upon this depends the possibility of obtaining the value of A from observation of the polarization as function of H, since the very laborious Paschen-Back effect calculations have to be carried through only for a suitably chosen set of values of H/A. If the dependence were upon H and A separately the task of computing would be so great that one would hesitate to undertake it.

[1] H. Schüler, Naturwiss. **16**, 512 (1926).
[2] L. Granath and C. M. Van Atta, Phys. Rev. **44**, 935 (1933).

THEORY

Where the separation of the levels making up a hyperfine multiplet is large compared to the natural breadth of an energy level, we may calculate polarizations by Heisenberg's method. For this the relative intensities of the Zeeman components of the hyperfine multiplet are re-

quired, and they may be calculated, as Goudsmit and Bacher[3] have pointed out, by a simple modification of the method applied to ordinary multiplets by Darwin.[4] The essential point for the present application is that the relative Zeeman intensities in the Paschen-Back effect depend upon a single argument which, as noted above, is essentially the ratio of the Larmor frequency to the separation constant of the multiplet. That intensities are function of $g(J)(eH/4\pi mcA)$ is immediately evident upon inspection of the chains of equations for the Fourier coefficients of the perturbed functions. These chains are

$$-X_{M_J-1,M_I+1}(A/2)(J-M_J+1)(I+M_I+1)+X_{M_JM_I}(E-AM_JM_I-M_J\omega)$$
$$-X_{M_J+1,M_I-1}(A/2)(J+M_J+1)(I-M_I+1)=0, \quad (1)$$

where $\omega=g(J)(eH/4\pi mc)$. The roots of the secular determinant are seen to be functions of $\Omega=\omega/A$ only, and consequently on substituting these roots back into the chains and solving for the X's we find that they depend upon A and H through Ω only.

As an illustration we may show that $3^2S_{1/2}-n^2P_{1/2}$ resonance radiation is unpolarized whatever the value of the nuclear moment may be and whatever the intensity of the applied magnetic field so long as it produces no Paschen-Back effect of the gross multiplet. That is to say, we take the unperturbed characteristic functions to be of the form

$$\overset{J}{\Psi}_{M_JM_I}=\overset{J}{\Psi}_{M_J}\overset{M_I}{P_I}(\cos\theta)e^{iM_I\Phi},$$

where $\Psi^J_{M_J}$ is the characteristic function for the atom with no nuclear spin. Strictly speaking the $\Psi^J_{M_J}$ are not independent of H, but as long as the Zeeman separations produced by the applied field are very small compared to the separation of the $^2P_{1/2,\,3/2}$ levels we may treat them as though independent of H. The perturbed characteristic functions may then be written

$$\overset{JF}{\Psi}_{M_F}=\sum X^{JF}_{M_JM_I}\overset{J}{\Psi}_{M_JM_I},$$

where the summation is over all values of M_J and M_I such that $M_J+M_I=M_F$. For either $^2P_{1/2}$ or $^2S_{1/2}$ the possible values of M_J are $\pm\frac{1}{2}$. The chains of equations reduce to two members, except when $M_F=\pm(I+\frac{1}{2})$ when there is only one. Writing $M_F=M_J+M_I$ these are

$$\begin{aligned}-X_{-\frac{1}{2},M_F+\frac{1}{2}}(A/2)(I+M_F+\tfrac{1}{2})+X_{\frac{1}{2},M_F-\frac{1}{2}}[E-(A/2)(M_F-\tfrac{1}{2})-\omega/2]=0,\\ X_{-\frac{1}{2},M_F+\frac{1}{2}}[E+(A/2)(M_F+\tfrac{1}{2})+\omega/2]-X_{\frac{1}{2},M_F-\frac{1}{2}}(A/2)(I-M_F+\tfrac{1}{2})=0.\end{aligned} \quad (2)$$

The normalizing equation is

$$(X_{-\frac{1}{2},M_F+\frac{1}{2}})^2(I+M_F+\tfrac{1}{2})!(I-M_F-\tfrac{1}{2})!+(X_{\frac{1}{2},M_F-\frac{1}{2}})^2(I+M_F-\tfrac{1}{2})!(I-M_F+\tfrac{1}{2})!=1.$$

If we write $\epsilon=2E/A$, $\Omega=\omega/A$ the roots of the secular equation are

$$\epsilon=(-1\pm\Delta)/2; \qquad \Delta=[1+4\Omega(2M_F+\Omega)+4I(I+1)]^{\frac{1}{2}}.$$

The X's are

$$\begin{aligned}\overset{I+\frac{1}{2}}{X}_{\pm\frac{1}{2},M_F\mp\frac{1}{2}}&=\left[\frac{\tfrac{1}{2}\Delta\pm(M_F+\Omega)}{\Delta(I+M_F\mp\tfrac{1}{2})!(I-M_F\pm\tfrac{1}{2})!}\right]^{\frac{1}{2}},\\ \overset{I-\frac{1}{2}}{X}_{\pm\frac{1}{2},M_F\mp\frac{1}{2}}&=\left[\frac{\tfrac{1}{2}\Delta\mp(M_F+\Omega)}{\Delta(I+M_F\mp\tfrac{1}{2})!(I-M_F\pm\tfrac{1}{2})!}\right]^{\frac{1}{2}}.\end{aligned} \quad (3)$$

[3] S. Goudsmit and R. F. Bacher, Phys. Rev. **34**, 1499 (1929).
[4] C. G. Darwin, Proc. Roy. Soc. **A115**, 1 (1927).

Labelling levels by their weak field quantum numbers F and M_F and writing transitions in the form $\begin{bmatrix} F\to F' \\ M_F\to M_F' \end{bmatrix}$ the intensities of parallel transitions from $F=I+\frac{1}{2}$ are

$$\left[\begin{matrix} I+\frac{1}{2}\to I+\frac{1}{2} \\ M_F\to M_F \end{matrix}\right]=\left[\frac{(\frac{1}{2}\Delta+M_F+\Omega)^{\frac{1}{2}}(\frac{1}{2}\Delta'+M_F+\Omega)^{\frac{1}{2}}-(\frac{1}{2}\Delta-M_F-\Omega)^{\frac{1}{2}}(\frac{1}{2}\Delta'-M_F-\Omega)^{\frac{1}{2}}}{\Delta\Delta'}\right]^2, \tag{4}$$

$$\left[\begin{matrix} I+\frac{1}{2}\to I-\frac{1}{2} \\ M_F\to M_F \end{matrix}\right]=\left[\frac{(\frac{1}{2}\Delta+M_F+\Omega)^{\frac{1}{2}}(\frac{1}{2}\Delta'-M_F-\Omega)^{\frac{1}{2}}+(\frac{1}{2}\Delta-M_F-\Omega)^{\frac{1}{2}}(\frac{1}{2}\Delta'+M_F+\Omega)^{\frac{1}{2}}}{\Delta\Delta'}\right]^2. \tag{5}$$

The sum of these is seen to be unity, and the same is readily found to be true for the sum of the parallel transitions from any sublevel of $F=I-\frac{1}{2}$. The total intensity (viewed perpendicular to the applied field) of the perpendicular components originating from any upper level is also readily found to be unity, as it obviously must be, since all levels have the same weight. Since the radiation from any upper magnetic sublevel shows no net polarization the line is unpolarized in resonance radiation. This result, it may be noted, is independent of the intensity distribution in the source.

The polarization of $^2S_{1/2}-{}^2P_{3/2}$ resonance radiation for a nuclear moment of unity has been calculated by Larrick.[5] We have carried out similar calculations for $I=3/2$. In this case the secular equation for $M_F=0$ is a biquadratic, while those for $M_F=\pm 1$ are cubics. If the cubics are reduced to the so-called cannonical form $E^3+aE+C=0$ they become identical, so that the labor of calculation is considerably reduced. We find also that the X's for $M_F=\pm 1$ are related, $X_{r,s}$ being the same as $X_{-s,-r}$. The reduction of the cubics to the same form and the relation between the X's is a result of the symmetry introduced into the chains of equations when I and J are equal.

The energies (in terms of A) have been calculated for $\Omega=0$, 1, 2, 3, 4, 6, 10, 15. The roots of the secular determinants were calculated to an accuracy of ± 1 in the fifth significant figure while the intensities[6] of the parallel transitions in the hyperfine multiplet were obtained to an accuracy of one part in 10^4.

Having the intensities of the Zeeman components making up the hyperfine multiplet we may compute the relative populations of excited states produced by radiation of given polarization and intensity distribution. Emissions from these excited states then give the relative intensities of the emitted radiation polarized in various azimuths. This procedure is unambiguous as long as the separations in the hyperfine multiplet are large compared to the breadth of a level. When this condition is no longer satisfied the specification of the state of polarization and frequency of an absorbed quantum no longer suffices to determine the excited atomic state resulting from its absorption. The degeneracy which thus arises is evidently not without effect upon the polarization of the resonance radiation for as the coupling with the nuclear magnetic moment approaches zero we should expect in some way to pass over to the situation prevailing when there is no nuclear moment and no hyperfine structure. How this occurs and how in such cases the polarization may be calculated has been discussed by Breit.[7]

In order to form an estimate of the importance of this effect we may bear in mind that the $^2S_{1/2}-{}^2P_{1/2,\,3/2}$ doublet excited to resonance by unpolarized incident light may show anywhere from 10.48 percent to 42.8 percent polarization in zero magnetic field, the first being the value when line breadth is completely negligible, the latter that when the coupling to the nuclear spin is so slight as to produce no effect. Now the observed value is only slightly greater than 10.48 percent so that we may expect to represent our results fairly well without taking into account the finite breadth of levels, especially in view of the fact that the separation of magnetic levels due to the applied field will remove

[5] Larrick, Phys. Rev. **46**, 581 (1934).

[6] These numerical results, together with those for $I=5/2$ are on file in the Physics Library of the University of Iowa and are available for loan to any one who may have use for them.

[7] G. Breit, Rev. Mod. Phys. **5**, 91 (1933) especially Art. 4, p. 117 ff.

the degeneracy due to breadth of levels sometime before the Paschen-Back effect is complete.

In Fig. 1 the broken curve represents the polarization of resonance radiation for a $^2S_{1/2} - {}^2P_{1/2, 3/2}$ doublet excited by unpolarized incident radiation (in a magnetic field parallel to the direction of the incident light beam), as a function of the argument Ω for the case where

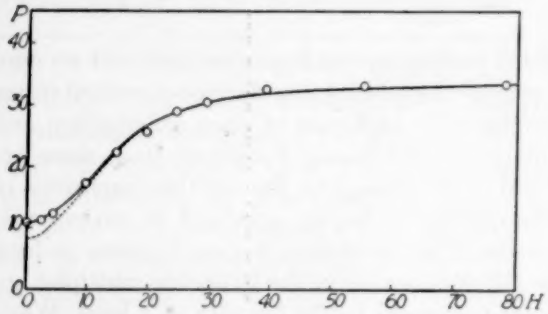

FIG. 1. Polarization as a function of magnetic field. Circles represent observations. Heavy curve computed with $A(4^2P_{3/2}) = 1.87\times10^{-4}$ cm^{-1}, $\tau = 3.13\times10^{-8}$ sec. Broken curve computed neglecting effect of proximity of hyperfine levels.

the hyperfine separations are very large compared to the breadth of energy levels. The incident radiation is supposed to come from a source emitting broad lines with the intensity ratio in the doublet 2 : 1. On the same figure the circles are the observed values of polarization plotted against the intensity of the applied magnetic field.

With a proper choice of scales for Ω and H the observed points may be made to coincide with the computed curve fairly closely for $\Omega > 4$. Since $\Omega = g(J)(eH/4\pi mcA)$ we conclude that the constant A for the hyperfine multiplet $4^2P_{3/2}$ is of the order of 2×10^{-4} cm^{-1}. We may now expect to improve the agreement and obtain a better value for A by taking into account the two effects so far neglected—first that due to finite breadth of energy levels and second that due to the fact that our source, while emitting fairly broad lines, is nevertheless not quite uniform across the absorption lines. As both these "corrections" are small we may treat them as though independent—that is, in computing the correction for intensity distribution in the source we will neglect the effect of finite breadth of energy levels, while in computing the change effected by the finite breadth of energy levels we will regard the intensity as uniform across the absorption line. Taking the simplest one first we consider the effect of non-uniform intensity.

Effect on Non-Uniform Source

Because of the very small hyperfine separation in $4^2P_{3/2}$ the line $3^2S_{1/2} - 4^2P_{3/2}$ is effectively a close doublet whose separation is nearly that of the $3^2S_{1/2}$ level. This according to Granath and Van Atta is 0.0583 cm^{-1}. We take the line form to be adequately represented by the superposition of two Rayleigh curves spaced 0.058 cm^{-1}, having maximum ordinates in the ratio of the statistical weights of the lower levels, 5 : 3, and a breadth corresponding to a source temperature of 1000°K. With this line form the energy absorbed by an absorption line of unit intensity whose center lies at a frequency distant ν_1 and ν_2, respectively, from the centers of the components of the doublet will be proportional to

$$3\exp(-\alpha\nu_1^2)+5\exp(-\alpha\nu_2^2),$$

in which

$$\alpha = Mc^2/2\nu_0R(T_r+T_s),$$

where ν_0 is a mean frequency, T_s and T_r the temperatures of source and resonance lamp. The factors 3 and 5 take account of the relative weights of the two hyperfine levels making up $^2S_{1/2}$. The difference in values of the polarization computed taking into account the actual intensity distribution in the source and that computed on the assumption of a uniform intensity varies from +1 in the third significant figure in zero field, to −4 in the fourth figure in a field of 30 gauss. As the correction is less than the experimental error it has been neglected.

Finite Breadth of Energy Levels

Breit[7] has discussed the effect of finite breadth in detail for the case of zero applied field. He finds, for the case of incident light plane polarized along the x axis, observation along z

$$I_z = \sum_{\phi,\mu}\left(\frac{C}{g_a}\right)(A_{x^{\phi\mu}})^2 + \sum_{f,f';\phi>\phi'}\left(\frac{2C}{g_a}\right)\frac{Sp[(e\dot{x})^{\phi f}(e\dot{x})^{f\phi'}(e\dot{x})^{\phi' f'}(e\dot{x})^{f'\phi}]}{[1+(2\pi\tau\nu_{\phi\phi'})^2]}, \qquad (6)$$

$$I_x+2I_y=(CA^2/3g_a)\sum_{\phi}(2\phi+1). \qquad (7)$$

Here and in what follows M and f are magnetic and total spin quantum numbers for sub-levels of the normal state (here $3^2S_{1/2}$), μ and ϕ corresponding quantities for the excited state ($^2P_{3/2}$). We reproduce these equations for the purpose of calling the reader's attention to the following points; Eq. (7) which is also valid when the applied field is not zero merely states that the total amount of energy absorbed does not depend on the degeneracy but merely upon the total weight of the system of nondegenerate levels into which a suitable perturbation will resolve the upper multiplet. Eq. (6) exhibits the intensity of the radiation polarized along x as the sum of two parts, a term $\sum_{\phi\mu}(C/g_a)(A_x^{\phi\mu})^2$ which is just what we would have obtained by the usual method of calculating populations of and emissions from the levels of the upper states, and which would tell the whole story if there were no degeneracy due breadth of levels; and another term, the balance of Eq. (6), which we will call δ. The term δ represents the change in intensity brought about by interference between the states which enter as linear combinations because of the degeneracy. It may be noted that we may write

$$I_x=I_x'+\delta; \qquad I_y=I_y'-\delta/2,$$

where I_x' and I_y' are the values of I_x and I_y obtained when the breadth of levels is negligible. Let us consider the term δ more closely. The summation

$$\sum_{f,\,f'} Sp[(e\dot{x})^{\phi f}(e\dot{x})^{f\phi'}(e\dot{x})^{\phi' f'}(e\dot{x})^{f'\phi}]$$

may, as Breit shows, be written

$$\sum_{\mu}|\sum_{f}(e\dot{z})_{\mu\mu}^{\phi f}(e\dot{z})_{\mu\mu}^{f\phi'}|^2;$$

that is, it involves the product of the probability amplitudes associated with transitions from two given upper levels ϕ, μ; ϕ', μ to *all common* lower levels f, $m_f=\mu$. That this term represents an interference effect, that is to say, that the relative phases of the probability amplitudes are of importance, is to be seen in the fact that the summation over the various possible lower levels is carried out before squaring. In the denominator of this term as it occurs in δ is the expression $1+(2\pi\tau\nu_{\phi\phi'})^2$ characteristic of such interference effects and involving the frequency difference of the interfering probability amplitudes. In zero applied field this frequency difference is the same for all terms involved in the further summation over μ. As this summation does not represent an interference (we are dealing now with the sum of squared terms) we may anticipate that we have merely to write for the more general case

$$\delta=\sum_{\mu,\ \phi>\phi'}\frac{|\sum_f(e\dot{z})^{\phi f}(e\dot{z})^{f\phi'}|^2}{[1+(2\pi\tau\nu_{\mu\mu}^{\phi\phi'})^2]}.$$

In the solution of the problem of the Paschen-Back effect of the hyperfine multiplet we have calculated the probability amplitudes which enter into this expression and the energy values whose differences divided by h are the $\nu_{\mu\mu}^{\phi\phi'}$, so the calculation of δ is merely a matter of numerical computation. A useful numerical check is afforded by the observation that if τ is small enough so that $(2\pi\tau\nu_{\mu\mu}^{\phi\phi'})^2$ may be neglected in comparison to unity we must get the same polarization as we would with zero coupling to the nuclear moment, in the present case 0.60. The polarization for the case of unpolarized incident light and field parallel to the light beam may be obtained from the above equations by use of the relation $P_\perp=P_{||}/(2-P_{||})$, where $P_{||}$ and $P_\perp$ are the polarizations for polarized and unpolarized incident light, respectively.

In the quantity δ there are two constants at our disposal, A, which enters through Ω in the probability amplitudes and in the frequency differences, and τ. We have seen that $A\sim 2\times10^{-4}$ cm^{-1}. Using this value of A as a first approximation we may give τ a value such that the calculated polarization in zero field agrees with that observed (after correction for intensity distribution, if necessary). The entire curve may now be calculated with these A and τ values, and if it shows systematic deviation from the observed curve the values of A and τ may be changed in the sense required to secure better agreement. By this process we have arrived at $A=1.87\times10^{-4}$ cm^{-1} with $\tau=3.13\times10^{-8}$ sec. as giving the best fit. The upper heavy curve in Fig. 1 is drawn through points calculated with these A and τ values.

Apparatus and Experimental Conditions

The interpretation of our results is based upon two principal assumptions regarding the experimental conditions. These are: first, that the vapor pressure of sodium in the resonance lamp is small enough so that errors due to secondary radiation, to depolarization by collision, and to change in the intensity distribution in the exciting beam as it passes through the resonance lamp are negligible; and second, that the vapor pressure in the source is so low that all effects due to reabsorption in the source are also negligible. We may test whether these conditions are met by progressively lowering the vapor pressure in resonance lamp and source. If we find that below a certain vapor pressure the polarization does not change over a considerable further range of reduction we may suppose that these sources of error have been eliminated. Our measurements of polarization were made with a resonance bulb temperature of 170°C which corresponds to a vapor pressure of sodium of 2.36×10^{-5} mm of mercury. With this vapor pressure it was possible to obtain a photograph of the resonance beam of sufficient intensity for measuring purposes with an exposure time of about 10 minutes. Lowering the temperature to 157°C at which the vapor pressure of sodium is 1×10^{-5} mm increased the necessary exposure time to about 30 minutes but did not cause any change in the polarization.

A photograph of the resonance beam with the slit between the bulb and camera removed showed a well-defined image of the beam with no blackening beyond the confines of the incident beam. This is evidence that the vapor pressure used was low enough that no secondary resonance radiation was present. Further evidence is derived from the observation that the image of the resonance beam was of nearly the same intensity at points where the exciting light entered and left the resonance bulb, showing that the intensity of the exciting light had not changed appreciably in passing through the absorbing sodium vapor in the bulb.

The source was a discharge tube of the type first used for resonance radiation work by one of the authors. Hydrogen is admitted through a capillary leak so adjusted that with continuous pumping of the discharge tube with a Cenco Hyvac pump the hydrogen pressure is just high enough to eliminate overheating of the tube by positive ion bombardment. The side tube containing a small amount of sodium is heated by an electric heater so wound that the metallic sodium is in the coldest part of the tube. The temperature of the side tube was 270°C which for equilibrium conditions would correspond to a vapor pressure of sodium of 4×10^{-3} mm of mercury. However, the sodium vapor pressure in the discharge is certainly less than this since diffusion to cooler parts of the discharge tube, convection by the steady current of hydrogen flowing through the discharge and reaction with the quartz walls all remove sodium from the discharge. If the heater on the side tube is turned off the yellow color disappears from the source almost as soon as the side tube has become cool. The reaction of sodium with the quartz walls ultimately produces a slight yellow discoloration and reduces the ultraviolet transmission to such an extent that a new quartz section must be inserted after about ten hours of operation.

The temperature of the side tube could be lowered to 255°C corresponding to a decrease in pressure of fifty percent without changing the polarization and also raised to a temperature of at least 275°C without any effect. It is therefore safe to assume that the vapor pressure used in the discharge tube was below that at which appreciable self-reversal takes place.

Nuclear Moment of Sodium

The calculation of nuclear magnetic moments from hyperfine structure A values has been discussed by Goudsmit[8] and by Fermi and Segré.[9] From Goudsmit's Eq. (6)

$$g(I)=\frac{aZ_i j(j+1)(l+\frac{1}{2})}{\Delta\nu l(l+1)}\times\frac{\lambda(lZ_i)}{k(jZ_i)}.$$

We can calculate $g(I)$ provided we know Z_i. The best that we can do at present is to use the value of Z_i obtained from the ordinary spin doublet formulas and the results of such calculations are presented in Table I. (The A values

[8] S. Goudsmit, Phys. Rev. **43**, 636 (1933).
[9] E. Fermi and E. Segré, Zeits. f. Physik **82**, 729 (1933).

TABLE I. *Hyperfine structure splitting constants (A) with corresponding nuclear magnetic moments and g factors together with values of effective nuclear charge used in computing them.*

	$3^2S_{1/2}$	$3^2P_{3/2}$	$4^2P_{3/2}$
A	0.029	$6.6\text{–}7.5\times10^{-4}$	1.87×10^{-4}
$g(I)$	1.35	1.5–1.7	1.33
$\mu(I)$	2.02	2.25–2.6	1.99
Z_i	11	7.66	7.55

for $3^2S_{1/2}$ and $3^2P_{3/2}$ are taken from Granath and Van Atta[2] and the preceding paper of Larrick.) As both Goudsmit and Fermi point out this Z_i value is not quite correct, since the hyperfine structure constant depends essentially on $\overline{1/r^3}$ while the spin doublet separation depends upon $\overline{(1/r)(dV/dr)}$. The values of the nuclear moment calculated from the splittings of $3^2S_{1/2}$ and $4^2P_{3/2}$ are in good agreement, but differ by almost thirty percent from that based on the $3^2P_{3/2}$ separation. This is no doubt due to some extent to the Z_i values used, and also to errors in polarization measurements. In the determination of A values from polarization *vs.* field strength curves the greatest weight should be attached to those points lying on the steeply sloping part of the curve, as it is here that a small error in the measurement of polarization will least affect the result. In the present case these are the points lying in the region 8–30 gauss. Of five points in this region only one is badly off the curve, that at 19.38 gauss, which corresponds to an A value of 2.05×10^{-4} cm^{-1}, about ten percent higher than that which we have chosen as giving the best fit. The results probably warrant writing $A(4^2P_{3/2})=1.87\pm0.05\times10^{-4}$ cm^{-1}.

The value of $A(3^2P_{3/2})$ is less certain, the points on Larrick's polarization field strength curve (see the preceding paper) scatter so that the A value is uncertain by about 10 percent. The present writers have measured one point in the critical region of this curve photographically and find 31.2 percent polarization in a field of 39.2 gauss applied parallel to the electric vector of plane polarized exciting radiation. To these values corresponds $A(3^2P_{3/2})=6.6\times10^{-4}$ cm^{-1}. Larrick's observed values at 19.4 and 48.5 gauss will lie very close to a curve drawn for this value of $A(3^2P_{3/2})$, and we are inclined to suppose that a curve run by the more accurate photographic method will give an A value somewhat lower than he has obtained, but not very much lower than 6.6×10^{-4} cm^{-1}.

Note added in proof. Regarding the computation of $g(I)$ values of the ^2P states (Table I supra), Breit writes that the value of Z_i which must be used is 8.9, or practically 9, but that the use of a Z_i has a sense only insofar as the central field picture applies. The value 8.9 is the ratio $(Z_{i\Delta})^2/Z_{iS}$ where $Z_{i\Delta}$ is the Z_i of the Landé doublet splitting formula and the Z_{iS} is the Z_i in Goudsmit's formula for the hyperfine splitting in terms of $g(I)$. He remarks that it is possible that this picture is sufficiently inaccurate to make the difference between $Z_i=7$ and $Z_i=9$ meaningless.

Radiation Damping and the Polarization of Fluorescence Radiation

G. BREIT AND I. S. LOWEN, *Physics Department, New York University, University Heights, N. Y.*

(Received August 15, 1934)

If the distance between two or more energy levels is comparable to their natural breadth, the levels cease to act independently. The coupling between the levels is then describable by means of a "damping constant matrix." The usual discussions concern themselves with a diagonal damping constant. Below a systematic treatment of emission, absorption and fluorescence is given without this restriction and it is shown how in general the frequencies of emission lines are affected by this radiation coupling. The theory is applied to the calculation of the polarization of fluorescence radiation. It is shown that the coupling state of the lower group of levels of the fluorescence line does not influence the polarization. Results of detailed calculations are given for the polarization of Hα excited by absorption of the second line of the Lyman series.

PHENOMENA associated with radiation damping have been treated by various authors[1–5] from the point of view of Dirac's theory of light quanta. In most of the phenomena investigated the effect of the coupling of matter and radiation turned out to be that of broadening the sharp line emission of frequency $\nu=\Delta W/h$ into a band of width proportional to the damping constant. It has been shown by Weisskopf and Wigner[2] that the width of the frequency band may be thought of as the sum of the widths of the initial and final level. In this way the old question of diffuse quantization has found its quantitative treatment. One may say that on account of the coupling between radiation and matter the concept of the stationary state is only partially exact and that the finite life of the stationary states makes their energy diffuse to the degree demanded by the uncertainty relation. The question arises whether the effect of the interaction with radiation is entirely that of broadening the energy levels or may also produce more vital effects on the quantization. In order to discuss this one must give a definition of quantization which applies in the presence of a damping constant. If the frequency spectrum emitted by an atom is of the type *const.* $\times[(\nu-\nu_0)^2+\Gamma^2]^{-1}$ we may say that the energy difference between the initial and final level is $h\nu_0$ and that the sum of the widths of the levels corresponds to a damping constant Γ. We can thus measure ν_0 even though the energy is diffuse just as we can measure the center of gravity of a wave packet in a properly defined state even though the position of the particle is indefinite. Let there be two levels close together situated so that the combination frequencies to a third level, as calculated by neglecting the coupling to radiation and given by the Bohr frequency condition, are ν_1, ν_2. In some cases it is possible to prepare an atomic state of such a kind that one will have a frequency distribution $[(\nu-\nu_1)^2+\Gamma_1^2]^{-1}d\nu$ emitted, and to prepare another state the emission from which will be $[(\nu-\nu_2)^2+\Gamma_2^2]^{-1}d\nu$. In such cases we may say that the coupling to the radiation had only a broadening effect. We are particularly concerned with another condition which makes it impossible to prepare such states. The general case[6] is one in which the spectra that may be prepared are of the form $[(\nu-f_1(\nu_1,\nu_2))^2+\Gamma_1^2]^{-1}$ and $[(\nu-f_2(\nu_1,\nu_2))^2+\Gamma_2^2]^{-1}$. In this condition the effect of the coupling to the radiation is not only to broaden each line, but also to shift its center of gravity. We shall first discuss qualitatively these effects for emission, absorption and fluorescence.

(a) *Emission.* A complete treatment of the emission of radiation from nondegenerate states has been given by Weisskopf and Wigner. It applies only as long as the energy levels of the atomic system are separated by intervals which are appreciably larger than the natural breadth due to radiation damping. When this is not the case one has to work[6] with a "damping constant matrix" instead of an ordinary "damping constant." Thus consider two energy levels μ, μ' located so close to each other that their energy

[1] F. Hoyt, Phys. Rev. **36**, 860 (1930).
[2] V. Weisskopf and E. Wigner, Zeits. f. Physik **63**, 54 (1930).
[3] V. Weisskopf, Ann. d. Physik **9**, 23 (1931).
[4] E. Fermi, Rev. Mod. Phys. **4**, 87 (1932).
[5] G. Breit, Rev. Mod. Phys. **5**, 91 (1933).

[6] Reference 5. See Eq. (156), p. 118. The special case of the text above corresponds to $\Gamma^{\mu\mu'}$ being diagonal.

difference is comparable with their average natural breadth. If the atom is put into the level μ, its coupling to the radiation will produce intermediate states of nearly the same energy in which a light quantum has been emitted and these intermediate states, through the absorption of a light quantum, will cause the production of μ'. Only in special cases will the radiation be describable as a simple exponential decay of the probability of the level μ, as may be seen without elaborate calculation by means of the following argument. Suppose for the moment that μ and μ' are two states such that either can emit independently of the other and suppose that they result from the application of an external, say magnetic, field to a degenerate level. Let their wave functions be ψ_μ and $\psi_{\mu'}$. We may as a rule neglect the change in ψ_μ and $\psi_{\mu'}$ due to the field. For the important thing about these wave functions is their effect on matrix elements to other levels and if these elements are appreciable before the field is applied, we may neglect the small change produced in them by the field. Let now the magnetic field be removed and a field of another type, say an electric field, be applied. The new energy levels will be described by $\psi_{\bar{\mu}}=c_1\psi_\mu+c_2\psi_{\mu'}$, $\psi_{\bar{\mu}'}=c_3\psi_\mu+c_4\psi_{\mu'}$. Neither $\psi_{\bar{\mu}}$ nor $\psi_{\bar{\mu}'}$ can now decay exponentially since the rate of decay is, in general, different for μ and μ'. This discussion applies only to very weak fields since energy differences also enter the exponents.[7]

A brief treatment of this question has been given by Bethe[8] for the case of hydrogen. He showed how the metastability of the $2s$ level is removed by a weak electric field and how, as the field decreases to zero, one approaches continuously to the existence of a metastable level. Bethe's treatment makes no explicit use of the theory of light quanta. It is not altogether rigorous because the form of the result is assumed without proof. One may regard some of the calculations which follow as substantiating the validity of this form.

The radiation coupling discussed here is similar, but not identical with, that treated by Weisskopf and Wigner[2] for a harmonic oscillator. In both cases it is essential that the radiation emitted in a jump between two energy levels be of the right frequency to be selectively absorbed in a transition between another pair. In our calculations the lower levels of the two pairs are either identical or close together and the energy differences of the two pairs are not equal. In these respects the coupling considered here is different from that of Weisskopf and Wigner. In neither case is the coupling describable as the result of the addition of probabilities for emissions and absorptions. It is correctly thought of only in terms of additions of probability amplitudes.

(b) *Absorption and fluorescence radiation.* A treatment of absorption and of the polarization of resonance radiation has been given by Weisskopf.[3] His results apply either to nondegenerate systems or to the special case of a nondegenerate normal level and a triply degenerate excited level with constant angular momentum. A more complete theory given by Breit[5] took into account explicitly possible degeneracies (hyperfine structure) of both levels for resonance radiation, and applied the results to cases of constant angular momentum as well as some closely related cases in which the "damping constant matrix" is diagonal. In weak magnetic fields only the splittings of the upper group of levels and their mean life were found to be of importance. It will be seen below[9] that as long as the incident radiation has a uniform energy spectrum[10] this result applies also to fluorescence radiation. The natural breadths and the energy differences among the lower group of levels do not matter for the polarization of this radiation. On the other hand, according to Weisskopf and Wigner,[2] it is the sum of the breadths of the initial and final levels that determines the width of the emission lines. It is thus impossible to replace the fluorescence transition by a virtual oscillator, since

[7] The fact that the damping constants of atoms with a constant angular momentum are necessarily equal, by spectroscopic stability, is not an objection to the above argument because the angular momentum need not be constant.

[8] H. Bethe, Handb. d. Physik, H. Geiger and K. Scheel; Springer, 1933, 2nd edition XXIV/1, pp. 452–456.

[9] I. S. Lowen and G. Breit, Phys. Rev. **45**, 120 (1934).

[10] If the incident energy spectrum is non-uniform the splitting of the normal level affects the result, as is obvious from qualitative considerations and also appears in Eq. (7.4) below. The splitting and width of the lower level c of the energy level pair giving the fluorescence line is immaterial also in this case as follows by combining Eq. (7.4) with Eq. (7.8).

the damping constant of that oscillator varies for different phenomena.

The same is found to be true if the damping constant is nondiagonal. The lack of influence of the lower level may be understood qualitatively in the sense that the cause of broadening is unimportant within certain limits. Thus if this level is split by interaction with the nuclear spin there is no effect on the polarization,[5] just as there is no effect if it is broadened by possible transitions to levels below it.

(c) *Fluorescence of hydrogen.* For purposes of illustration of the general theory we calculate the polarization of the line $H\alpha$ produced by absorption of the second line of the Lyman series. The atomic hydrogen gas is supposed to be in an electric field. The polarization changes as the electric field increases as soon as the Stark effect splittings are of the order of the natural breadth of the $n=3$ sublevels. No explicit calculations were made for the influence of the nuclear spin which must affect the polarization in weak fields. If the experimental arrangement for observing the polarization of such fluorescence should prove practical, we should be able to determine the h.f.s. of the $3s$ level of hydrogen by measurements of the polarization of the fluorescent $H\alpha$ radiation.

1. General Theory

An absorbing atom in the normal state a is supposed to be exposed to radiation from a distant emitting atom I. The state a as well as the other states with which we deal is supposed to consist of groups of sublevels such as would be produced by applying an external field to a degenerate level. The maximum frequency difference between sublevels in the same group is supposed to be small in comparison with the emission and the absorption frequencies dealt with. The same is supposed to hold for the damping constants. No restriction on the relative magnitudes of damping constants and the frequency differences of sublevels in the same group is made. The frequency ν_I of the incident radiation is supposed to lie close to the absorption frequency from a to another state b. We also take into account the presence of two other states c, d (Fig. 1) to which the atom may fall in succession from b. The light quanta emitted are called s, s', respectively. The state d is supposed to be metastable. The above arrangement of levels enables one to generalize to most of the other possible cases. The equations which describe the process are[11]

$$[(d/idt)+\omega(b')]C(b')=\sum(sc')(B_s^{c'b'})^*C(sc')+\sum(sa')(B_s^{a'b'})^*C(sa') +K_{b'a}\exp\{-i[\omega(\mathrm{I})+\omega(a)-i\gamma(\mathrm{I})]t\}\cdots, \quad (1.1)$$

$$[(d/idt)+\omega(c')+\omega(s)]C(sc')=\sum(b')B_s^{c'b'}C(b')+\sum(d's')(B_{s'}^{d'c'})^*C(ss'd')\cdots, \quad (1.2)$$

$$[(d/idt)+\omega(d')+\omega(s)+\omega(s')]C(ss'd')=\sum(c')B_{s'}^{d'c'}C(sc'). \quad (1.3)$$

Here C are the probability amplitudes for the states considered. Thus, e.g., $C(ss'd')$ refers to the state in which there is one light quantum of type s, one light quantum of type s', and in which the atom is in a sublevel d' of the state d. We use a and a', b and b', etc. interchangeably for the sublevels of a, b, etc. The additive energy constant is supposed to be adjusted so that the energy is zero if there are no light quanta and if the atom is in an arbitrarily chosen sublevel of a Also $\omega=2\pi\nu$

$$B_s^{ab}=(h\nu_s V)^{-\frac{1}{2}}(\sum e_i\mathbf{f}_i\mathbf{f}_s)_{ab}\exp\{-i\mathbf{k}_s\mathbf{R}\} \quad (1.4)$$

where

$\mathbf{f}_s$ = unit vector in the direction of electric intensity of light quantum s.

e_i and $\dot{\mathbf{r}}_i$ = charge and velocity vector of atomic particle i.

$\mathbf{k}_s$ = vector of magnitude $2\pi\nu_s/c$ in the direction of propagation of light quantum s.

$\mathbf{R}$ = vector from origin of coordinates to center of atom and

$$K_{ba}=(\sum e_i\mathbf{r}_i)^{(p)}{}_{ba}(e\mathbf{r}_\mathrm{I})^{(p)}{}_{n_\mathrm{I}n_\mathrm{I}'}/R_{\mathrm{II}\,\mathrm{I}}\hbar c^2 \quad (1.5)$$

where the superscript (p) changes a vector into its projection on the plane perpendicular to the line joining the emitter I to the absorber, and where n_I, n_I' are, respectively, the normal and excited states of the emitter.

We solve these equations using the customary approximations introduced by Dirac, Weisskopf

[11] Reference 5, VII §4; VI §4.

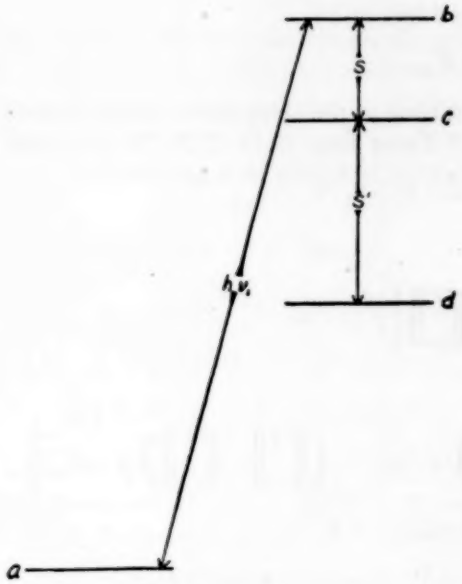

FIG. 1. Energy diagram.

and Wigner and by Hoyt. Thus the summations over possible light quanta on the right side of Eq. (1) will be replaced by integrations. These will be performed approximately by extending the range to $-\infty$ and by considering the number of possible kinds of light quanta in unit frequency range as being constant. The procedure for obtaining the solutions is very similar to that of the simpler case already discussed.[11] We introduce the following abbreviations:

$$\begin{bmatrix} A & \\ & B \end{bmatrix} = e^{-iAt} - e^{-iBt};$$

$$\left[\!\!\left[\begin{matrix} A & \\ & B \end{matrix} \right]\!\!\right] = \begin{bmatrix} A & \\ & B \end{bmatrix} \Big/ (B-A) \quad (2)$$

and we have

$$\int_{-\infty}^{+\infty} \left[\!\!\left[\begin{matrix} A & \\ & B \end{matrix} \right]\!\!\right] dB = \pi i e^{-iAt}. \quad (3)$$

The description of the emission from c to d is obtained by solving Eqs. (1.2), (1.3) omitting the first sum in Eq. (1.2) altogether. The solution is

$$C(sc') = \sum(\bar{c}) a_{\bar{c}} a_{c'}^{\bar{c}} \exp\{-i[\omega(\bar{c}) + \omega(s) - i\gamma(\bar{c})]\}, \quad (4.1)$$

$$C(ss'd') = \sum a_{\bar{c}} a_{c'}^{\bar{c}} B_{s'}^{d'c'} \left[\!\!\left[\begin{matrix} \omega(\bar{c}) + \omega(s) - i\gamma(\bar{c}) & \\ & \omega(d') + \omega(s) + \omega(s') \end{matrix} \right]\!\!\right], \quad (4.2)$$

where the $a_{\bar{c}}$ are determined by

$$\sum a_{\bar{c}} a_{c'}^{\bar{c}} = C(sc')_{t=0} \quad (4.3)$$

and $a_{c'}^{\bar{c}}$, $\omega(\bar{c})$, $\gamma(\bar{c})$ are given by

$$a_{c'}^{\bar{c}}[\omega(c') - \omega(\bar{c}) + i\gamma(\bar{c})] = i\sum \gamma^{c'c''} a_{c''}^{\bar{c}} \quad (4.4)$$

with

$$\gamma^{c'c''} = (\pi/\Delta\omega(s'))\overline{\sum(d')(B_{s'}^{d'c'})^* B_{s'}^{d'c''}}, \quad (4.5)$$

where the ——— indicates averaging over all directions and polarizations of s'.

Eq. (5.3) gives, in general, nonvanishing values of all $a_{\bar{c}}$. It is thus not possible to have only one level c' of the group c excited at all times. If it is the only excited level at $t=0$ other levels will become excited later according to Eq. (4.1). If the levels c', c'', etc., are widely spaced, the solutions of the Eqs. (4.4) will be such that a possible $\bar{c}$ will lie close to a c' and the $a_{c'}^{\bar{c}}$ for this pair of values will be much larger than the other $a_{c'}^{\bar{c}}$; the emission can then take place with the excitation of only one level c'. If, however, the differences $\omega(c') - \omega(c'')$ are of the same order as the $\gamma^{c'c''}$ then one should take into account more than one term in Eq. (4.1) and the energy levels lose their identity as the radiation couples them by the matrix $\gamma^{c'c''}$. The quantity $\omega(s)$ is, of course, irrelevant to the discussion of emission, playing the part of an additive constant in the energy.

In the solution of Eqs. (1) the terms in $C(b')$ will bring into Eq. (1.2) terms of the type $K_{sc'} \exp\{-i(\Omega - i\Gamma)t\}$. We consider this equation with one of these terms replacing the first sum. We obtain the following solution of the thus modified Eqs. (1.3), (1.2) subject to the initial conditions $C(sc') = C(ss'd') = 0$

$$C(sc') = \sum (Ka^{-1})_{s\bar{c}} a_{c'}^{\bar{c}} \left[\!\!\left[\begin{matrix} \Omega - i\Gamma & \\ & \omega(\bar{c}) + \omega(s) - i\gamma(\bar{c}) \end{matrix} \right]\!\!\right], \quad (5.1)$$

$$C(ss'd') = \sum (Ka^{-1})_{s\bar{c}} a_{c'}^{\bar{c}} B_{s'}^{d'c'} \left[\left[\!\!\left[\begin{matrix} \Omega - i\Gamma & \\ & \omega(d') + \omega(s) + \omega(s') \end{matrix} \right]\!\!\right] - \left[\!\!\left[\begin{matrix} \omega(\bar{c}) + \omega(s) - i\gamma(\bar{c}) & \\ & \omega(d') + \omega(s) + \omega(s') \end{matrix} \right]\!\!\right] \right] \Big/ [\omega(s) + \omega(\bar{c}) - i\gamma(\bar{c}) - \Omega + i\Gamma], \quad (5.2)$$

the summations being over $\bar{c}$ and where $(Ka^{-1})_{s\bar{c}}$ is defined by:

$$\sum (Ka^{-1})_{s\bar{c}} a_{c'\bar{c}} = K_{sc'}. \tag{5.3}$$

This solution except for the presence of $\omega(s)$ is of the same form as the absorption solution from d to c, and its properties have been already partly discussed.[11] Using Eqs. (5.1), (5.2), (3) we solve Eqs. (1.1), (1.2), (1.3) subject to the initial conditions $C(b')=C(sc')=C(ss'd')=0$ and obtain

$$C(b') = \sum (\bar{b})(KA^{-1})_{\bar{b}a} A_{b'\bar{b}} \left[\!\left[\begin{matrix} x \\ z \end{matrix} \right]\!\right], \tag{6.1}$$

$$C(sc') = \sum (\bar{b}\bar{c})(KA^{-1})_{\bar{b}a} A_{b'\bar{b}} B_{s}^{c''b'} (a^{-1})_{\bar{c}}^{c''} a_{c'\bar{c}} \left[\left[\!\left[\begin{matrix} x \\ u \end{matrix} \right]\!\right] - \left[\!\left[\begin{matrix} z \\ u \end{matrix} \right]\!\right]\right] \Big/ (z-x), \tag{6.2}$$

$$C(ss'd') = \sum (KA^{-1})_{\bar{b}a} A_{b'\bar{b}} B_{s}^{c''b'} (a^{-1})_{\bar{c}}^{c''} a_{c'\bar{c}} B_{s'}^{d'c'} (z-x)^{-1}$$

$$\times \left[\left(\left[\!\left[\begin{matrix} x \\ y \end{matrix} \right]\!\right] - \left[\!\left[\begin{matrix} u \\ y \end{matrix} \right]\!\right] \right) (u-x)^{-1} - \left(\left[\!\left[\begin{matrix} z \\ y \end{matrix} \right]\!\right] - \left[\!\left[\begin{matrix} u \\ y \end{matrix} \right]\!\right] \right) (u-z)^{-1} \right], \tag{6.3}$$

where

$$A_{b'\bar{b}}[\omega(b') - \omega(\bar{b}) + i\gamma(\bar{b})] = i\sum \gamma^{b'b''} A_{b''\bar{b}}, \tag{6.4}$$

$$x = \omega(\mathrm{I}) + \omega(a) - i\gamma(\mathrm{I}), \quad y = \omega(d') + \omega(s) + \omega(s'), \quad z = \omega(\bar{b}) - i\gamma(\bar{b}), \quad u = \omega(\bar{c}) + \omega(s) - i\gamma(\bar{c}). \tag{6.5}$$

On account of the presence of $\gamma(\bar{b})$ in z and $\gamma(\bar{c})$ in u both $C(b')$ and $C(sc')$ vanish when $t\to\infty$. The only terms in $C(ss'd')$ which do not vanish are those due to y in the [ ]. Thus for sufficiently large t

$$C(ss'd') = \sum (\bar{b}\bar{c})(KA^{-1})_{\bar{b}a} (ABa^{-1})_{s\bar{c}} \bar{b}(aB)_{s'\bar{c}d'} [X - \omega(s) - \omega(s')]^{-1} [Z(\bar{b}) - \omega(s) - \omega(s')]^{-1}$$

$$\times [U(\bar{c}) - \omega(s')]^{-1} \exp\{-i[\omega(d') + \omega(s) + \omega(s')]t\}, \tag{7.1}$$

where

$$X = \omega(\mathrm{I}) - \omega(d'a) - i\gamma(\mathrm{I}); \quad Z(\bar{b}) = \omega(\bar{b}d') - i\gamma(\bar{b}); \quad U(\bar{c}) = \omega(\bar{c}d') - i\gamma(\bar{c}). \tag{7.2}$$

The above expression (7.1) gives the final values for the probability amplitudes of states in which, light quanta s, s' were emitted, respectively, in transitions $b\to c$, $c\to d$ and the atom fell into state d'. In order to obtain the probability of finding simultaneously a photon s with a given polarization and directional property and a photon s' with another polarization and directional property we must calculate

$$\sum_{\omega(s)\omega(s')} |C(ss'd')|^2 = [1/\Delta\omega(s)\Delta\omega(s')] \int_0^\infty \int_0^\infty |C(ss'd')|^2 d\omega(s) d\omega(s'), \tag{7.3}$$

where $1/\Delta\omega(s)$ is the number of photons of the type considered in the unit frequency range of $\omega(s)$. Using Eqs. (7.1), (7.2), we have

$$\sum_{\omega(s)\omega(s')d'} |C(ss'd')|^2 = \frac{2\pi^2}{i\gamma(\mathrm{I})\Delta\omega(s)\Delta\omega(s')} \sum (\bar{b}'\bar{c}'\bar{b}\bar{c}) \frac{(\bar{b}'\bar{c}'|G|\bar{b}\bar{c})}{[\omega(\bar{c}\bar{c}') - i(\gamma(\bar{c}') + \gamma(\bar{c}))][\omega(\bar{b}\bar{b}') - i(\gamma(\bar{b}) + \gamma(\bar{b}'))]}$$

$$\cdot \left\{ \frac{1}{\omega(\bar{b}'a) - \omega(\mathrm{I}) + i(\gamma(\bar{b}') + \gamma(\mathrm{I}))} + \frac{1}{\omega(\mathrm{I}) - \omega(\bar{b}a) + i(\gamma(\mathrm{I}) + \gamma(\bar{b}))} \right\}, \tag{7.4}$$

$$(\bar{b}'\bar{c}'|G|\bar{b}\bar{c}) = \sum (KA^{-1})_{\bar{b}'a}{}^{*} (AB_{s}a^{-1})_{\bar{c}'}\bar{b}'^{*} (aB_{s'})_{\bar{c}d'}{}^{*} (aB_{s'})_{\bar{c}d'} (AB_{s}a^{-1})_{\bar{c}}\bar{b} (KA^{-1})_{\bar{b}a}. \tag{7.5}$$

For large $\gamma(\mathrm{I})$ the general Eq. (7.4) simplifies to

$$\sum |C(ss'd')|^2 = \frac{4\pi^2}{\gamma^2(\mathrm{I})\Delta\omega(s)\Delta\omega(s')} \sum (\bar{b}'\bar{c}'\bar{b}\bar{c}) \frac{(\bar{b}'\bar{c}'|G|\bar{b}\bar{c})}{[\gamma(\bar{c}') + \gamma(\bar{c}) + i\omega(\bar{c}\bar{c}')][\gamma(\bar{b}) + \gamma(\bar{b}') + i\omega(\bar{b}\bar{b}')]}. \tag{7.6}$$

From this Eq. (7.6) one can obtain the properties of the radiation s emitted in jumps from b to c or the properties of the radiation s' emitted in jumps from c to d by summing, respectively, over all the directions of polarization and of propagation of s' and s, respectively. We make the calculation for s and we must thus average $(\bar{b}'\bar{c}'|G|\bar{b}\bar{c})$ over all possible polarizations of s'. We have by Eq. (4.5)

$$(\pi/\Delta\omega(s'))\sum\overline{(d')(aB_{s'})^{\bar{c}'d'*}(aB_{s'})^{\bar{c}d'}}=\sum(c'c'')a_{c''}{}^{\bar{c}'*}\gamma^{c''c'}a_{c'}{}^{\bar{c}}. \tag{7.7}$$

But it follows from Eq. (4.4) that

$$\sum(c'c'')a_{c''}{}^{\bar{c}'*}\gamma^{c''c'}a_{c'}{}^{\bar{c}}=(1/2)[\gamma(\bar{c})+\gamma(\bar{c}')+i\omega(\bar{c}\bar{c}')]\sum(c)a_{c}{}^{\bar{c}'*}a_{c}{}^{\bar{c}}. \tag{7.8}$$

Hence

$$\overline{\sum|C(ss'd')|^2}=(2\pi/\gamma^2(\mathrm{I})\Delta\omega(s))\sum(\bar{b}\bar{b}')\beta(\bar{b}'\bar{b})\kappa(\bar{b}\bar{b}')/[\gamma(\bar{b})+\gamma(\bar{b}')+i\omega(\bar{b}\bar{b}')], \tag{9}$$

where

$$\beta(\bar{b}'\bar{b})=\sum(c)(AB_s)^{\bar{c}\bar{b}'*}(AB_s)^{\bar{c}\bar{b}}\cdots. \tag{9.1}$$

$$\kappa(\bar{b}\bar{b}')=\sum(a)(KA^{-1})_{b'a}{}^{*}(KA^{-1})_{\bar{b}a}. \tag{9.2}$$

It is seen from Eq. (9) that the frequency differences among levels c do not matter for the intensity of fluorescence radiation due to light quanta s. Neither do the damping constants $\gamma^{c'c''}$ enter the result. Thus the breadth of the lower level has nothing to do with the polarization of the fluorescence radiation.

In the above calculation we considered explicitly only the level groups a, b, c, d. The presence of other level groups introduces no essential difference. Thus the matrix $\gamma^{b'b''}$ is given by a formula similar to (4.5):

$$\gamma^{b'b''}=(32\pi^4e^2/3hc^3)[\sum(d)\nu^3(bd)\mathfrak{r}(b'd)\mathfrak{r}(db'')+\sum(c)\nu^3(bc)\mathfrak{r}(b'c)\mathfrak{r}(cb'')+\sum(a)\nu^3(ba)\mathfrak{r}(b'a)\mathfrak{r}(ab'')].$$

Similarly there is, in general, a like term for every group of levels below b to which a transition is possible.

Eq. (7.1) is more general than the formula derived by Weisskopf[12] inasmuch as it includes non-diagonal damping terms. It is more special inasmuch as it does not consider chains of more than two successive reemissions and because it does not include the different permutations in the order of emission of the light quanta. An obvious extension of Eq. (7.1) can be made by including in it the extra terms of Weisskopf's formula.

2. Application to Hydrogen in an Electric Field

We consider an atom of hydrogen in an electric field. We suppose the field to be weak enough to have the Stark effect small in comparison with the distances between levels with different j. We may then approximate the wave function[13] by considering it as a linear combination of wave functions with the same j, m and different l. We calculate the contribution to $\gamma^{b'b''}$ due to a level of total quantum number n'. In terms of $(32\pi^4\nu(nn')^3e^2/3hc^3)$ this contribution is

$$\frac{2j+3}{8(j+1)}(R_{n',\,j+3/2}^{n,\,j+1/2})^2+\frac{2j+1}{8(j+1)}(R_{n',\,j-1/2}^{n,\,j+1/2})^2+(-)^{\alpha'+\alpha''}\left[\frac{2j+1}{8j}(R_{n',\,j+1/2}^{n,\,j-1/2})^2+\frac{2j-1}{8j}(R_{n',\,j-3/2}^{n,\,j-1/2})^2\right]. \tag{10}$$

Here n is the total quantum number of the state b, $R_{n'l'}^{n,\,l}$ is the radial integral of r, referred to the states n, l and n', l'; for $\alpha'=0$, 1 the state b' is, respectively, symmetric and antisymmetric, its wave function being supposed to be:[14]

$$2^{-1}\{(n,j+\tfrac{1}{2},j,m)+(-)^{\alpha}(n,j-\tfrac{1}{2},j,m)\}.$$

[12] V. Weisskopf, Zeits. f. Physik **85**, 451 (1933).

[13] R. Schlapp, Proc. Roy. Soc. **A119**, 313 (1928); V. Rojansky, Phys. Rev. **33**, 1 (1929).

[14] Since the result depends only on $\alpha+\alpha'$ and not on α, α' individually, the choice of signs for the wave functions (n, l, j, m) is immaterial for the present purpose. The radial and angular parts of the wave functions are supposed to be normalized to 1 separately.

Expression (10) has values for the states of interest to us given in Table I.

TABLE I.

n	n'	j	$(3hc^3/32\pi^4\nu(nn')^3e^2)\gamma^{b'b''}$
3	2	3/2	$(1/5)(R_{2p}^{3d})^2+(-)^{a+a'}(1/6)(R_{2s}^{3p})^2$
3	1	3/2	$(-)^{a+a'}(1/6)(R_{1s}^{3p})^2$
3	2	1/2	$(1/6)(R_{2s}^{3p})^2+(-)^{a+a'}(1/2)(R_{2p}^{3s})^2$
3	1	1/2	$(1/6)(R_{1s}^{3p})^2$

The second and fourth lines give also the values for $n=2$, $n'=1$ on changing $3p$ into $2p$ and $3s$ into $2s$. The Eqs. (4.4) are now

$$(\bar{\Gamma}-\Gamma_1)A_1=gA_2; \qquad (\bar{\Gamma}-\Gamma_2)A_2=gA_1, \tag{11}$$

where

$$\bar{\Gamma}=\bar{\gamma}+i\bar{\omega}, \qquad \Gamma_1=\gamma+i\omega_1, \qquad \Gamma_2=\gamma+i\omega_2, \qquad \gamma^{12}=g, \qquad \gamma^{11}=\gamma^{22}=\gamma \tag{11.1}$$

and by 1,2 are meant, respectively, the symmetric and antisymmetric states. There are two roots for Γ which satisfy Eq. (11). We call them $\Gamma_{\bar{1}}$, $\Gamma_{\bar{2}}$. We may take

$$A_1{}^{\bar{1}}=A_1{}^{\bar{2}}=g, \qquad A_2{}^{\bar{1}}=\Gamma_{\bar{1}}-\Gamma_1, \qquad A_2{}^{\bar{2}}=\Gamma_{\bar{2}}-\Gamma_1 \tag{11.2}$$

and we have

$$(\Gamma_{\bar{1}},\Gamma_{\bar{2}})=\bar{\Gamma}=(1/2)(\Gamma_1+\Gamma_2)\pm[g^2-(1/4)(\omega_1-\omega_2)^2]^{1/2}. \tag{11.3}$$

If $|\omega_1-\omega_2|\gg\gamma, g$ the two values of $\bar{\Gamma}$ are Γ_1, Γ_2. In this case the nondiagonal matrix element g has no effect. For $|\omega_1-\omega_2|<2g$ the imaginary parts of $\Gamma_{\bar{1}}$, $\Gamma_{\bar{2}}$ are equal to each other. In this case one has no effect of the electric field on the emission frequencies $\omega_{\bar{1}}/2\pi$, $\omega_{\bar{2}}/2\pi$. Since $\omega_{\bar{1}}=\omega_{\bar{2}}=(\omega_1+\omega_2)/2$. If finally $|\omega_1-\omega_2|\ll 2g$ we may take in addition $\gamma_{\bar{1}}=\gamma+g$, $\gamma_{\bar{2}}=\gamma-g$. For $n=2$, $j=\frac{1}{2}$ in accordance with Table I we have $\gamma=g$ so that $\gamma_{\bar{1}}=2\gamma$, $\gamma_{\bar{2}}=0$. This corresponds to the fact that the $2s$ level is metastable. The first effect of the introduction of a weak field is to make

$$\begin{aligned}\gamma_{\bar{2}}&=\gamma-[\gamma^2-(\omega_1-\omega_2)^2/4]^{1/2}\leqq(\omega_1-\omega_2)^2/8\gamma\\ \gamma_{\bar{1}}&=\gamma+[\gamma^2-(\omega_1-\omega_2)^2/4]^{1/2}\leqq 2\gamma.\end{aligned} \tag{11.4}$$

Thus, in agreement with Bethe,[8] the presence of an electric field destroys the metastability of the $2s$ level gradually and at first in proportion to the square of the electric field.

It is of interest to note that for $|\omega_1-\omega_2|<2g$ the observation of radiation from the $n=2$ state does not show the presence of two distinct frequencies ω_1, ω_2. Instead there is only one frequency $\bar{\omega}=(\omega_1+\omega_2)/2$ and two damping constants given by Eq. (11.4). We may say that in this case the coupling of the atom to the radiation is so strong as to make the distinction between the different Stark effect levels meaningless. The state which radiates in accordance with the simple formula $\exp\{-i(\bar{\omega}+i\bar{\gamma})t\}$ is in this case not a stationary state of the matter but a linear combination of two stationary states approaching as a limit either the $2s$ or $2p$ state for $|\omega_1-\omega_2|\to 0$.

In the calculation of the polarization of fluorescence radiation we may neglect a factor common to all intensities. We may thus use for the values of K the matrix elements of the coordinates of the absorbing atom instead of the complete expression (1.5). We also omit the factor $(R_{1s}^{3p})^2/9$ which is common to the squares of all the matrix elements. Similarly, instead of the complete B_s entering Eq. (9.1) we use the matrix elements of the coordinates. We calculate first the polarization for the case in which the incident light is polarized with its electric vector parallel to the electric intensity of the field applied to the hydrogen atom. The calculation is conveniently performed separately for $|\omega_2-\omega_1|>2g$ and $|\omega_2-\omega_1|<2g$. One obtains the same formula for the final answer. We indicate an intermediate step for $x<g$, $x=(\omega_2-\omega_1)/2$ and for the polarization of the fluorescence radiation parallel to that of

the incident radiation. We have

$$\begin{pmatrix}\kappa(\bar{1}\bar{1}), & \kappa(\bar{1}\bar{2})\\ \kappa(\bar{2}\bar{1}), & \kappa(\bar{2}\bar{2})\end{pmatrix}=[4g^2(g^2-x^2)]^{-1}\begin{pmatrix}|Z_2|^2, & -Z_1^*Z_2\\ -Z_2^*Z_1, & |Z_1|^2\end{pmatrix}\cdots, \tag{12.1}$$

$$\begin{pmatrix}\beta(\bar{1}\bar{1}), & \beta(\bar{1}\bar{2})\\ \beta(\bar{2}\bar{1}), & \beta(\bar{2}\bar{2})\end{pmatrix}=\frac{51}{450}(R_{2p}{}^{3d})^2\begin{pmatrix}|Z_1|^2, & Z_1^*Z_2\\ Z_2^*Z_1, & |Z_2|^2\end{pmatrix}+\frac{1}{9}(R_{2s}{}^{3p})^2\begin{pmatrix}|Z_2|^2, & Z_1^*Z_2\\ Z_2^*Z_1, & |Z_1|^2\end{pmatrix}, \tag{12.2}$$

where

$$Z_1=g+(g^2-x^2)^{1/2}+ix=A_1{}^{\bar{1}}+A_2{}^{\bar{1}}=(A_1{}^{\bar{2}}-A_2{}^{\bar{2}})^* \tag{12.3}$$

$$Z_2=g-(g^2-x^2)^{1/2}-ix=A_1{}^{\bar{2}}+A_2{}^{\bar{2}}=(A_1{}^{\bar{1}}-A_2{}^{\bar{1}})^*, \tag{12.4}$$

$$x=(\omega_2-\omega_1)/2, \qquad (n, j, m)=(3, 3/2, 1/2). \tag{12.5}$$

Using Z_1, Z_2 as defined by Eqs. (12.3), (12.4), (12.5) but with different values of g, γ, x we have for

$$(n, j, m)=(3, 1/2, 1/2), \tag{13.1}$$

$$\begin{pmatrix}\kappa(\bar{1}\bar{1}), & \kappa(\bar{1}\bar{2})\\ \kappa(\bar{2}\bar{1}), & \kappa(\bar{2}\bar{2})\end{pmatrix}=[4g^2(g^2-x^2)]^{-1}\begin{pmatrix}|Z_1|^2, & -Z_2Z_1^*\\ -Z_1Z_2^*, & |Z_2|^2\end{pmatrix}, \tag{13.2}$$

$$\begin{pmatrix}\beta(\bar{1}\bar{1}), & \beta(\bar{1}\bar{2})\\ \beta(\bar{2}\bar{1}), & \beta(\bar{2}\bar{2})\end{pmatrix}=\frac{1}{18}(R_{2s}{}^{3p})^2\begin{pmatrix}|Z_1|^2, & Z_1^*Z_2\\ Z_2^*Z_1, & |Z_2|^2\end{pmatrix}+\frac{1}{6}(R_{2p}{}^{3s})^2\begin{pmatrix}|Z_2|^2, & Z_1^*Z_2\\ Z_2^*Z_1, & |Z_1|^2\end{pmatrix}. \tag{13.3}$$

Substituting these values into Eq. (9) we obtain I_z the intensity of the fluorescence radiation polarized along the z axis which we suppose to be parallel to the electric vector of the incident radiation. Similarly one may calculate $I=I_x+I_y+I_z$ and hence I_x as $(I-I_z)/2$. For the degree of polarization $P=(I_z-I_x)/(I_z+I_x)$ we find

$$P=A/(B+C), \tag{14}$$

where

$$A=\{[(7/50)(R_{2p}{}^{3d})^2x^2+(1/6)(2\gamma^2+2\gamma g+x^2)(R_{2s}{}^{3p})^2]\gamma^{-1}(\gamma^2-g^2+x^2)^{-1}\}_{j=3/2}, \tag{14.1}$$

$$B=\{[(141/450)(R_{2p}{}^{3d})^2x^2+(5/18)(2\gamma^2+2\gamma g+x^2)(R_{2s}{}^{3p})^2]\gamma^{-1}(\gamma^2-g^2+x^2)^{-1}\}_{j=3/2}, \tag{14.2}$$

$$C=\{[(1/9)(2\gamma^2-2\gamma g+x^2)(R_{2s}{}^{3p})^2+(1/3)(R_{2p}{}^{3s})^2x^2]\gamma^{-1}(\gamma^2-g^2+x^2)^{-1}\}_{j=1/2}. \tag{14.3}$$

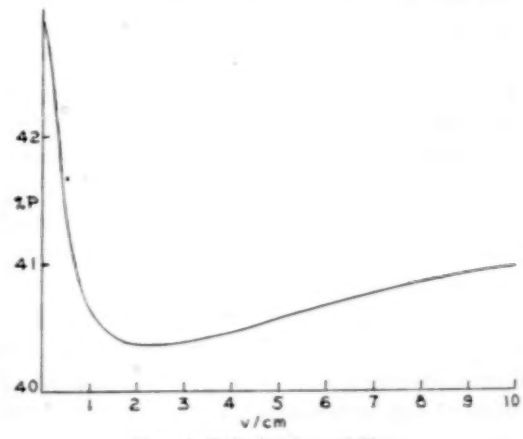

FIG. 2. Polarization of $H\alpha$.

As already mentioned, this result holds for $g<x$ as well as for $g>x$. The fact that the same analytic expression applies whether Eq. (11.3) gives different values of $\bar{\omega}$ or not is due to the continuity in the variation of the radiated spectrum with the electric field. The way in which P depends on the electric field is shown in Fig. 2.

It should be noted that in the geometrical arrangement to which Eq. (14) applies the $\kappa(\bar{b}\bar{b}')$ are diagonal with respect to m and that we have neglected the matrix elements between states with same m but different j. We are justified in doing so because the levels with different j are separated by appreciably more than the natural breadths. The values of the separations and half value widths are: $W(5/2)-W(3/2)=0.036$ cm^{-1}; $W(3/2)-W(1/2)=0.108$ cm^{-1}; $\gamma(5/2)/\pi=1/2\pi\tau(5/2)=0.00018$ cm^{-1}; $\gamma(3/2)/\pi=0.00068$ cm^{-1}; $\gamma(1/2)/\pi=0.00053$ cm^{-1}. The change in polarization with the field calculated here is thus due entirely to the radiation coupling between Stark effect levels with the same m and j.

The Specific Isotope Effect in the Hyperfine Spectrum of the Lead Atom

BERYL H. DICKINSON, *Ryerson Laboratory, University of Chicago*

(Received August 17, 1934)

A calculation by the method of Hughes and Eckart is performed for the specific isotope separation of Pb^{206} and Pb^{208} levels for terms arising from the $6p^2$, $6p7s$, $6p6d$, $6p7d$ and $6p8s$ configurations. The electron wave functions used are an ortho-normal set having the effective nuclear charge as parameter. From the perturbation calculation a double sum is obtained. Slater's method of sums is used to remove the degeneracy existing in the magnetic quantum number. The double sums for the various configurations of lead are found to contain a great number of terms which are common for all configurations and only a few terms which differ for the various configurations. These terms which are different for the various configurations are calculated and summed to obtain a "net specific isotope separation." It is found that an effective nuclear charge of only about 55 is necessary to make this net specific isotope separation equal to the observed isotope separation. A small variation from term to term of the same configuration requires that some other effect also be postulated. An upper limit argument for the specific isotope separation leads to a result of the order of thousands of wave numbers. This is shown to result from the vast number of terms in the double sum. It is not to be expected that this high upper limit for the separation would be approached by the actual separation. A set of wave functions which would be accurate enough to permit evaluating and subtracting the double sums does not seem obtainable.

1. Calculation of the Specific Isotope Separation Using Orthogonal Functions

THE effect of the motion of the nucleus upon the spectrum of an atom having more than one orbital electron has been discussed by Hughes and Eckart.[1] The results which they obtained for the two and three electron systems were in good numerical agreement with the measured values of isotope displacements in the Li I and Li II spectra. Recently Bartlett and Gibbons[2] calculated the isotope shifts for singlet and triplet levels in the Ne I spectrum. In this paper it is proposed to apply the method of Hughes and Eckart to the calculation of isotope displacements in the spectrum of the Pb-atom.

The kinetic energy operator for an atomic system of N electrons and one nucleus is given by Hughes and Eckart in the following form:

$$T=-\hbar^2\left\{\sum_{k=1}^{N}[\nabla_k/2\mu]+\sum_{(k,\,j)}[\nabla_k\cdot\nabla_j/M]+[\nabla^2/2(M+Nm)]\right\}, \quad (1)$$

in which

$$\nabla_k=\mathbf{i}\partial/\partial x_k+\mathbf{j}\partial/\partial y_k+\mathbf{k}\partial/\partial z_k,$$
$$\nabla=\mathbf{i}\partial/\partial X+\mathbf{j}\partial/\partial Y+\mathbf{k}\partial/\partial Z,$$

x_k, y_k, z_k = coordinates of the kth electron for which the origin is located at the moving nucleus,

X, Y, Z = coordinates of the center of mass of the atom in an arbitrary system with fixed origin,

m = electronic mass,

M = nuclear mass,

$\mu=mM/m+M$ = reduced electronic mass.

The third term in the bracket of Eq. (1) is the kinetic energy operator for the motion of the center of mass of the atom. Since this motion is of no significance in the calculation of isotope effects, the third term may be dropped from the bracket. The first and second terms of the bracket give rise respectively to the normal isotope effect and to the specific isotope effect. Hughes and Eckart have discussed the calculation of the normal isotope effect for any atom and have shown that it may be accomplished by multiplying the term values for a stationary nucleus by the fraction μ/m.

The second term in the bracket, which accounts for the specific isotope effect, may be used as a perturbing term for the calculation of the energy displacement. The degeneracy existing in the magnetic quantum number is not taken into account in the perturbation calculation. Instead the problem is solved assuming no degeneracy and the method of sums of Slater is used to remove the degeneracy existing in the

[1] D. S. Hughes and Carl Eckart, Phys. Rev. **36**, 694 (1930).

[2] J. H. Bartlett and J. J. Gibbons, Phys. Rev. **44**, 538 (1933).

magnetic quantum number. In the event that the unperturbed wave function has been normalized the result of such calculation is:

$$\Delta W = \sum_{(k,\,j)} \Delta W_{kj}, \tag{2}$$

where

$$\Delta W_{kj} = \int u^*(-\hbar^2 \nabla_k \cdot \nabla_j / M) u d\tau. \tag{3}$$

The form of the wave function which it is intended to use is the one given by Slater[3]:

$$u = (1/N!) det[\psi(n_1|x_1)\psi(n_2|x_2) \cdots \psi(n_N|x_N)], \tag{4}$$

$$\text{where} \quad \psi(n|x) = R(nl|r)\, Y(lm|\theta\phi)\Xi(s|\sigma). \tag{5}$$

It is assumed that the ψ's form an ortho-normal set and hence it may be shown that u, as defined above, is normalized and that[4]

$$\Delta W_{kj} = (-1/M)|\mathbf{P}(n_k; n_j)|^2, \tag{6}$$

where $\mathbf{P}(n_k; n_j)$ is the vector momentum matrix element associated with the transition from orbit n_k to orbit n_j. As is well known, it may be expressed in terms of the corresponding coordinate matrix element:

$$\mathbf{P}(n_k; n_j) = (im/\hbar)(W_k - W_j)\mathbf{X}(n_k; n_j). \tag{7}$$

By using the substitution of the coordinate elements and the wave functions in a spherically symmetric field it is possible to perform the integration for ΔW_{kj}. The summation over the spin functions results in a delta-function of the spin quantum numbers. The integral of the spherical harmonics is well known from the calculation of intensity for a simple rotator:

$$\beta(k; j) = (X^2 + Y^2 + Z^2)/[r(k; j)]^2, \tag{8}$$

where

$$\Delta l = +1 \begin{cases} \Delta m = +1 & |X|^2 = |Y|^2 = \dfrac{1}{4}\dfrac{(l+m+1)(l+m+2)}{(2l+1)(2l+3)}[r(k;j)]^2 \quad |Z|^2 = 0, \\ \Delta m = 0 & |Z|^2 = \dfrac{(l+m+1)(l-m+1)}{(2l+1)(2l+3)}[r(k;j)]^2 \quad |X|^2 = |Y|^2 = 0, \\ \Delta m = -1 & |X|^2 = |Y|^2 = \dfrac{1}{4}\dfrac{(l-m+1)(l-m+2)}{(2l+1)(2l+3)}[r(k;j)]^2 \quad |Z|^2 = 0. \end{cases} \tag{9}$$

The expressions for $\Delta l = -1$ may be obtained from the foregoing, and all others are zero. The quantity $r(k; j)$ in these expressions is the integral of the radial functions:

$$r(k; j) = \int_0^\infty R(n_k l_k|r) R(n_j l_j|r) r^3 dr. \tag{10}$$

The resulting expression for the specific isotope displacement is in terms of wave numbers:

$$\Delta\nu = \sum_{(k,\,j)} \{ -Rm Z^4 \cdot [n_j^2 - n_k^2]^2 \cdot \delta(s_k; s_j) \cdot \beta(k; j) \cdot [r(k; j)]^2 / 2Ma^2 n_k^4 n_j^4 \}. \tag{11}$$

The radial integrals contain a common factor a/Z, in which a is the radius of the first Bohr orbit and Z is the nuclear charge. This leaves $\Delta\nu$ in Eq. (11) dependent upon the square of the nuclear charge.

The degeneracy in the perturbation calculation, which has been ignored in obtaining Eq. (11) for the specific isotope displacement, may be removed by Slater's method of sums. The result of the calculation by the method of sums is to correlate $\Delta\nu$ for any spectroscopic term with $\Delta\nu$ for an electronic configuration. For the purpose of discussing the electron configurations numbers have been assigned to the electrons starting with the innermost. Electrons having a spin of $+\frac{1}{2}$ are allotted the odd numbers while electrons having a spin of $-\frac{1}{2}$ are allotted the even numbers. The serial numbers are assigned encyclopedically from the quantum numbers nlm, in the order of increasing n and l and decreasing m. For example, number 6 is $n=2$, $l=1$, $m=1$, $s=\frac{1}{2}$ while number 61 is $n=5$, $l=0$, $m=0$, $s=\frac{1}{2}$. The single number system of designation is much more compact than the four quantum number system for writing the complicated lead configurations.

[3] J. C. Slater, Phys. Rev. **34**, 1293 (1929).

[4] For evaluation of the perturbation matrix refer to C. Eckart, Rev. Mod. Phys. **2**, 375 (1930).

In the normal lead atom there are four electrons outside of the completed $5n$ shell. Two of these electrons are fixed in the $6s$ shell for all of the configurations considered, so that it is only the two outermost electrons (numbered from 81 up) which will differ in the various configurations. This leads to an important simplification in Eq. (11). The summation over all pairs of electrons k and j contains a great many terms which will be common for all configurations. It is only when k (and/or j) is numbered greater than 80 that a term will occur in the summation which will not be a common term for all configurations. The common terms give rise to an additive constant in the term-values which is of no significance since it cannot be observed, the frequencies being differences between two term-values.

With this simplification it is now possible to state the result of the calculation by the method of sums assuming that the coupling is Russell-Saunders. The specific isotope displacement for one Russell-Saunders term has the form:

$$\Delta\nu(6p^2\ {}^1D)=\Delta\nu(81, 82), \tag{12}$$

in which $\Delta\nu(81, 82)$ is the result of the summation of Eq. (11) using for k the electrons numbers 81 and 82 and for j all electrons numbers 1, 2, $\cdots$, 80, 81, 82. The other Russell-Saunders terms require similar summations:

$$\Delta\nu(6p^2\ {}^3P) =\Delta\nu(81, 83), \tag{13}$$

$$\Delta\nu(6p^2\ {}^1S) =\Delta\nu(81, 86)+\Delta\nu(83, 84)+\Delta\nu(85, 82)-\Delta\nu(85, 86)-\Delta\nu(82, 84), \tag{14}$$

$$\Delta\nu(6p7s\ {}^3P)=\Delta\nu(81, 97), \tag{15}$$

$$\Delta\nu(6p7s\ {}^1P)=\Delta\nu(81, 98)+\Delta\nu(82, 97)-\Delta\nu(81, 97), \tag{16}$$

$$\Delta\nu(6p6d\ {}^3F)=\Delta\nu(81, 87), \tag{17}$$

$$\Delta\nu(6p6d\ {}^3D)=\Delta\nu(81, 89)+\Delta\nu(83, 87)-\Delta\nu(81, 87), \tag{18}$$

$$\Delta\nu(6p7d\ {}^3F)=\Delta\nu(81, 105), \tag{19}$$

$$\Delta\nu(6p7d\ {}^3D)=\Delta\nu(81, 107)+\Delta\nu(83, 105)-\Delta\nu(81, 105), \tag{20}$$

$$\Delta\nu(6p8s\ {}^3P)=\Delta\nu(81, 115), \tag{21}$$

$$\Delta\nu(6p8s\ {}^1P)=\Delta\nu(81, 116)+\Delta\nu(82, 115)-\Delta\nu(81, 115). \tag{22}$$

In Table I the summation is performed for the cases in which k of Eq. (11) is one of the orbital electrons numbered greater than 80. Instead of calculating the summations for an isotope of mass M, the table is calculated in terms of the difference in $\Delta\nu$ for the Pb^{206} and Pb^{208} isotopes. These isotopes give rise to very strong lines in the hyperfine spectrum which are not complicated by the effect of nuclear spin. A simple calculation will show that the normal isotope separation of spectroscopic levels for the two will be insignificant. Since actual separations are observed for term levels in the hyperfine spectrum, it is desirable to compare the observed separations with the sums calculated from Eq. (11). The nuclear charge is left as an undetermined parameter in the calculations.

Most of the integrals $r(k; j)$ for this table were evaluated by Kupper.[5] However, two additional integrals are necessary to complete the table:

$$[r(6p; nd)]^2=\frac{2^{19}3^9n^9(n^2-1)(n^2-4)(n-6)^{2n-14}}{5\ 7\ (n+6)^{2n+14}}\{-475n^6+23{,}364n^4-353{,}808n^2+1{,}632{,}960\}^2, \tag{23}$$

$$[r(6p; ns)]^2=\frac{2^{15}3^7n^9(n-6)^{2n-14}}{5\ 7\ (n+6)^{2n+14}}\times\{-2761n^8+132{,}528n^6-2{,}057{,}184n^4+11{,}757{,}312n^2-19{,}595{,}520\}^2. \tag{24}$$

With the summations performed in this table it is possible to find the separations of the Pb^{206} and the Pb^{208} isotope levels in the lead spectrum. Such isotope separations have been measured by many experimenters[6-9] in connection with

[5] A. Kupper, Ann. d. Physik **86**, 511 (1928).
[6] H. Schuler and G. Jones, Zeits. f. Physik **75**, 565 (1932).
[7] H. Kopfermann, Zeits. f. Physik **75**, 363 (1932).
[8] J. Rose and L. Granath, Phys. Rev. **40**, 775 (1932).
[9] K. Murakawa, Scientific Papers (Tokyo), Nos.: 191, 245, 367, 372, 398.

TABLE I.

Orbitals k	j	$\beta(k;j)$	$[r(k;j)]^2$	$10^6(\Delta\nu^{208}-\Delta\nu^{206})/Z^2$
81	1	1/3	0.0241	10.54
	3	1/3	0.292	6.69
	11	1/3	1.856	5.97
	19	2/5		
	21	1/5	0.0757	.049
	23	1/15		
	29	1/3	11.98	6.67
	37	2/5		
	39	1/5	1.263	1.41
	41	1/15		
	61	1/3	49.2	3.41
	69	2/5		
	71	1/5	15.3	2.12
	73	1/15		
				Total = 37.30
83	1	1/3	0.0241	10.54
	3	1/3	0.292	6.69
	11	1/3	1.856	5.97
	21	1/5		
	23	4/15	0.0757	0.49
	25	1/5		
	29	1/3	11.98	6.67
	39	1/5		
	41	4/15	1.263	1.41
	43	1/5		
	61	1/3	49.2	3.41
	71	1/5		
	73	4/15	15.3	2.12
	75	1/5		
				Total = 37.30
87	5	2/5	0.438	12.06
	13	2/5	3.03	11.71
	31	2/5	19.3	12.90
	47	3/7		
	49	1/7	0.32	0.34
	51	1/35		
	63	2/5	231.	19.20
				Total = 56.21
89	5	1/5	0.438	12.06
	7	1/5		
	13	1/5	3.03	11.71
	15	1/5		
	31	1/5	19.3	12.90
	33	1/5		
	49	2/7		
	51	8/35	0.32	0.34
	53	3/35		
	63	1/5	231.	19.20
	65	1/5		
				Total = 56.21

Orbitals k	j	$\beta(k;j)$	$[r(k;g)]^2$	$10^6(\Delta\nu^{208}-\Delta\nu^{206})/Z^2$
97	5	1/3		
	7	1/3	0.01414	1.03
	9	1/3		
	13	1/3		
	15	1/3	0.1566	1.78
	17	1/3		
	31	1/3		
	33	1/3	1.38	3.36
	35	1/3		
	63	1/3		
	65	1/3	35.0	18.70
	67	1/3		
	81	1/3	1560.	39.30
				Total = 64.17
105	5	2/5	0.2416	7.10
	13	2/5	1.439	6.58
	31	2/5	6.68	6.60
	47	3/7		
	49	1/7	0.080	0.19
	51	1/35		
	63	2/5	35.8	7.80
	81	2/5	408.	12.34
				Total = 40.61
107	5	1/5	0.2416	7.10
	7	1/5		
	13	1/5	1.439	6.58
	15	1/5		
	31	1/5	6.68	6.60
	33	1/5		
	49	2/7		
	51	8/35	0.080	0.19
	53	3/35		
	63	1/5	35.8	7.80
	65	1/5		
	81	1/5	408.	6.17
				Total = 34.44
115	5	1/3		
	7	1/3	0.00886	0.68
	9	1/3		
	13	1/3		
	15	1/3	0.0887	1.12
	17	1/3		
	31	1/3		
	33	1/3	0.598	1.83
	35	1/3		
	63	1/3		
	65	1/3	4.13	3.43
	67	1/3		
	81	1/3	16.04	1.10
				Total = 8.16

TABLE II. *Isotopic separations in head.*

Pb term	Specific isotope separation	Net specific isotope separation	Observed isotope separation	Effective nuclear charge
$(6p^2\ ^1D)$	$74.60\ Z_1^2\ \text{cm}^{-1}$	$(74.60\ Z_1^2-101.47\ Z_4^2)$	$-0.088\ \text{cm}^{-1}$	54.4
$(6p^2\ ^3P)$	$74.60\ Z_2^2$	$(74.60\ Z_2^2-101.47\ Z_4^2)$	−0.85	54.6
$(6p^2\ ^1S)$	$74.60\ Z_3^2$	$(74.60\ Z_3^2-101.47\ Z_4^2)$	−.077	55.7
$(6p7s\ ^3P)$	$101.47\ Z_4^2$	0	.000	55[a]
$(6p7s\ ^1P)$	$101.47\ Z_5^2$	$(101.47\ Z_5^2-101.47\ Z_4^2)$	−.017	
$(6p6d\ ^3F)$	$93.51\ Z_6^2$	$(93.51\ Z_6^2-101.47\ Z_4^2)$	−.030	54.6
$(6p6d\ ^3D)$	$93.51\ Z_7^2$	$(93.51\ Z_7^2-101.47\ Z_4^2)$	−.033	54.3
$(6p7d\ F)$	$77.91\ Z_8^2$	$(77.91\ Z_8^2-101.47\ Z_4^2)$		
$(6p7d\ D)$	$59.40\ Z_9^2$	$(59.40\ Z_9^2-101.47\ Z_4^2)$	−.241	33.6
$(6p8s\ P)$	$45.46\ Z_{10}^2$	$(45.46\ Z_{10}^2-101.47\ Z_4^2)$	−.017	80.2
$(6p8s\ P)$	$45.46\ Z_{11}^2$	$(45.46\ Z_{11}^2-101.47\ Z_4^2)$		

[a] The value of Z_4 was chosen equal to 55 because this value makes the other Z's have an identical average value.

the hyperfine spectrum. Most of the results have been stated upon the assumption that the isotope separation for the $6p7s\ ^3P$ term is zero. This convention is observed in Table II, in the column headed "net specific isotope separation." The values for this column are obtained by subtraction of the calculated specific isotope separation for the $6p7s\ ^3P$ term from the calculated values for all other terms. The nuclear charge which has been left as an undetermined parameter is established in such a way as to give results for the specific isotope separations which agree with the measured values. This is accomplished by assigning to each spectroscopic term in Table II, a different nuclear charge. Upon subtracting the specific isotope separation of the $6p7s\ ^3P$ term from the specific isotope separation for all other terms the net specific isotope separation is obtained, which depends upon two values of the effective nuclear charge. If the observed isotope separations are set equal to these values of the net specific isotope separation, equations are obtained which may be plotted using the squares of the nuclear charges for ordinate and abscissa. These equations are plotted in the form of straight lines from which it is easy to show that the specific isotope separations of the terms arising from the $6p^2$ $6p7s$, $6p6d$, configurations may be calculated with remarkable accuracy by using for all Z's the value 55. Another way to handle this is to assign $Z_4=55$ for the $6p7s\ ^3P$ term and to calculate the other Z's. This is done in the last column of Table II. For the $6p7d$ and $6p8s$ configurations the terms require different values of Z.

From the last column in this table a number of important deductions may be drawn concerning the specific isotope effect. The values listed are those which Z must have to bring the calculation into numerical agreement with the observations. In the first place, all values of Z^2 come out positive, which means that the calculated separations and observed separations agree in direction. Secondly, all values of Z are less than the true value. This indicates that the effect under consideration is by no means negligible; if it were, the effective values of Z would come out very much greater than 82. Finally it is evident that the values of Z for all terms of the $6p^2$ configuration are nearly equal, as they are also for all terms arising from each of the other configurations with the exception of $6p7d$. This is probably due, at least in part, to the approximate nature of the calculation, which cannot account for the smaller variations of the separation from term to term. Nevertheless, because of this it seems necessary to postulate contributions from other causes for the separation.

For the terms arising from the $6p7d$ configuration a special condition holds. While the specific isotope separation of only one of the terms has been measured, the calculated values are quite different. The difference arises in the summation

of Eq. (11) in the term in which j is a $6p$ electron while k is a $7d$ electron. In this term the value of $\beta(k;j)$ depends upon the m-values, so that the two Russell-Saunders terms from this configuration lead to different results upon summing. This condition does not occur in the $6p6d$ configuration since $r(6p;6d)$ is zero. The condition is also not found for any configuration $6pns$ since in this case $\beta(6p;ns)$ is the same for any m-value.

2. An Upper Limit to the Specific Isotope Displacement

In the case that non-orthogonal wave functions involving different nuclear charges Z are to be used for the various orbitals the number of terms in the summation in Eq. (2) becomes very great. It is for this reason that the effective nuclear charge was considered the same for all electrons in the preceding section. However, a very interesting calculation for the maximum limit may be performed without making use of the assumption of orthogonality.

For this calculation let the wave equation of a complex atom be written:

$$(T_0+V)u=Wu, \tag{25}$$

where

$$T_0=(-\hbar^2/m)\sum_i \nabla_i^2, \tag{26}$$

$$V=\sum_i (Ne^2/r_i)+\sum_{(i,j)}(e^2/r_{ij}). \tag{27}$$

Now if θ is a real quantity:

$$\sum_i\sum_j \int (\nabla_i u^*+\theta\nabla_j u^*)(\nabla_i u+\theta\nabla_j u)d\tau\geq 0, \tag{28}$$

$$\sum_i\sum_j \int (\nabla_i u^*\cdot\nabla_i u+\theta\nabla_i u^*\cdot\nabla_j u+\theta\nabla_j u^*\cdot\nabla_i u +\theta^2\nabla_j u^*\cdot\nabla_j u)d\tau\geq 0. \tag{29}$$

This latter expression may be integrated by parts and the integral

$$\int \nabla^2(u^*u)d\tau$$

set equal to zero. In this way Eq. (29) may be written:

$$\sum_i\sum_j -\int (u^*\nabla_i^2 u+2\theta u^*\nabla_i\cdot\nabla_j u +\theta^2 u^*_j\nabla u)d\tau\geq 0. \tag{30}$$

Since the operator T_1 for the specific isotope effect is defined by:

$$T_1=(-\hbar^2/2M)\sum_i\sum_j \nabla_i\cdot\nabla_j, \tag{31}$$

then Eq. (30) becomes:

$$N\tau_0+2M\theta\tau_1/m+\theta^2 N\tau_0\geq 0, \tag{32}$$

in which τ_0 is the average value of T_0 while τ_1 is the average value of T_1. Hence the discriminant of Eq. (32) must be negative:

$$N^2\tau_0^2-M^2\tau_1^2/m^2\leq 0, \tag{33}$$

$$\tau_1\leq mN\tau_0/M. \tag{34}$$

From the theorem of the virial it may be shown that the wave-mechanical mean of the kinetic energy is equal to one-half the wave-mechanical mean of the potential energy taken with the reverse sign. This result is also true in the case that each electron is acted upon by a different field:[10]

$$2\int u^*T_0 u d\tau=-\int u^*Vud\tau. \tag{35}$$

This result makes it possible to express the mean values of potential and kinetic energy in terms of the total energy:

$$\int u^*T_0 u d\tau=-W\int u^*ud\tau, \tag{36}$$

$$\int u^*Vud\tau=2W\int u^*ud\tau. \tag{37}$$

So that

$$\tau\leq mN|W|/M. \tag{38}$$

However, since $|W|$ is the energy required to strip the atom of all electrons and is very great, the upper limit of τ_1 becomes very great. Using the K energy level for an approximate value of W leads to a separation for the energy levels of Pb^{206} and Pb^{208} isotopes of the order of thousands of wave numbers. However, this huge limit is not surprising. In the summations of Eq. (2)

[10] J. C. Slater, J. Chem. Phys. 1, 667 (1933).

there are $N(N-1)/2$ ΔW_{kj}'s of which only from one to five are not common for all configurations. If the common terms were also summed the calculated magnitude of the energy level separations would be greatly increased, but would have no effect in the separation of the spectrum lines. This fact that the line-separation is the small difference of two large numbers probably accounts for the variation of the calculated effect with the choice of wave function, noted by Bartlett and Gibbons, and also encountered in attempts to refine the present calculation. In any event it is not to be expected that the separation of the isotope levels would approach this high limit, since it is merely a limit and since it is so large in comparison with observed isotope separations.

The writer wishes to thank Professor Carl Eckart for suggesting the problem and discussing its solution many times with him.

OCTOBER 1, 1934 PHYSICAL REVIEW VOLUME 46

Application of the Dirac Vector Model to the d^4 Configuration

M. OSTROFSKY, *Department of Physics, University of Wisconsin*

(Received August 3, 1934)

Formulae for the energies of multiplets belonging to d^4 are computed by the use of the vector model as developed by Van Vleck and Serber. Since insufficient data were available for d^4, the configuration md^4ns was used to check the formulae against experiment. Even here the data are rather meager. In order to obtain out of the above configuration the proper energies of the multiplets arising from d^4 alone, it was necessary to subtract from it the exchange energy between the s electron and the d^4 "core." The agreement with experiment is, at best, only fair, perhaps because of perturbations from neighboring levels.

INTRODUCTION

THE first calculation of the energies of multiplets was made by Slater[1] in his well-known paper on complex spectra. However, the method of diagonal sums, which he employed, does not yield the separation of multiplets occurring more than once in a given configuration; it only gives their mean energy. Slater's work was extended by Condon, Shortley and Ufford.[2] The latter two developed a method for separating multiplets occurring more than once in a given configuration. Later the problem was attacked from a somewhat different point of view by Van Vleck[3] by means of Dirac's[4] vector model. The restriction to a single configuration made by Van Vleck was removed in a subsequent paper by Serber.[5] He was able to separate multiplets occurring more than once and thus checked the results obtained previously by Ufford and Shortley[2] on the separation of the two ^2D terms in d^3. In the present paper Serber's procedure will be applied to the d^4 configuration, which apparently has not been examined previously. His method does not include spin-orbit interaction and, therefore, only the centers of gravity of the multiplets in question are calculated here.

CALCULATION OF THE FORMULAE

To begin with, the method of diagonal sums was applied to all the multiplets in d^4. This gave only the mean energies of ^3F, ^3P, ^1G, ^1D and ^1S, each of which occurs twice in d^4. In order to separate them Serber's scheme was employed. By way of illustration, the energy matrix necessary for the separation of $^3P_+$ and $^3P_-$ is given here. Vanishing matrix elements, which occur when the interacting states differ in more than two non-identical electronic orbits, are omitted.

[1] J. C. Slater, Phys. Rev. **34**, 1293 (1929).
[2] E. U. Condon, Phys. Rev. **36**, 1121 (1930); E. U. Condon and H. G. Shortley, Phys. Rev. **37**, 1025 (1931); G. H. Shortley, Phys. Rev. **40**, 185 (1932); C. W. Ufford and G. H. Shortley, Phys. Rev. **42**, 167 (1932).
[3] J. H. Van Vleck, Phys. Rev. **45**, 405 (1934).
[4] P. A. M. Dirac, *The Principles of Quantum Mechanics*, Chapter XI.
[5] Robert Serber, Phys. Rev. **45**, 461 (1934).

The states involved are:

A: $\delta\pi\sigma-\delta$ (three states); D: $\sigma\sigma\delta-\pi$;
B: $\delta\delta-\pi-\delta$; E: $\pi\pi\sigma-\pi$;
C: $-\pi-\pi\delta\pi$;

with $L=M_L=1$; $S=1$. The energies of the two ^3P's are now given by

$$^3P_{\pm}=\tfrac{1}{2}a\pm\tfrac{1}{2}(2b-a^2)^{\frac{1}{2}} \qquad (1)$$

where a is simply twice the mean value of ^3P as obtained by the method of diagonal sums while b is given by the sum of the squares of the elements in the energy matrix minus the squares of the energies of all triplets having $L>1$. To complete the computation it is only necessary to substitute for the elements of the energy matrix in terms of Slater's F's; no G's are involved, since, for equivalent electrons, F's and G's of the same index are equal.

The formulae for the energies of the multiplets arising from d^4 are:

$$^1D = 6F_0-21F_2-189F_4$$
$$^3H = 6F_0-17F_2-69F_4$$
$$^1G = 6F_0-12F_2-94F_4$$
$$^3F_{\pm} = 6F_0-5F_2-76.5F_4 \pm\tfrac{1}{2}(612F_2^2+20025F_4^2-4860F_2F_4)^{\frac{1}{2}}$$

A			B	C	D	E
$H_1^{AA}-H_{13}^{AA}-H_{34}^{AA}$	$\sqrt{\tfrac{1}{3}}[-H_{12}^{AA}+H_{14}^{AA}-H_{23}^{AA}+H_{24}^{AA}]$	$\sqrt{\tfrac{1}{3}}[H_{12}^{AA}+H_{14}^{AA}-H_{23}^{AA}-H_{24}^{AA}]$	$-H_{23}^{BA}$	0	H_{13}^{DA}	H_{14}^{EA}
$\sqrt{\tfrac{1}{3}}[-H_{13}^{AA}+H_{14}^{AA}-H_{23}^{AA}+H_{24}^{AA}]$	$H_1^{AA}-H_{12}^{AA}+H_{34}^{AA}-\tfrac{1}{3}[H_{12}^{AA}+H_{14}^{AA}+H_{23}^{AA}+H_{24}^{AA}]$	$\tfrac{1}{3}[-H_{13}^{AA}+H_{14}^{AA}+H_{23}^{AA}-H_{24}^{AA}]$	$\sqrt{\tfrac{1}{3}}H_{23}^{BA}$	$\sqrt{2}H^{CA}{}_{(13)(24)}$	$\sqrt{2}[-\tfrac{1}{3}H_{13}^{DA}+H^{DA}{}_{(24)(13)}]$	$\sqrt{\tfrac{1}{3}}H_{14}^{BA}$
$\sqrt{\tfrac{1}{3}}[H_{13}^{AA}+H_{14}^{AA}-H_{23}^{AA}-H_{24}^{AA}]$	$\tfrac{1}{3}[-H_{12}^{AA}+H_{14}^{AA}+H_{23}^{AA}-H_{24}^{AA}]$	$H_1^{AA}+H_{12}^{AA}-H_{34}^{AA}-\tfrac{1}{3}[H_{13}^{AA}+H_{14}^{AA}+H_{23}^{AA}+H_{24}^{AA}]$	$\sqrt{2}[H_1^{BA}-\tfrac{1}{3}H_{23}^{BA}]$	0	$-\sqrt{\tfrac{1}{3}}H_{13}^{DA}$	$\sqrt{2}[H_1^{EA}-\tfrac{1}{3}H_{14}^{EA}]$
$-H_{23}^{BA}$	$\sqrt{\tfrac{1}{3}}H_{23}^{BA}$	$\sqrt{2}[H_1^{BA}-\tfrac{1}{3}H_{23}^{BA}]$	$H_1^{BB}-H_{34}^{BB}-\tfrac{1}{3}[H_{13}^{BB}+H_{14}^{BB}+H_{23}^{BB}+H_{24}^{BB}]$	$-\tfrac{1}{3}[H_{13}^{CB}+H_{23}^{CB}]$	$\tfrac{1}{3}[H^{DB}{}_{(13)(24)}+H^{DB}{}_{(23)(24)}]$	0
0	$\sqrt{2}H^{CA}{}_{(13)(24)}$	0	$-\tfrac{1}{3}[H_{13}^{CB}+H_{23}^{CB}]$	$H_1^{CC}-H_{34}^{CC}-\tfrac{1}{3}[H_{13}^{CC}+H_{14}^{CC}+H_{23}^{CC}+H_{24}^{CC}]$	$-\tfrac{1}{3}[H_{13}^{DC}+H_{23}^{DC}]$	$-\tfrac{1}{3}[H_{14}^{EC}+H_{24}^{EC}]$
H_{13}^{DA}	$\sqrt{2}[-\tfrac{1}{3}H_{13}^{DA}+H^{DA}{}_{(24)(13)}]$	$-\sqrt{\tfrac{1}{3}}H_{13}^{DA}$	$\tfrac{1}{3}[H^{DB}{}_{(13)(24)}+H^{DB}{}_{(23)(24)}]$	$-\tfrac{1}{3}[H_{13}^{DC}+H_{23}^{DC}]$	$H_1^{DD}-H_{34}^{DD}-\tfrac{1}{3}[H_{13}^{DD}+H_{14}^{DD}+H_{23}^{ED}+H_{24}^{DD}]$	$-\tfrac{1}{3}[H_{13}^{ED}+H_{23}^{ED}]$
H_{14}^{EA}	$\sqrt{\tfrac{1}{3}}H_{14}^{EA}$	$\sqrt{2}[H_1^{EA}-\tfrac{1}{3}H_{14}^{EA}]$	0	$-\tfrac{1}{3}[H_{14}^{EC}+H_{24}^{EC}]$	$-\tfrac{1}{3}[H_{13}^{ED}+H_{23}^{ED}]$	$H_1^{EE}-H_{34}^{EE}-\tfrac{1}{3}[H_{13}^{EE}+H_{14}^{EE}+H_{23}^{EE}+H_{24}^{EE}]$

In the above matrix $H^{AA}{}_{ij}$ denotes the usual type of exchange integral wherein electrons i and j are interchanged, whereas $H^{AB}{}_{ij}$ differs from the usual type of exchange integral in that the initial wave function refers to a state of the type A and the final wave function to B. In $H_{(12)(34)}$, etc., there are two exchanges. When all the electronic orbits in a given state are different, the complete matrices P_{ij}, tabulated on page 466 of Serber's paper, are needed to represent the state in the energy matrix. Such is the case with A. When, on the other hand, orbits 1 and 2 are identical, as in states B, C, D, E, then, in considering the interactions between any of the latter and A, it must be remembered that all the rows in P_{12} having characteristic values of -1 are not allowed; of course, the corresponding rows in all the other P matrices must be excluded also. Thus matrix elements of the type $H^{XA}{}_{ij}$, ($X=B$, C, D, E), are given by the third row of Serber's P matrices. Similarly, in considering interactions between any two states in which orbits 1 and 2 are identical, both rows and columns of P_{12} having characteristic values of -1 are excluded. Therefore, matrix elements of the type $H^{XY}{}_{ij}$, (X, Y, $=B$, C, D, E), are given by the element in the third row, third column of the P matrices. For more detailed discussion on this point see Serber's paper.[5]

TABLE I. *Energies of all the multiplets arising from the $3d^4$ configuration.*[6]

Terms	*Vanadium* Calc. $3d^4<4s>$ $F_2=779.5$ $F_4=69.3$	*Vanadium* $F_2=790$ $F_4=62$	Obs. V I $3d^4<4s>$	Obs. V II $3d^3$	*Chromium* Calc. $3d^4<4s>$ $F_2=1152$ $F_4=99$	Obs. Cr II $3d^4<4s>$	Obs. Cr III $3d^3$
^5D	0 cm^{-1}	0 cm^{-1}	0 cm^{-1}	0 cm^{-1}	0 cm^{-1}	0 cm^{-1}	
^3H	11435	10600	11435		16488	16494	
$^3F_-$	13101	12197	12166	13354	18913	17370	17441 cm^{-1}
$^3P_-$	13221	12088	11848	11500	18997		
^3G	13600	13000	13600	16240	19773	19780	19780
^3D	16630	16360			24372		
^1I	17152	15900			24732		
$^1G_-$	17514	16114			25213		
$^1S_-$	19001	17684			27405		
$^1D_-$	21545	20844			31280		
^1F	23647	23100			34587		
$^3P_+$	27317	27170			40141		
$^3F_+$	27437	27059			40225		
$^1G_+$	32723	31796			47785		
$^1D_+$	40821	41240			60114		
$^1S_+$	56369	55476			82629		

[6] All the experimental values were taken out of Bacher and Goudsmith's book on *Atomic Energy States.*

$$^3D \quad = 6F_0 - 5F_2 - 129F_4$$
$$^3P_\pm = 6F_0 - 5F_2 - 76.5F_4 \pm \tfrac{1}{2}(912F_2^2 + 38025F_4^2 - 9960F_2F_4)^{\frac{1}{2}}$$
$$^1I \quad = 6F_0 - 15F_2 - 9F_4$$
$$^1G_\pm = 6F_0 - 5F_2 - 6.5F_4 \pm \tfrac{1}{2}(708F_2^2 + 30825F_4^2 - 6420F_2F_4)^{\frac{1}{2}}$$
$$^1F \quad = 6F_0 - 84F_4$$
$$^1D_\pm = 6F_0 + 9F_2 - 76.5F_4 \pm \tfrac{1}{2}(1296F_2^2 + 30825F_4^2 - 10440F_2F_4)^{\frac{1}{2}}$$
$$^1S_\pm = 6F_0 + 10F_2 + 6F_4 \pm \tfrac{1}{2}(3088F_2^2 + 133200F_4^2 - 20640F_2F_4)^{\frac{1}{2}}.$$

COMPARISON WITH EXPERIMENT

Unfortunately there are very little experimental data with which to check the above computations. Obviously three multiplets are needed to determine the paremeters involved in the above equations. Only in the case of V II are there as many as four levels and even so, after the three parameters have been determined, there is but one level left to check. However, in his paper on the vector model Van Vleck[3] showed that, in case of a configuration of the form sa^k, the energy due to the addition of an s electron to the "core" a^k enters in a very simple manner, namely:

$$W = W(a^k) - \tfrac{1}{2}K_{as}\{k + 2[S(S+1) - S_k(S_k+1) - 3/4]\} + kJ_{as}, \quad (2)$$

where W is the energy of sa^k, $W(a^k)$ the energy of a^k alone, K_{as} is the exchange energy between the s electron and a^k "core," J_{as} the coulomb energy, S is the resultant spin and S_k the spin of the "core" a^k. It follows at once that the interval between two states $S = S_k \pm \frac{1}{2}$ originating from a given configuration L_k, S_k of a^k is:

$$h\Delta\nu = 2|K_{as}|(S_k + \tfrac{1}{2}). \quad (3)$$

Thus, if any two levels arising from such a configuration are known, it is possible, with the help of Eq. (3), to compute K_{as} and then, using Eq. (2), to determine the energy of any level arising from a^k alone. Once K_{as} has been determined, either one of any known pair of levels $S = S_k \pm \frac{1}{2}$ belonging to sa^k may be used to compute the energy of that particular multiplet, (belonging to a^k), from which this pair of levels originated. It is to be noted that the energies of the various multiplets computed in the above manner are obtained, except for an additive constant kJ_{as}, which, however, need not concern one here as one is interested only in the relative positions of the levels.

V I and Cr II have in their respective spectra levels belonging to the configuration $3d^44s$. In each case are found ^4D and ^6D, both arising from ^5D of d^4. The separation between ^4D and ^6D was hence used to determine K_{as} by means of (3). In accordance with the results of the previous paragraph, the energies of all the multiplets arising from $3d^4$ alone were computed and are given in Table I. In it, under the columns headed by $3d^4<4s>$, is to be understood a set of energy levels arising from $3d^4$ alone but computed from $3d^44s$. In order to obtain out of these energies those actually belonging to the multiplets of $3d^44s$, i.e., those which can be observed experimentally, it is, of course, necessary to reapply Eq. (2). The values of K_{ds} for V I and Cr II as obtained by the author are 1259 cm^{-1} and 1508.6 cm^{-1}, respectively.

In the above table the energy of ^5D is always taken as zero. There are two adjustable param-

eters F_2 and F_4 which are to be so selected as to fit the observed data as well as possible. The values of F_2 and F_4 used for the calculations in the first column were so chosen as to fit ^3H and ^3G of V I exactly. The fifth column is based on a corresponding choice for Cr II instead of V I. In the case of vanadium, $^3F_-$ and $^3P_-$ proved to be in the wrong order as compared with the observed values. However, this situation can be rectified by changing slightly the values of F_2 and F_4, as is evident from the second column of the table. The agreement for ^3H and ^3G is, of course, then to a certain extent impaired. The calculated positions of the terms not yet found experimentally should not be taken too literally, as the parameters cannot be fixed with any precision from the existing experimental data. Nevertheless it has seemed advisable to tabulate these computed positions since they at least show the general trend of the various states belonging to the configuration. Part of the inability to fit the few observed levels very accurately may be due to perturbations by other configurations. In particular, the actual value of ^3G for V II may be abnormally high because of perturbation by the known $3d^34s$ ^3G level at 14,573 cm^{-1}. It is hard, however, to see how the displacement due to this perturbation could amount to more than 800 cm^{-1}. In the case of Cr II, the position of $^3F_-$ may be abnormally low, as the ^4F term from which it is obtained is, no doubt, strongly perturbed by the d^5 ^4F level located about 1600 cm^{-1} above the former. There is no reason why the parameters F_2 and F_4 should have exactly the same values in V I and V II, or in Cr II and Cr III, as the addition of the $4s$ electron may influence the core d^4 to a slight extent. The experimental values for Cr II and Cr III are remarkably nearly equal.

The writer wishes to express his sincerest thanks to Dr. J. H. Van Vleck for suggesting this problem.

OCTOBER 1, 1934 PHYSICAL REVIEW VOLUME 46

Effect of Temperature and Pressure on the Mercury Afterglow

DAVID W. CARPENTER* AND WALTER M. NIELSEN, *Department of Physics, Duke University*

(Received July 17, 1934)

Measurements have been made on the rate of escape of resonance radiation from a slab of mercury vapor 4.0 cm thick. The measurements extended over a range of pressures from 0.133 to 0.720 mm of mercury and over a range of temperature from 390°K to 585°K. Calculations have also been made of the decay constants on the basis of Kenty's theory of radiation diffusion. The variations of the disagreement between the experimental results and Kenty's theory as affected by both pressure and temperature are hence made available. Some of the difficulties for present theories in the interpretation of the experimental results are pointed out.

INTRODUCTION

DURING the last few years several studies[1] have been made on the rate of escape of resonance radiation from a slab of mercury vapor after the initial excitation has been cut off. These experiments are in agreement in showing, that for low vapor pressures, the decay constant, β, of the exponential curve representing the decay of resonance radiation emitted by the mercury vapor, decreases as the mercury vapor pressure increases. As the mercury vapor pressure is further increased, the decay constant passes through a minimum value after which it slowly rises with increased vapor pressure.

The final interpretation of these results has not as yet been definitely fixed. In his earlier work Zemansky[2] interpreted his results on the basis of repeated atomic absorptions and reemissions; the increase in β at higher pressures

* Part of a dissertation presented for the degree of Doctor of Philosophy in the Graduate School of Arts and Sciences of Duke University.

[1] H. W. Webb, Phys. Rev. **24**, 113 (1924); L. J. Hayner, Phys. Rev. **26**, 364 (1925); H. W. Webb and H. A. Messenger, Phys. Rev. **33**, 319 (1929); H. W. Webb and H. A. Messenger, Phys. Rev. **40**, 466 (1932); E. W. Samson, Phys. Rev. **40**, 940 (1932).

[2] M. W. Zemansky, Phys. Rev. **29**, 513 (1927).

was thought to be connected with the quenching of excited states. Later Zemansky[3] re-interpreted his results on the basis of a metastable atom theory in which the radiation emitted from the cell after cut-off was regarded as being due to the raising of metastable 6^3P_0 atoms up to 6^3P_1 state. On this theory the decreasing values of β in regions of low vapor pressure was believed to be due to the reduction in the rate of diffusion of metastable atoms to the walls of the experimental tube; the increase at higher vapor pressures was thought to be due to the destruction of metastable atoms by being raised from the 6^3P_0 to the 6^3P_1 state.

Recently Kenty[4] has given an additional theory of such experiments in which he devises a means of calculating the equivalent opacity of a slab of mercury vapor to resonance radiation as affected by the Doppler broadening of the emission and absorption line, assuming the motions of both absorbing and emitting atoms to have a Maxwellian distribution. Such values of the equivalent absorption coefficient when used with Milne's theory of radiation diffusion lead to predicted values of the exponential decay constants. Zemansky[5] has calculated the decay constants to be expected in his experiment on the basis of Kenty's theory and finds agreement as to order of magnitude between theory and experiment particularly in the region of the lower opacities. Marked deviations were, however, noted at the higher vapor pressures and the suggestion was made that Holtsmark or other broadening might be responsible for such discrepancies between theory and experiment.

In view of the unsatisfactory state of the interpretation of such experiments it seems that there is need for further measurements extending over a wider range of pressures and temperatures than has heretofore appeared in the literature. It is the purpose of the present paper to report additional measurements of this kind. In view of the success of Kenty's theory for the lower opacities, already referred to, it seemed desirable to extend the comparison to the results herein reported. It is hoped that this procedure will give some indication as to the modification required in the present theories of the diffusion of resonance radiation through mercury vapor.

[3] M. W. Zemansky, Phys. Rev. **34**, 213 (1929).
[4] C. Kenty, Phys. Rev. **42**, 823 (1932).
[5] M. W. Zemansky, Phys. Rev. **42**, 843 (1932).

Experimental Arrangements and Procedure

The apparatus shown in Fig. 1 is essentially the same as that used by Zemansky.[2] A is a vertical type water-cooled and magnetically deflected Uviarc mercury lamp. The total radiation from this lamp passed through a horizontal slit S, and a quartz window of a furnace F_1 into a cylindrical resonance cell C. The cell (Fig. 4) was of clear fused quartz with circular plane face 5 cm in diameter, 4.0 cm deep and was mounted as shown in the furnace F_1. F_2 and F_3 were furnaces to control the temperature of other parts of the tube as shown. H is a quartz to Pyrex seal and M is a small iron ball that could be pulled up into the ground glass socket by means of an electromagnet. In this way the tube could be sealed off during a run and the vapor pressure of the mercury controlled. Furnace F_3 was always 20°C to 30°C above the temperature of F_2. The temperatures of F_1 and F_2 were controlled by the use of two mercury regulators

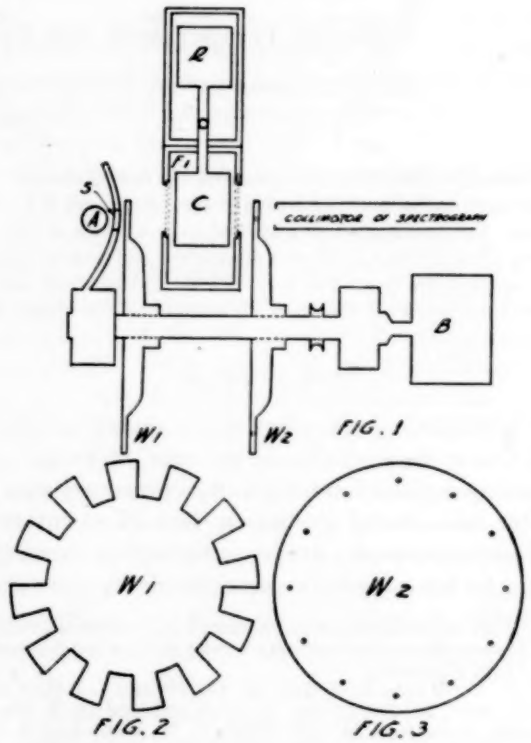

FIGS. 1, 2 AND 3. Experimental arrangements.

K_1 and K_2, which operated two relays. The temperatures of the furnaces were measured with copper-advance thermocouples. In furnace F_1 thermocouples were placed near the top and bottom of cell C. With the disk at rest no difference was noted in the reading of the temperatures at the various points. On rotation of the disks a difference in temperature was noticed between the sides of cell C. Such temperature differences between the sides were reduced by controlling additional heating elements placed on the sides of furnace F_1. In F_2 a thermocouple was placed at the point of condensation of the mercury in cell R.

The temperature of cell C did not vary during an exposure by more than ± 2°C and that of cell R was held constant to within ± 0.3°C. It required from $1\frac{1}{2}$ to 2 hours for the temperatures to become constant.

Between slit S and the furnace F_1 was a rotating disk 25 cm in diameter with 12 teeth (Fig. 2). This disk alternately transmitted the light and cut it off 12 times per revolution. Mounted on the same shaft as W_1 was a second disk of the same diameter (Fig. 3). This disk contained 12 holes 0.6 mm in diameter placed $\frac{3}{4}$ cm from the edge of the disk. The holes acted as a moving slit for the spectrograph.

B(Fig. 1) was a Model 44 Type A Weston magneto connected to the axle of the disk by gears and connected to a Weston Model 45 meter which had been calibrated by the manufacturer to read in revolutions per minute. The speed of the disk could be read to ± 10 r.p.m.

In order to measure the time after cut-off corresponding to any point on the photographic trace it is necessary to know the relationship between distances along the trace and such elapsed time. To obtain this relationship a small mirror was mounted at the center on the end of the axle of the disks. The mirror was mounted in such a way as to reflect a beam of light onto a galvanometer scale. A series of photographs were made of one of the illuminated holes for different positions along the slit of the spectrograph. The angle through which the disks had been rotated was calculated from the displacement of the reflected beam of light and the geometry of the apparatus. A template was made so that the photographic plate would be moved in such a way that the beam of light of the Moll microphotometer passed through the centers of each of the images at λ2537 of the above exposures. The photograph containing the exposures was run through the microphotometer and the distances between these exposures measured on the microphotometer photographic trace. A curve was plotted between distances on the microphotometer trace and angle of rotation of the disk. By the use of this curve the time after cut-off could be measured directly from the microphotometer trace of an exposure.

To show the relationship between light intensity and the blackening of the photographic plate, the characteristic curve of each photographic plate was plotted. This curve was determined experimentally by exposing the plate to the radiation from another mercury arc after it had passed through a Zeiss step filter calibrated for λ2537 by means of a photoelectric cell and a suitable amplifying system. In order to eliminate any possible error due to the intermittency effect, the density marks were photographed under the same condition as that of the afterglow. A third disk, on separate mounting, of the same diameter as W_2 and containing 12 slits each of 0.6 mm width was rotated in front of a narrow slit placed in the beam of light from a 220 volt Uviarc lamp. Cellophane was placed in the beam of light from this arc lamp so that the intensity falling on the photographic plate would be about the same as that of the afterglow. This disk was always rotated at the same speed as the disk W_2 and the exposure time was the same as that of the experiment, so that the intermittency effect in each case would be the same. Means were provided by which the spectrograph could be returned to the same position in front of the resonance cell for each photograph of the afterglow.

The tubes were baked out for several days at a temperature considerable higher than that to be used in the experiment. The pumps were always in operation while the furnaces were being heated up. After the desired temperature was reached the tube was sealed off from the vacuum system by raising the ball M (Fig. 4) into the socket L by means of the electromagnet.

The exposure time was one hour. During this time the temperatures were read every five

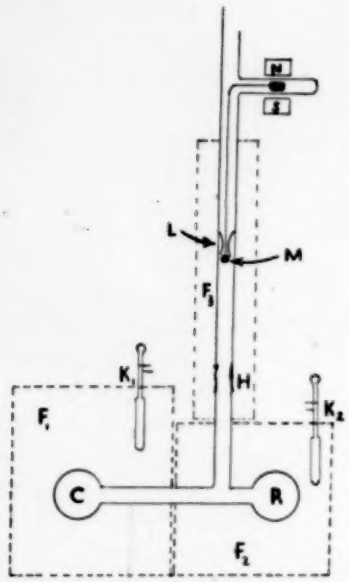

FIG. 4. Quartz cell and furnaces.

minutes and the speed of the disks held constant at 2800 r.p.m. Eastman 50 plates were used.

After the completion of the exposure the spectrograph was shifted in position to make an exposure with the step filter fastened in front of the slit of the spectrograph. This comparison exposure was also of one hour duration and the speed was 2800 r.p.m.

A reproduction of a typical spectrogram is shown in Fig. 5.

Fig. 6 and Fig. 7 are microphotometer traces of the afterglow and calibrating density marks, respectively.

The relative intensities of the radiation emitted by the mercury vapor at different times after the cut-off was obtained by measuring the photographic density at points 0.5 cm apart along each trace: each point representing a known interval of time after the cut-off. This time after cut-off was read from the curve plotted, as previously described, between distance along the microphotometer trace and the angle of rotation, since the angle of rotation is directly proportional to the time.

RESULTS AND CONCLUSIONS

Photographs were taken of the afterglow for various pressures and temperatures as shown in columns 1 and 2 of Table I. A microphotometer

FIG. 5. Photograph of density marks and afterglow.

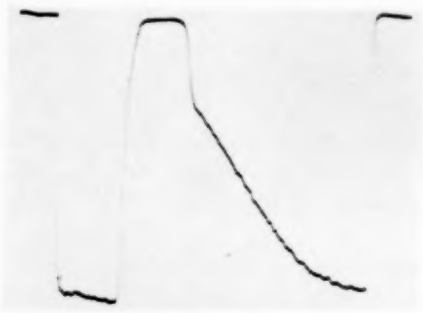

FIG. 6. Microphotometer trace of afterglow.

FIG. 7. Microphotometer trace of density marks.

trace was made of each photographic plate as previously described, and the intensity of the afterglow was measured at known intervals of time after cut-off. The curves plotted between the logarithm of the intensities and the time after cut-off gave a straight line. The fact that the first few points after cut-off fall in general below the curve may be due to the fact that certain terms, which enter into the law of decay, persist only for a short time after cut-off. The values of β, either for successive exposures or for exposures with several days intervening, checked within the limits of experimental error

TABLE I. *Experimental and calculated values of decay constant.*

1	2	3	4	5	6	7	8	9
Press. (mm) Hg.*	T (°K)	$N\times10^{-18}$	$\frac{NL}{\Delta\nu_D}\times10^{-7}$	k_0L	$\bar{k}L$	β Theor.	β Exp.	Diff. (Exp. and Theor.)
.133	393	4.34	1.47	1955	112.5	1840	3820	1980
.133	413	4.13	1.36	1809	108.0	1990	4160	2170
.133	435	3.92	1.26	1676	103.0	2200	4460	2260
.133	483	3.53	1.08	1436	94.5	2580	5220	2640
.133	543	3.14	.90	1197	85.0	3240	6390	3150
.133	586	2.91	.81	1077	80.0	3660	7070	3410
.151	393	4.94	1.70	2260	121.5	1570	3170	1600
.151	434	4.48	1.44	1915	111.0	1890	3460	1570
.151	490	3.97	1.20	1596	100.0	2330	3880	1550
.151	529	3.67	1.07	1423	94.0	2640	4220	1580
.151	578	3.36	.94	1250	87.5	3050	5100	2050
.165	393	5.43	1.83	2434	126.5	1450	2900	1450
.165	438	4.87	1.56	2074	116.0	1730	2990	1260
.165	484	4.41	1.34	1782	106.5	2050	3170	1120
.165	531	4.02	1.17	1556	98.5	2410	3280	870
.165	582	3.67	1.02	1357	91.5	2790	3730	940
.238	388	8.09	2.75	3658	158.0	927	2380	1453
.238	435	7.21	2.32	3086	144.0	1120	2400	1280
.238	484	6.48	1.97	2620	132.0	1330	2460	1130
.238	538	5.83	1.68	2234	121.0	1590	2460	870
.238	583	5.39	1.50	1995	116.5	1710	2690	980
.279	398	9.31	3.13	4163	168.0	820	2290	1470
.279	454	8.16	2.57	3418	152.5	990	2290	1300
.279	504	7.35	2.19	2913	139.5	1190	2270	1080
.279	538	6.89	1.99	2646	132.5	1320	2230	910
.279	585	6.34	1.76	2341	128.0	1420	2400	980
.312	396	10.5	3.54	4708	180.0	714	2140	1426
.312	455	9.16	2.88	3830	162.0	881	2110	1229
.312	503	8.28	2.47	3285	149.0	1040	2140	1100
.312	543	7.67	2.21	2939	140.0	1180	2140	960
.312	581	7.17	1.99	2647	132.5	1320	2320	1000
.429	415	14.0	4.61	6131	207.5	535	2550	2015
.429	456	12.7	3.99	5307	192.0	626	2520	1894
.429	504	11.5	3.43	4562	177.0	737	2580	1843
.429	543	10.7	3.08	4096	167.5	873	2520	1647
.429	581	10.0	2.80	3724	160.0	904	2610	1706
.720	422	23.8	7.76	10320			3250	
.720	452	22.0	6.93	9217			3280	
.720	507	19.9	5.93	7887	239.5	401	3220	2819
.720	549	18.3	5.23	6956	223.0	463	3220	2757
.720	585	17.2	4.77	6344	211.0	518	3250	2732

* International Critical Tables, Vol. III, p. 206.

of 5 percent. The decay constant, β, is given by the slope of this curve and a typical curve for determining β is shown in Fig. 8. The experimental values of β determined by the above method are shown in column 8 of Table I. When these values of β, at constant temperature, are plotted against vapor pressure the resulting curves are similar to those obtained by Zemansky.[2]

It is of interest to compare these experimental values of β with those to be expected when the values of the equivalent absorption coefficient of mercury vapor to resonance radiation, as calculated on the basis of Kenty's theory, are used in Milne's[6] theory of radiation diffusion. It has been shown by Milne[6] that

$$\beta=(1/\tau)/[1+(\bar{k}L/\lambda_1)^2], \qquad (1)$$

[6] E. A. Milne, J. Lond. Math. Soc. **1**, 1 (1926).

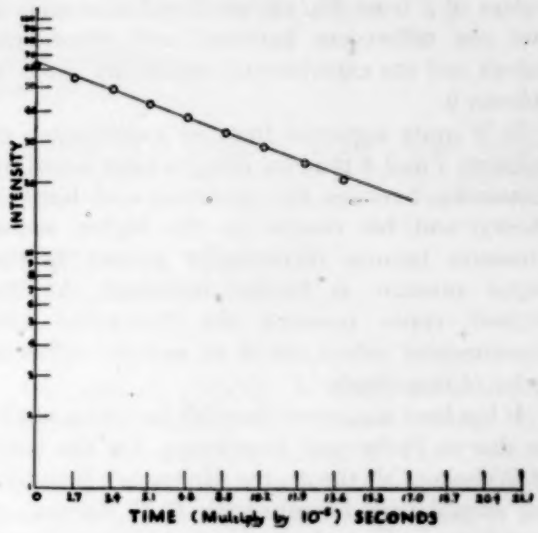

FIG. 8. Curve showing logarithm of intensity of afterglow as a function of time in seconds after cut-off.

where τ is the lifetime of the excited state, $\bar{k}$ is the equivalent absorption coefficient, L is the thickness of the slab of mercury and λ_1 is the first root of the equation

$$\tan y=\bar{k}L/y. \qquad (2)$$

Zemansky[5] has calculated values of the equivalent absorption coefficient on the basis of Kenty's theory for various values of k_0L where k_0 is the absorption coefficient for the center of the line. In the calculations[7] it is necessary to compute the Doppler breadth of the radiation from the equation

$$\Delta\nu_D=5.97\times10^7T^{\frac{1}{2}}. \qquad (3)$$

Values of k_0L were then obtained from the equation[8]

$$k_0L=1.33\times10^{-4}NL/\Delta\nu_D, \qquad (4)$$

where N is the number of molecules per cc.

Values of k_0L obtained in this way are shown in column 5 of Table I. Corresponding values of $\bar{k}L$ were obtained[9] from a plot of Kenty's equivalent opacity as a function of k_0L and are listed in column 6 of Fig. 1. The theoretical

[7] For further details see Mitchell and Zemansky, *Resonance Radiation and Excited Atoms.*

[8] Reference 7, pp. 100 Eq. (35) or Eq. (3) of a paper by M. W. Zemansky, Phys. Rev. **36**, 219 (1930). The numerical coefficient in the latter case is different from that in Eq. (3) and reference 7 due to the use of a probably less accurate value of τ.

[9] See reference 7, pp. 331.

values of β from Eq. (1) are listed in column 7 and the differences between such theoretical values and the experimental results are listed in column 9.

It is quite apparent from an examination of columns 7 and 8 that the disagreement noted by Zemansky between the predictions of Kenty's theory and his results at the higher vapor pressures become increasingly greater as the vapor pressure is further increased. At the highest vapor pressure the theoretical and experimental values are of an entirely different order of magnitude.

It has been suggested that this deviation might be due to Holtsmark broadening. On the basis of Weisskopf's[10] theory the Holtsmark broadening should vary linearly with P/T. Because of such increased broadening at the higher pressures one would expect $\bar{k}L$ to have larger values than are calculated on the basis of Kenty's theory so that β should increase with pressure. On the other hand one might expect that due to Holtsmark broadening alone β should decrease with increasing temperature at constant pressure due to the lowering of the density to maintain constant pressure. This may be the reason for the fact that the experimental value of β decreases with increasing temperatures for pressures of 0.151 mm and above. In this same region of pressure (0.151 mm–0.312 mm) the value of β at a given temperature decreases with increase in pressure, a result difficult to reconcile with the expected effect of Holtsmark broadening. The observations at higher pressure (0.429 mm and 0.720 mm) on the other hand do show a decrease with increase in pressure for the same temperature.

The results obtained at the lowest pressure, namely, an increase in β with rise in temperature is in marked contrast with the results obtained at higher pressures. Heretofore experiments of this kind on pure mercury vapor have been conducted in such a manner that in the main the pressure only has been varied. When attempts[4] have in the past been made to explain the results of such experiments on the basis of Kenty's theory it has been assumed that differences corresponding to column 9 Table I may be due to the presence of Holtsmark or other broadening. The results of the lowest pressure are of such a nature that it is extremely difficult on present theories to understand how such broadening can be alone responsible for these discrepancies.

In Zemansky's earlier theory and later in the work of Kenty,[4] the suggestion has been made that the rise in the value of β beyond the minimum in $\beta-P$ curves may be due to quenching of the excited state. Inasmuch as the number of collisions at constant pressure varies as $T^{-\frac{1}{2}}$ it is difficult to associate the marked increase of β with temperature at the lowest pressure (and for the highest temperature for some of the other pressures) with quenching unless the efficiency of this process is a markedly increasing function of temperature.

No doubt the phenomena are complex and the present experiments indicate additional difficulties for present theories. The complete explanation must await a detailed calculation of the effect of Holtsmark broadening on the equivalent absorption coefficient. There is of course the possibility that the results at the lower pressure may finally be accounted for by a combination of Kenty's theory and Zemansky's metastable atom theory. We hope soon to undertake similar observations as herein reported with the same and a thinner resonance cell over the region of lower vapor pressures.

[10] V. Weisskopf, Phys. Zeits. **34**, 1 (1933).

Nuclear Energy Levels and the Model of a Potential Hole

HENRY MARGENAU, *Yale University*

(Received August 7, 1934)

Part I contains the solution of the problem of a particle for which the potential energy $V(r)$ is a simple rectangular hole of finite depth, such a model being of interest in connection with the spacing of nuclear energy levels. Formulae are given by which a numerical determination of energies can be carried out for any assumed depth of the hole. In part II the results are extended to finite holes of different shape, and an argument is presented which proves the inadequacy of any such model to explain the arrangement of α-ray levels in Ra C′.

TO correlate the empirical data concerning atomic nuclei with the theoretical properties of assumed nuclear models becomes a problem of increasing importance as the amount of experimental material grows. The present note is devoted to one aspect of this problem which permits a clear solution, insofar as it establishes the impossibility of accounting for the observed positions of α-particle energies by means of simple hypotheses regarding the nuclear potential, which are so fruitful in explaining α-ray decay.

Rutherford and his collaborators[1] have determined the positions of the nuclear levels in Ra C′ with a precision which permits an application of analysis. Gamow[2] was the first to attempt an explanation of their arrangement on the basis of a nuclear model consisting of an infinitely deep potential hole within which the α-particle moves. His analysis is intended to be only qualitative but shows at first sight some promising features.

There are two respects in which the model used by Gamow may be refined: (1) the hole should be taken of finite depth, (2) its walls should not be vertical. In the first part of this note we shall incorporate into the theory the first refinement and work out the arrangement of the energy levels of a particle for which the potential energy $V(r)$ is a simple rectangular hole of finite depth (a problem which has perhaps some mathematical interest independently of its connection with nuclear theory). In the second part we shall consider the other refinement and discuss the conclusions regarding nuclear levels to which this theory leads.

[1] Rutherford, Proc. Roy. Soc. **A131**, 684 (1931). Rutherford, Lewis and Bowden, Proc. Roy. Soc. **A142**, 347 (1933).

[2] Gamow, Nature **131**, 433 (1933); Cf. also Solvay Congress (1933).

I

Our present problem is simply to solve the Schrödinger equation for a potential energy $V(r)$ given by the solid line in Fig. 1. The Coulomb potential outside of this hole, while producing an appreciable width of the energy levels, is not essential in determining their positions and need not be considered in this connection.

Let us first recall the position of the levels inside a hole of *infinite* depth. If we reckon the energy W of the particle from the bottom of the hole and define $k^2 \equiv 8\pi^2 MW/h^2$, M being the reduced mass of particle and nucleus, then the solution of Schrödinger's equation, multiplied by r, is

$$P(r) = cr^{\frac{1}{2}} J_{l+\frac{1}{2}}(kr),$$

and k must be determined in such a way that

$$J_{l+\frac{1}{2}}(kr_0) = 0, \qquad (1)$$

where r_0 is the radius of the hole. In this expression, l is the usual azimuthal quantum number.

Thus is produced an infinite set of levels, the position of which depends on the values of M and r_0. In Table I we list the first few values of

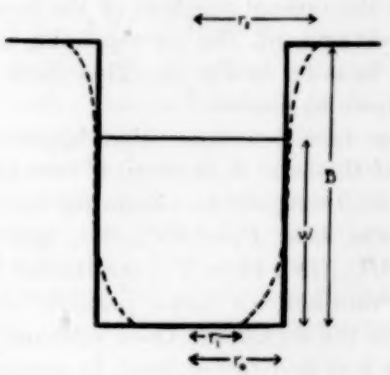

FIG. 1.

TABLE I. *Values of* Wr_0^2.

l	$Wr_0^2 \cdot 10^{19}$			
0	5.081 (1)	20.32 (4)	45.73 (10)	81.29 (17)
1	10.39 (2)	30.72 (6)	61.21 (13)	101.74
2	17.10 (3)	42.58 (8)	78.18 (16)	
3	25.15 (5)	55.85 (11)	96.59	
4	34.45 (7)	70.54 (15)	116.44	
5	45.2 (9)			
6	57.0 (12)			

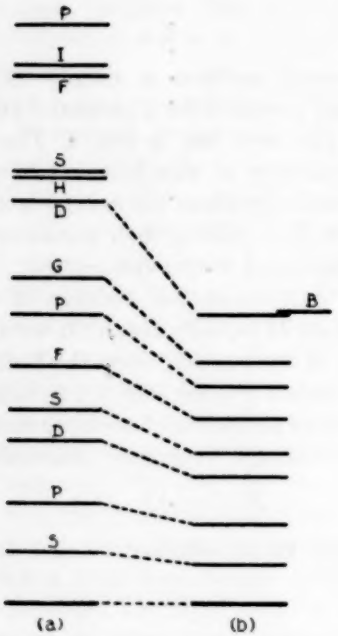

FIG. 2. (a) Arrangement of levels in an infinitely deep hole with spectroscopic designation of l-values. (b) Arrangement of levels in a hole of depth B.

$W \cdot r_0^2$, in electron-volts $\times$ cm^2, taking for M the mass of an alpha-particle. The parentheses contain the ordinal numbers of the levels from the lowest upward. The corresponding levels are plotted in order in Fig. 2a. They have already been drawn by Gamow.[2]

Let us now determine what happens if the depth of the hole, B, is *finite*. If then we define $\kappa^2 \equiv 8\pi^2 M(B-W)/h^2$, we obtain for the solution inside the hole $P_i = c_1 r^{\frac{1}{2}} J_{l+\frac{1}{2}}(kr)$, and outside $P_0 = c_2 r^{\frac{1}{2}} H_{l+\frac{1}{2}}(i\kappa r)$. Here H is the Hankel function which vanishes for large positive imaginary values of the argument. These solutions, as well as their first derivatives, must be continuous at r_0, a circumstance which leads to the relation

$$\frac{J_{l+\frac{1}{2}}(kr_0)}{J_{l-\frac{1}{2}}(kr_0)} = \frac{H_{l+\frac{1}{2}}(i\kappa r_0)}{H_{l-\frac{1}{2}}(i\kappa r_0)}. \tag{2}$$

This equation is to be used for determining k.

The right hand side of (2), for which we shall write $R_l(\kappa r_0)$, can be expanded as a quotient of finite sums. Thus one finds

$$\begin{aligned}
-R_0(x) &= 1+x^{-1}, \\
-R_1(x) &= 1+3x^{-1}+3x^{-2}, \\
-R_2(x) &= \frac{1+6x^{-1}+15x^{-2}+15x^{-3}}{1+x^{-1}}, \\
-R_3(x) &= \frac{1+10x^{-1}+45x^{-2}+105x^{-3}+105x^{-4}}{1+3x^{-1}+3x^{-2}}, \\
-R_4(x) &= \frac{1+15x^{-1}+105x^{-2}+420x^{-3}+945x^{-4}+945x^{-5}}{1+6x^{-1}+15x^{-2}+15x^{-3}}.
\end{aligned} \tag{3}$$

If the barrier is infinitely high, then according to (3) $\kappa \to \infty$, and every $R(\kappa r_0)$ takes on the value -1. In that case, Eq. (2) states: $J_{l+\frac{1}{2}} + J_{l-\frac{1}{2}} = 0$. But this is identical with $J_{l+\frac{1}{2}}(kr_0) = 0$. Thus we have arrived at condition (1).

Let us now put $kr_0 = (8\pi^2 MW/h^2)^{\frac{1}{2}} r_0 \equiv x$, $(8\pi^2 BM/h^2)^{\frac{1}{2}} r_0 \equiv b$, so that (2) finally takes the form

$$J_{l+\frac{1}{2}}(x)/J_{l-\frac{1}{2}}(x) = R_l(b^2-x^2)^{\frac{1}{2}}. \tag{4}$$

The solutions x of this equation determine the permissible W's. They can be obtained with little labor by plotting the R's (cf. (3)) as well as the ratios of the Bessel functions. The energies, in electron-volts, are then given by

$$5.148 \times 10^{-20} x^2 / r_0^2.$$

It is easily seen that the finite height of the barrier depresses all the levels of Table I, as might be expected. One can find the maximum depression of any given level by the following consideration.

For the highest level, i.e., the one most strongly depressed, x will be but slightly smaller than b. The depression is a maximum when $b = x$. In this case the right hand side of (4) is $R_l(0)$, which tends toward $-\infty$ for every l. Hence this relation is satisfied when $J_{l-\frac{1}{2}}(x) = 0$. Now the root of $J_{l-\frac{1}{2}}$ determines the energy in an infinitely deep hole, but of a level with an l-value smaller

by 1 than that under consideration. Therefore the maximum displacement of a level is from its value in Table I to the value immediately above it in the same column of the table. By virtue of this fact one can circumvent actual calculations when a mere estimate of the effect of finite depth upon the "normal" position of the energy levels is desired, since it permits a determination of the quantum number of the *highest* energy state as well as its approximate position. To show the effect of finite depth of the hole upon the "normal" arrangement of the levels (Fig. 2a) we have calculated graphically the roots of 4, taking for B a value which will produce a maximum depression of the levels assumed by Gamow[3] for Ra C′. The results are plotted in Fig. 2b. All levels above B merge into a continuum. Comparison with Gamow's postulated level scheme shows that, to be sure, the finite depth produces the desired compression, but there is no strong crowding of the upper levels as in Gamow's diagram. This example is now merely hypothetical, however, since Gamow's assignment has been superseded by the recent determination of the levels due to Rutherford, Lewis and Bowden.

II

The considerations of part I will be helpful as we turn to the next question: what precise form of the potential walls will give the arrangement of levels required experimentally? This can of course only be found by trying various potential energy curves, such as the dotted one in Fig. 1, with the known levels in a finite rectangular hole serving as a guide. Given the dotted curve, one can simply start with the eigenvalue and eigenfunction calculated in part I, integrate the latter numerically from r_1 to r_0 and from r_2 to r_0, and see what change in the eigenvalue is necessary to make the solutions join. In doing this one is readily convinced that *very implausible* potential energy curves are required to produce the spacing of the levels proposed either by Gamow or by Rutherford, Lewis and Bowden. The major discrepancy which one encounters appears plainly from the following argument.

Suppose the energy difference between the lowest and, say, the nth level to be known. We can then, by choosing r_0 properly, construct a finite rectangular hole which will produce this energy difference. To obtain the minimum value of r_0 compatible with the given energy difference we will agree to place the barrier height B just above the position of the nth level. It is then at once evident (and may be shown rigorously) that, if the true potential hole differs at all from the assumed rectangular hole but still produces the same energy difference between the lowest and the nth level, its radius must be smaller than r_0 near the bottom and greater than r_0 near the top. Hence, if r is the radius of the actual hole near the top, $r > r_0$.

Let us now consider Gamow's level scheme. It assigns to the energy difference between the lowest and the 8th level the value 17.8×10^6 e. v. According to Table I this difference is $37.5\times10^{-19}\times r_0^{-2}$ e. v. if the hole is infinitely deep, $25.64\times10^{-19}r_0^{-2}$ e. v. if the hole has its minimum possible depth. In the first case, $r_0=1.45\times10^{-12}$ cm, in the second, $r_0=1.2\times10^{-12}$. Hence we are led to suppose that, even with the most favorable choice of B,

$$r > 1.2\times10^{-12} \text{ cm}.$$

This is hopelessly irreconcilable with the value[4] 8.2×10^{-13} cm $< r < 8.6\times10^{-13}$ cm which is required to obtain the correct decay constant for Ra C′.

The situation is no less unsatisfactory if we assume the assignment of levels given by Rutherford, Lewis and Bowden. Here the difference between the lowest and the 16th level is 27×10^6 e. v. This, according to Table I, is at least $61.2\times10^{-19}r_0^{-2}$ e.v. Thus $r_0\sim1.5\times10^{-12}$ cm, and

$$r > 1.5\times10^{-12} \text{ cm}.$$

In view of these considerations we must regard the model of a potential hole as inadequate to explain the distribution of α-particle energies within nuclei. The α-particle can not be said to move essentially in a potential field due to the other nuclear constituents; its potential appears to depend strongly on its own state of motion, in such a manner that, if the α-particle changes its energy, the entire nuclear configuration is altered.

[3] Gamow, Nature **131**, 433 (1933).

[4] Cf. Mott, Handb. d. Physik **XXIV**, 1, p. 807.

The Ionization Potentials of Formaldehyde and Halogen Derivatives of Methane

T. N. JEWITT, *Laboratory of Physical Chemistry, Cambridge, and Imperial Chemical Industries, Limited*

(Received July 9, 1934)

The ionization potentials of CH_2O, CH_3Cl, CH_3Br, CH_3I were measured by a molecular ray method, and found to be 11.3, 10.7, 10.0, and 9.1 volts, respectively.

IN the course of experiments following the lines of the program laid down by Fraser[1] on the application of molecular ray methods to the study of chemical reactions, an apparatus was built which lent itself to the rapid and easy measurement of the ionization potentials of a number of organic molecules.

The molecules investigated were HCHO, CH_3Cl, CH_3Br and CH_3I. These were chosen because the analysis of their spectra is comparatively far advanced, and a determination of their first ionization potentials would furnish an independent value of the electronic series limits.

The principle of the method is as follows: When a beam of molecules is allowed to enter the space between cathode and anode of a diode, ionization begins when the filament-anode voltage is greater than the ionization potential. If now the emission is controlled by space-charge conditions, the positive ions partially neutralize the negative space-charge of the electrons, and the emission increases. Further, if the anode is made a closed cylinder the efficiency of the positive ions in neutralizing space-charge is greatly increased, since the life of the ions in the neighborhood of the cathode is lengthened.[2]

Since the actual increase in emission is of the order of a thousandth of the emission current itself, a bridge-balanced circuit was used. A second similar closed-anode diode, into which the beam did not enter, was placed in the arm of the bridge adjacent to that containing the ionizing "Kingdon cage". With this arrangement the increase of emission current on entry of the beam is read directly as a galvanometer deflection. The use of the second diode also eliminates disturbances due to stray pressure fluctuations.[3] The extrapolation of the deflection *vs.* anode voltage curve to zero deflection gives the value of the ionization potential.

The apparatus and circuit (see Fig. 1, which is self-explanatory) were, except for a few minor improvements, the same as those used by Estermann and Stern[4] in their application of the Kingdon principle as a general method for detecting molecular beams.

The correct voltage scales were obtained by calibration with mercury, with the spectroscopic value (10.4 volts) of its ionization potential. The results are shown in Figs. 2 and 3 and in Table I.

TABLE I. *Ionization potentials.*

Substance	V_i(volts)	cm^{-1}
H·CHO	11.3±0.5	91,600
CH_3Cl	10.7±0.3	86,700
CH_3Br	10.0±0.25	81,100
CH_3I	9.1±0.25	73,800

There is of course a finite concentration of dissociation products in the cage due to decomposition at the hot filament. The corresponding stationary pressure is however certainly less than 5 percent of that of the undissociated molecules, the ratio of the stationary pressures of each dissociated product (p') and of the undissociated

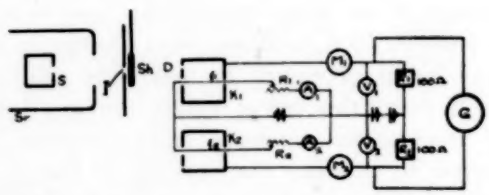

FIG. 1. Diagram of apparatus and electrical connections. *S*, Source; *I*, image aperture; *D*, entrance for beam; *Sh*, shutter; *Sr*, cooled screen; f_1, f_2, filaments; K_1, K_2, closed anodes; A_1, A_2, ammeters; M_1, M_2, milliammeters; V_1, V_2, anode voltmeters; *G*, galvanometer, $S_i = 100$.

[1] R. G. J. Fraser, Faraday Soc. Trans. **30**, 182 (1934).
[2] Kingdon, Phys. Rev. **21**, 408 (1923).
[3] Cf. Knauer and Stern, Zeits. f. Physik **53**, 766 (1929).
[4] Estermann and Stern, Zeits. f. Physik **85**, 135 (1933).

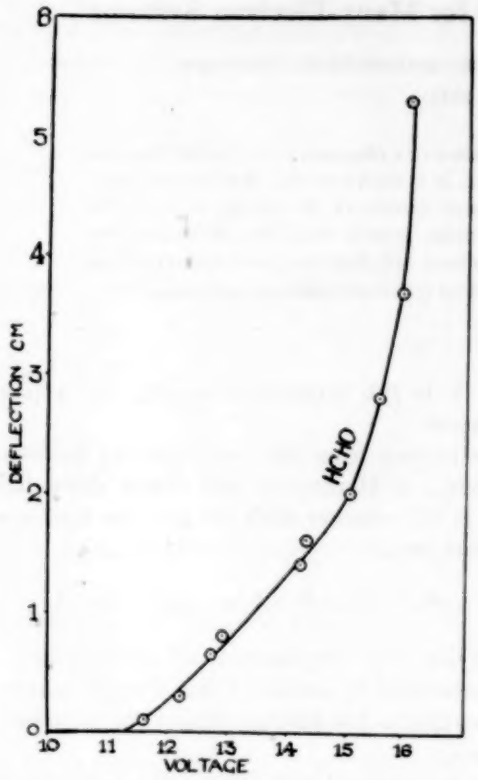

FIG. 2. Curve showing ionization potential of formaldehyde.

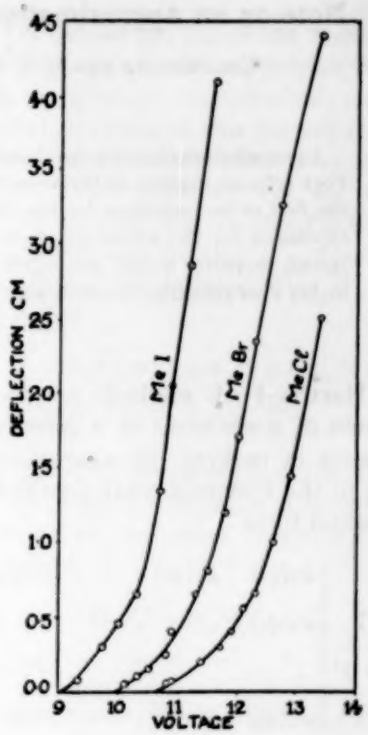

FIG. 3. Curves showing ionization potentials of methyl iodide, methyl bromide and methyl chloride.

molecules (p_0) being given by

$$p'/p_0 = (T_0/T_1)^{\frac{1}{2}}(a/a') \cdot \exp E/RT,$$

where T_0 is taken to be the temperature of the walls of the cage, T_1 is the filament temperature, a, a' are the areas of filament and anode apertures, respectively, and E is the energy of activation necessary for dissociation at the filament, the accommodation coefficient being assumed to be unity.

Under the conditions of the experiment $T_0 = ca.$ 600°K, $T_1 = 2400$°K, $a = 6 \times 10^{-2}$ cm², $a' = 8 \times 10^{-2}$ cm². Taking $E = 10{,}000$ cals., $p'/p_0 = 0.045$.

I have to thank Mr. W. G. Penney and Dr. G. B. B. M. Sutherland for helpful discussions; also Mr. S. A. McKay for his technical assistance.

Note on an Approximation Treatment for Many-Electron Systems

CHR. MØLLER AND M. S. PLESSET,* *Institut for teoretisk Fysik, Copenhagen*

(Received July 14, 1934)

A perturbation theory is developed for treating a system of n electrons in which the Hartree-Fock solution appears as the zero-order approximation. It is shown by this development that the first order correction for the energy and the charge density of the system is zero. The expression for the second-order correction for the energy greatly simplifies because of the special property of the zero-order solution. It is pointed out that the development of the higher approximation involves only calculations based on a definite one-body problem.

THE Hartree-Fock method[1] for treating a system of n electrons in a given external field consists in making the approximation of assigning to the system a wave function of the determinantal form

$$\Phi^0=\frac{1}{(n!)^{\frac{1}{2}}}\begin{vmatrix}\varphi_1(q_1) & \varphi_1(q_2) & \cdots & \varphi_1(q_n)\\ \varphi_2(q_1) & \cdot & \cdots & \cdot\\ \cdot & & & \cdot\\ \cdot & & & \cdot\\ \varphi_n(q_1) & \cdot & \cdots & \varphi_n(q_n)\end{vmatrix}, \quad (1)$$

where the variables q_i represent space and spin coordinates, and the n functions $\varphi_r(q)$ are a set of orthogonal normalized solutions of the equation

$$ih(\partial/\partial t)\varphi_r(q)=(H_0+B-A)\varphi_r(q). \quad (2)$$

In (2) H_0 is the Hamiltonian for an electron in the external field, and the matrix elements of B and A in the q-representation are given by[2]

$$(q|B|q')=\int\int(qq''|V|q'q''')dq''dq'''(q'''|\rho|q''), \quad (3)$$

$$(q|A|q')=\int\int(qq''|V|q'''q')dq''dq'''(q'''|\rho|q''), \quad (4)$$

where the matrix of ρ is defined by

$$(q|\rho|q')=\sum_{r=1}^{n}\varphi_r(q)\varphi_r^*(q'), \quad (5)$$

and V is the interaction energy for a pair of electrons.

As follows from the definition (5) the density matrix ρ is Hermitean and obeys the equation $\rho^2=\rho$; (5) together with (2) give the equation of motion for ρ

$$ih\dot{\rho}=(H_0+B-A)\rho-\rho(H_0+B-A). \quad (6)$$

As Dirac has emphasized, all probabilities can be expressed by means of this density matrix ρ;[3] in particular the charge density at q is given by $(q|\rho|q)$.

It is supposed throughout the following that H_0 does not contain the time explicitly. We may then consider solutions of (2) and (6) which belong to a stationary state μ so that our equations become

$$F_\mu\varphi_r^{(\mu)}(q)\equiv(H_0+B_\mu-A_\mu)\varphi_r^{(\mu)}(q)=\lambda_r^{(\mu)}\varphi_r^{(\mu)}(q); \quad (7)$$

$$F_\mu\rho_\mu-\rho_\mu F_\mu=0. \quad (8)$$

It is clear that the form of the operator F_μ depends on the stationary state considered. The energy of the system is, in the present approximation, given by

$$W_\mu^0=D\{\rho_\mu(H_0+\tfrac{1}{2}B_\mu-\tfrac{1}{2}A_\mu)\}, \quad (9)$$

where D denotes the diagonal sum. The corresponding wave function for a stationary state of the whole system is an eigenfunction of the operator

$$G_\mu\equiv\sum_{i=1}^{n}\{H_0^{(i)}+B_\mu^{(i)}-A_\mu^{(i)}\}=\sum_{i=1}^{n}F_\mu^{(i)}, \quad (10)$$

* National Research Fellow.

[1] V. Fock, Zeits. f. Physik **61**, 126 (1930); P. A. M. Dirac, Proc. Camb. Phil. Soc. **26**, Part III, 376 (1930).

[2] $\int\cdots dq$ is always understood to include summation over the spin coordinate.

[3] Dirac, Proc. Camb. Phil. Soc. **27**, Part II, 240 (1930).

where by $F_\mu^{(i)}$ is meant the operator $H_0+B_\mu-A_\mu$ (or F_μ) operating only on functions of the coordinates of the ith electron. We have

$$G_\mu\Phi_\mu^\circ=\lambda_\mu\Phi_\mu^\circ, \tag{11}$$

in which

$$\lambda_\mu=\sum_{r=1}^{n}\lambda_r^{(\mu)}.$$

From (7) it follows that

$$\lambda_\mu=\sum_{r=1}^{n}\int\varphi_r^{(\mu)*}\cdot F_\mu\varphi_r^{(\mu)}dq$$

$$=\sum_{r=1}^{n}\int\int\varphi_r^{(\mu)*}(q)(q|F_\mu|q')\varphi_r^{(\mu)}(q')dqdq'$$

$$=\int\int(q'|\rho_\mu|q)(q|F_\mu|q')dqdq'=D(\rho_\mu F_\mu). \tag{12}$$

Comparison of (12) with (9) gives

$$\lambda_\mu=W_\mu^\circ+\tfrac{1}{2}D\{\rho_\mu(B_\mu-A_\mu)\}. \tag{13}$$

We may now write (11) as follows

$$H_\mu\Phi_\mu^\circ\equiv[G_\mu-\tfrac{1}{2}D\{\rho_\mu(B_\mu-A_\mu)\}]\Phi_\mu^\circ=W_\mu^\circ\Phi_\mu^\circ. \tag{14}$$

so that the operator H_μ has the eigenvalue W_μ° and the eigenfunction Φ_μ°.

We now wish to compare the above equation with the exact one in order to determine the degree of accuracy of the Hartree-Fock approximation. If V_{ik} denoted the interaction energy between the ith and kth electron, then the exact equation for the eigenstates of the system is

$$\mathfrak{H}\Phi\equiv\left\{\sum_{i=1}^{n}H_0^{(i)}+\tfrac{1}{2}\sum_{i\neq k}^{n}V_{ik}\right\}\Phi=W\Phi. \tag{15}$$

It is, of course, understood that only antisymmetrical solutions of (15) are to be considered. We now compare the operators occurring in (14) and (15) and define a new operator Γ_μ as their difference,

$$\Gamma_\mu=\mathfrak{H}-H_\mu=\tfrac{1}{2}\sum_{i\neq k}^{n}V_{ik}-\sum_{i=1}^{n}(B_\mu^{(i)}-A_\mu^{(i)})+\tfrac{1}{2}D\{\rho_\mu(B_\mu-A_\mu)\}. \tag{16}$$

It is now proposed for the succeeding development to take the Hartree-Fock-approximation as the zero-order approximation to the exact theory. The deviation, Γ_μ, of the Hartree-Fock operator H_μ from the exact operator $\mathfrak{H}$ is here regarded as a small perturbation; and it is evident that the form of this perturbation term depends on the stationary state considered. We develop the exact eigenfunction Φ_μ, which is supposed to lie near the Hartree-Fock solution Φ_μ°, and the exact eigenvalue W_μ, which is supposed to lie near the corresponding W_μ°, in the following series

$$\Phi_\mu=\Phi_\mu^\circ+\Phi_\mu^{(1)}+\Phi_\mu^{(2)}+\cdots, \tag{17}$$

$$W_\mu=W_\mu^\circ+W_\mu^{(1)}+W_\mu^{(2)}+\cdots. \tag{18}$$

If these expansions are introduced into the exact equation $(H_\mu+\Gamma_\mu)\Phi_\mu=W_\mu\Phi_\mu$ it is found on collecting terms of the same magnitude in the usual way that

$$H_\mu\Phi_\mu^\circ=W_\mu^\circ\Phi_\mu^\circ; \tag{19}$$

$$\{H_\mu-W_\mu^\circ\}\Phi_\mu^{(1)}=\{W_\mu^{(1)}-\Gamma_\mu\}\Phi_\mu^\circ; \tag{20}$$

$$\{H_\mu-W_\mu^\circ\}\Phi_\mu^{(2)}=W_\mu^{(2)}\Phi_\mu^\circ+\{W_\mu^{(1)}-\Gamma_\mu\}\Phi_\mu^{(1)}; \tag{21}$$

Eq. (19) is of course fulfilled from the definition (14) of the zero-order approximation; (20) and (21) are the equations determining the first and second order corrections, respectively.

Let us consider the complete set of eigenfunctions $\Phi_{\mu\nu}^\circ$ of the Hartree-Fock operator H_μ associated with a definite zero-order state μ; we have

$$H_\mu\Phi_{\mu\nu}^\circ=W_{\mu\nu}^\circ\Phi_{\mu\nu}^\circ, \tag{22}$$

where $W_{\mu\nu}^\circ$ are the corresponding eigenvalues, and where we choose ν so that $\Phi_{\mu 0}^\circ=\Phi_\mu^\circ$. The functions $\Phi_\mu^{(1)}$, $\Phi_\mu^{(2)}$, $\cdots$ may be developed in terms of the complete set of functions $\Phi_{\mu\nu}^\circ$; that is,

$$\Phi_\mu^{(1)}=\sum_\nu a_{\mu\nu}^{(1)}\Phi_{\mu\nu}^\circ; \tag{23}$$

$$\Phi_\mu^{(2)}=\sum_\nu a_{\mu\nu}^{(2)}\Phi_{\mu\nu}^\circ; \tag{24}$$

. . . . . .

Substitution of (23) into (20) and application of (22) gives

$$\sum_\nu a_{\mu\nu}^{(1)}(W_{\mu\nu}^\circ-W_\mu^\circ)\Phi_{\mu\nu}^\circ=\{W_\mu^{(1)}-\Gamma_\mu\}\Phi_\mu^\circ. \tag{25}$$

If the right side of Eq. (25) is expanded in terms

of the functions $\Phi_{\mu\nu}^{\circ}$ and corresponding coefficients equated, one gets at once

$$a_{\mu\nu}^{(1)}(W_{\mu\nu}^{\circ}-W_{\mu}^{\circ}) = \int\cdots\int \Phi_{\mu\nu}^{\circ *}\{W_{\mu}^{(1)}-\Gamma_{\mu}\}\Phi_{\mu}^{\circ}dq. \quad (26)$$

Let us for simplicity suppose that $W_{\mu\nu}^{\circ} \neq W_{\mu}$ for $\nu \neq 0$; the alterations in the procedure which arise in the presence of degeneracies are of the usual kind and will not be considered here. From (26) for $\nu=0$ we have

$$W_{\mu}^{(1)} = \int\cdots\int \Phi_{\mu}^{\circ *}\Gamma_{\mu}\Phi_{\mu}^{\circ}dq; \quad (27)$$

and for $\nu \neq 0$

$$a_{\mu\nu}^{(1)} = \frac{\int\cdots\int \Phi_{\mu\nu}^{\circ *}\Gamma_{\mu}\Phi_{\mu}^{\circ}dq}{W_{\mu}^{\circ}-W_{\mu\nu}^{\circ}}. \quad (28)$$

The normalization condition for Φ_{μ} gives $a_{\mu 0}^{(1)}=0$. The second order correction may be carried through in a similar way by the introduction of (24) into (21); it is readily found that the second order correction in the energy is

$$W_{\mu}^{(2)} = \sum_{\nu\neq 0}\frac{\int\cdots\int \Phi_{\mu}^{\circ *}\Gamma_{\mu}\Phi_{\mu\nu}^{\circ}dq\cdot\int\cdots\int \Phi_{\mu\nu}^{\circ *}\Gamma_{\mu}\Phi_{\mu}^{\circ}dq}{W_{\mu}^{\circ}-W_{\mu\nu}^{\circ}}. \quad (29)$$

The complete set of antisymmetric eigenfunctions in (22) may be expressed in terms of the complete set of eigenfunctions of the one-electron operator F_{μ}. In addition to the n functions $\varphi_r^{(\mu)}$, which enter into the determinant Φ_{μ}°, we have an infinite set of eigenfunctions $\psi_{\rho}^{(\mu)}(\rho=1, 2, \cdots)$ of F_{μ} with the associated eigenvalues κ_{ρ}. We now get all the functions $\Phi_{\mu\nu}^{\circ}$ from

$$\Phi_{\mu}^{\circ} = \frac{1}{(n!)^{\frac{1}{2}}}\begin{vmatrix} \varphi_1^{(\mu)}(q_1) & \varphi_1^{(\mu)}(q_2) & \cdots & \varphi_1^{(\mu)}(q_n) \\ \varphi_2^{(\mu)}(q_1) & \cdot & \cdots & \cdot \\ \cdot & & & \cdot \\ \cdot & & & \cdot \\ \varphi_n^{(\mu)}(q_1) & \cdot & \cdots & \varphi_n^{(\mu)}(q_n) \end{vmatrix}, \quad (30)$$

by replacing one or more of the functions $\varphi^{(\mu)}$ by functions $\psi^{(\mu)}$. We denote by $\Phi^{\circ}{}_{(\mu)r,\ s\cdots;\ \rho,\ \sigma,\ \ldots}$ that $\Phi_{\mu\nu}^{\circ}$ which is obtained by replacing $\varphi_r^{(\mu)}$, $\varphi_s^{(\mu)}\cdots$ by $\psi_{\rho}^{(\mu)}$, $\psi_{\sigma}^{(\mu)}$, $\cdots$ respectively; the indices $r, s\cdots$ may take on independently all the values $1\cdots n$, and $\rho, \sigma\cdots$ take on all values.

It will be understood in the following that all quantities refer to a given stationary state, and the suffix μ will be dropped. From (27) and (16) we get for the first order correction in the energy

$$W^{(1)} = (1/(n!2))\sum_{i\neq k}^{n}\int\cdots\int (q_iq_k|\,V\,|q_i'q_k')\sum_{PP'}\delta_P P\varphi_1^*(q_1)\varphi_2^*(q_2)\cdots\varphi_n^*(q_n)\delta_{P'}P'\varphi_1(q_1)\varphi_2(q_2)$$
$$\cdots\varphi_i(q_i')\cdots\varphi_k(q_k')\cdots\varphi_n(q_n)dq_1dq_2\cdots dq_ndq_i'dq_k'$$
$$-(1/n!)\sum_{i=1}^{n}\int\cdots\int (q_i|\,B-A\,|q_i')\sum_{PP'}\delta_P P\varphi_1^*(q_1)\cdots\varphi_n^*(q_n)\delta_{P'}P'\varphi_1(q_1)\cdots\varphi_i(q_i')$$
$$\cdots\varphi_n(q_n)dq_1\cdots dq_ndq_i'+\tfrac{1}{2}D\{\rho(B-A)\}, \quad (31)$$
$$=\mathrm{I}+\mathrm{II}+\tfrac{1}{2}D\{\rho(B-A)\},$$

where P denotes a permutation of the arguments of the functions φ^*, δ_P is $+1$ or -1 according as P is an even or odd permutation, and $\sum_P$ includes $n!$ possible permutations; similarly P' denotes all permutations of the arguments of the functions φ. To calculate the first of the integrals in (31) we consider that term in $\sum_{PP'}$ which comes from $P=P'$, a definite permutation; a typical term, for the given P, in $\sum_{i\neq k}$ is

$$\frac{1}{n!2}\int\int\int\int (q_iq_k|\,V\,|q_i'q_k')\varphi_r^*(q_i)\varphi_s^*(q_k)\varphi_r(q_i')\varphi_s(q_k')dq_idq_kdq_i'dq_k'$$

$$=\frac{1}{n!2}\int\int\int\int (qq'|\,V\,|q''q''')\varphi_r^*(q)\varphi_s^*(q')\varphi_r(q'')\varphi_s(q''')dqdq'dq''dq''', \quad (32)$$

where r, s are the respective places to which P has taken q_i, q_k. If now the summation over i, k is carried out, we get

$$\frac{1}{n!2}\sum_{r\neq s}^{n}\int\int\int\int (qq'|\,V\,|q''q''')\varphi_r^*(q)\varphi_s^*(q')\varphi_r(q'')\varphi_s(q''')dqdq'dq''dq'''.$$

Clearly, every $P=P'$ gives this same result so that $\sum_{P=P'}$ gives a factor $n!$ and the contribution to I is, using (5) and (3),

$$\tfrac{1}{2}\int\int (q''|\,\rho\,|q)(q|\,B\,|q'')dqdq''$$

$$-\sum_{i=1}^{n}\int\int\int\int (qq'|\,V\,|q''q''')\varphi_i^*(q)\varphi_i^*(q')\varphi_i(q'')\varphi_i(q''')dqdq'dq''dq'''; \quad (33)$$

the first term in this expression, we note, is $\frac{1}{2}D(\rho B)$. We now consider the contribution to I arising from the remaining permutations $P'\neq P$. On account of the orthogonality of the functions φ_r, for a given P the only P' in $\sum_{P'}$ which contributes will differ from P merely by a transposition of the arguments of φ_r and φ_s in a typical term in $\sum_{i\neq k}$; thus the analogue of (32) is

$$-\frac{1}{n!2}\int\int\int\int (q_iq_k|\,V\,|q_i'q_k')\varphi_r^*(q_i)\varphi_s^*(q_k)\varphi_r(q_k')\varphi_s(q_i')dq_idq_kdq_i'dq_k';$$

the negative sign enters since $\delta_P=-\delta_{P'}$. As before $\sum_{i\neq k}$ and $\sum_P$ may be immediately carried out to give

$$-\tfrac{1}{2}D(\rho A)+\tfrac{1}{2}\sum_{i=1}^{n}\int\int\int\int (qq'|\,V\,|q''q''')\varphi_i^*(q)\varphi_i^*(q')\varphi_i(q'')\varphi_i(q''')dqdq'dq''dq'''. \quad (34)$$

Thus from (33) and (34)

$$\mathrm{I}=\tfrac{1}{2}D\{\rho(B-A)\}. \quad (35)$$

In a similar way we find that $\mathrm{II}=-D\{\rho(B-A)\}$; and we have finally from (31) that

$$W^{(1)}=0. \quad (36)$$

Thus, the perturbation method shows that the theory of the self-consistent field including exchange is accurate in the determination of energy to the second approximation.

We shall now consider the matrix elements entering into the determination of the first order correction (28) in the eigenfunction and the second order correction (29) in the energy. It is evident that those integrals, $\int\cdots\int\Phi_r^\circ\Gamma\Phi^\circ dq$ in which Φ_r° has more than two of the functions φ_r replaced by functions ψ_ρ will vanish identically because of the orthogonality of the functions φ and ψ. The only integrals, therefore, which remain are of the form

$$\int\cdots\int\Phi^\circ{}_{r;\ \rho}\Gamma\Phi^\circ dq \quad (37) \qquad \text{and} \qquad \int\cdots\int\Phi^\circ{}_{rs;\ \rho\sigma}\Gamma\Phi^\circ dq. \quad (38)$$

A straight forward calculation of the integrals of the type (37) shows that it is a special property of the Hartree-Fock theory that all these integrals vanish; however, we get a nonvanishing contribution from the integrals (38) of the form

$$\int\cdots\int\Phi^{\circ}{}_{rs;\ \rho\sigma}\Gamma\Phi^{\circ}dq=\int\int\int\int\psi_{\rho}^{*}(q)\psi_{\sigma}^{*}(q')(qq'|\,V\,|q''q''')\cdot\{\varphi_{r}(q'')\varphi_{s}(q''')-\varphi_{r}(q''')\varphi_{s}(q'')\}dqdq'dq''dq'''. \tag{39}$$

Eq. (29) now reduces to

$$W^{(2)}=\sum_{rs;\ \rho\sigma}\frac{|\int\int\int\int\psi_{\rho}^{*}(q)\psi_{\sigma}^{*}(q')(qq'|\,V\,|q''q''')\{\varphi_{r}(q'')\varphi_{s}(q''')-\varphi_{r}(q''')\varphi_{s}(q'')\}dqdq'dq''dq'''|^{2}}{\lambda_{r}+\lambda_{s}-\kappa_{\rho}-\kappa_{\sigma}} \tag{40}$$

where we have used the relations

$$W^{\circ}=\sum_{i=1}^{n}\lambda_{i}-\tfrac{1}{2}D\{\rho(B-A)\};\qquad\text{and}\qquad W^{\circ}{}_{rs;\ \rho\sigma}=\kappa_{\rho}+\kappa_{\sigma}+\sum_{i\neq r,\ s}\lambda_{i}-\tfrac{1}{2}D\{\rho(B-A)\}.$$

As we now see from (40) and (28), to carry the procedure to this higher approximation it is only necessary to find the solutions of the equation $F_{\mu}\psi=\kappa\psi$; that is, to solve a one-body problem.

The wave functions including the first order correction are in a similar way reduced to

$$\Phi^{\circ}+\Phi^{(1)}=\Phi^{\circ}+\sum_{rs;\ \rho\sigma}a^{(1)}{}_{rs;\ \rho\sigma}\Phi^{\circ}{}_{rs;\ \rho\sigma} \tag{41}$$

as $a^{(1)}{}_{rs;\ \rho\sigma}$ are the only non-zero coefficients from (28). The charge distribution corresponding to (41) is

$$\rho(q)=n\int\cdots\int\left|\Phi^{\circ}(q,q_{2},q_{3}\cdots q_{r})+\sum_{rs;\ \rho\sigma}a^{(1)}{}_{rs;\ \rho\sigma}\Phi^{\circ}{}_{rs;\ \rho\sigma}(q,q_{2},q_{3}\cdots q_{n})\right|^{2}dq_{2}dq_{3}\cdots dq_{n}. \tag{42}$$

It is readily seen that the cross terms in (42) which give the first order correction to $\rho(q)$ all vanish so that the Hartree-Fock electric density as given by the diagonal elements of (5) is accurate to the second order.

Segregation of Polonium in Bismuth Crystals

ALFRED B. FOCKE,* *Sloane Physics Laboratory, Yale University*

(Received August 9, 1934)

Single crystals of bismuth containing polonium as an impurity are studied in order to determine the distribution of the polonium. Number-distance relations for α-particles emitted normally through cleavage surfaces afford the means of investigation, measurements being made with a Geiger counter. When present in very small concentrations polonium is found to be segregated into small regions which have nearly regular spacings when viewed in several directions. These average spacings, $(0.54\pm0.03)\mu$ for planes parallel to the (111) plane and $(0.90\pm0.1)\mu$ for planes parallel to the (11$\bar{1}$) plane, are unaffected by the speed of growth of the bismuth crystal and by subsequent heat treatment. The addition of tellurium suppresses alternate layers parallel to the (111) plane and removes all evidence of layers parallel to the (11$\bar{1}$) plane.

IN a recent paper, Goetz and Focke[1] were led to make several assumptions in order to explain the effect of impurities on the magnetic properties of bismuth single crystals. Two of these assumptions were that metals possess a secondary or superstructure, such as has been predicted by Zwicky,[2] and that the impurities locate in these planes. For example, elements belonging to subgroup 6*b* of the periodic system enter planes parallel to the perfect cleavage plane (111). Since polonium is a member of this group it offers a good test of these assumptions.

If the assumptions are correct and if the ranges of the α-particles emitted normally through a perfect cleavage surface of a polonium-infected bismuth crystal are determined, it should be found that the ranges of individual particles differ by integral multiples of some least difference. Conversely, if it is found that the observed ranges are so related, the polonium atoms must have been arranged in equally spaced planes parallel to the perfect cleavage plane.

Preparation of Crystals

The polonium was introduced into the bismuth by rotating a thin sheet of bismuth in an acid solution containing about three millicuries of polonium, for a period of two hours at a rate of one revolution per minute. In this time one millicurie of polonium was deposited on the bismuth (1 atom Po to 10^7 atoms Bi). This was measured, and freedom from Ra D and Ra E was checked after the bismuth had been carefully washed and dried. The metal was then melted under hydrogen to form a small button. This was subsequently divided into three parts, each weighing about 0.1 gram. In order to form the single crystals the 0.1 gram samples were again melted under hydrogen and allowed to cool slowly. The resulting buttons were in general found to be single crystals. As the orientation of the crystals could not conveniently be predetermined, the cleavage planes were located by means of the pattern revealed by etching the samples in a 50 percent water solution of HNO_3. The crystals were then cleaved with a razor blade and very good cleavage surfaces were obtained.

Apparatus and Method of Measurement

A diagram of the apparatus used to determine the ranges of the α-particles is shown in Fig. 1. The crystal was mounted with its cleavage surface normal to the axis of a screw which provided a convenient method for adjusting the location of the crystal within the vacuum chamber. A mica window 1.5 mm in diameter and 8 mm stopping power (air equivalent), was set perpendicular to the axis of the screw. The distance from the crystal face to the window was kept at about 38 mm to facilitate the conversion of cm of Hg

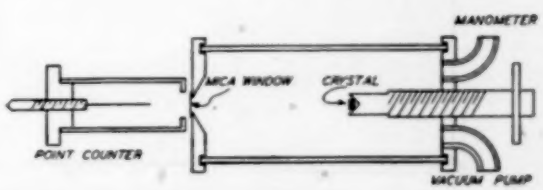

FIG. 1. Arrangement of apparatus for α-particle range determination.

* National Research Fellow.

[1] A. Goetz and A. B. Focke, Phys. Rev. **45**, 170 (1934).

[2] F. Zwicky, Proc. Nat. Acad. Sci. **16**, 211 (1930).

pressure within the chamber to equivalent air path of the α-particles. A 2 cm change of pressure thus had the same effect as a 1 mm displacement of the crystal at standard pressure. As the largest dimension of the crystal face was 3 mm, the error introduced into the determination of the ranges of the α-particles, due to obliquity of paths, amounted to about 0.1 percent and was therefore completely negligible. The number of α-particles passing through the window was determined by means of a Geiger-point counter coupled through a two-stage amplifier and a sensitive relay to a Cenco impulse counter. The arrangement was found to be entirely satisfactory for counting α-particles up to rates of 500 per minute.

In making the measurements counts were taken for pressure steps of one cm Hg and the number of α-particles reaching the counter in ten minutes was recorded for each pressure. The entire number-distance curve for each cleavage face was plotted without interruption in order to make sure that external conditions were as uniform as possible. Counts were taken at 76 cm pressure at the beginning and end of each run and

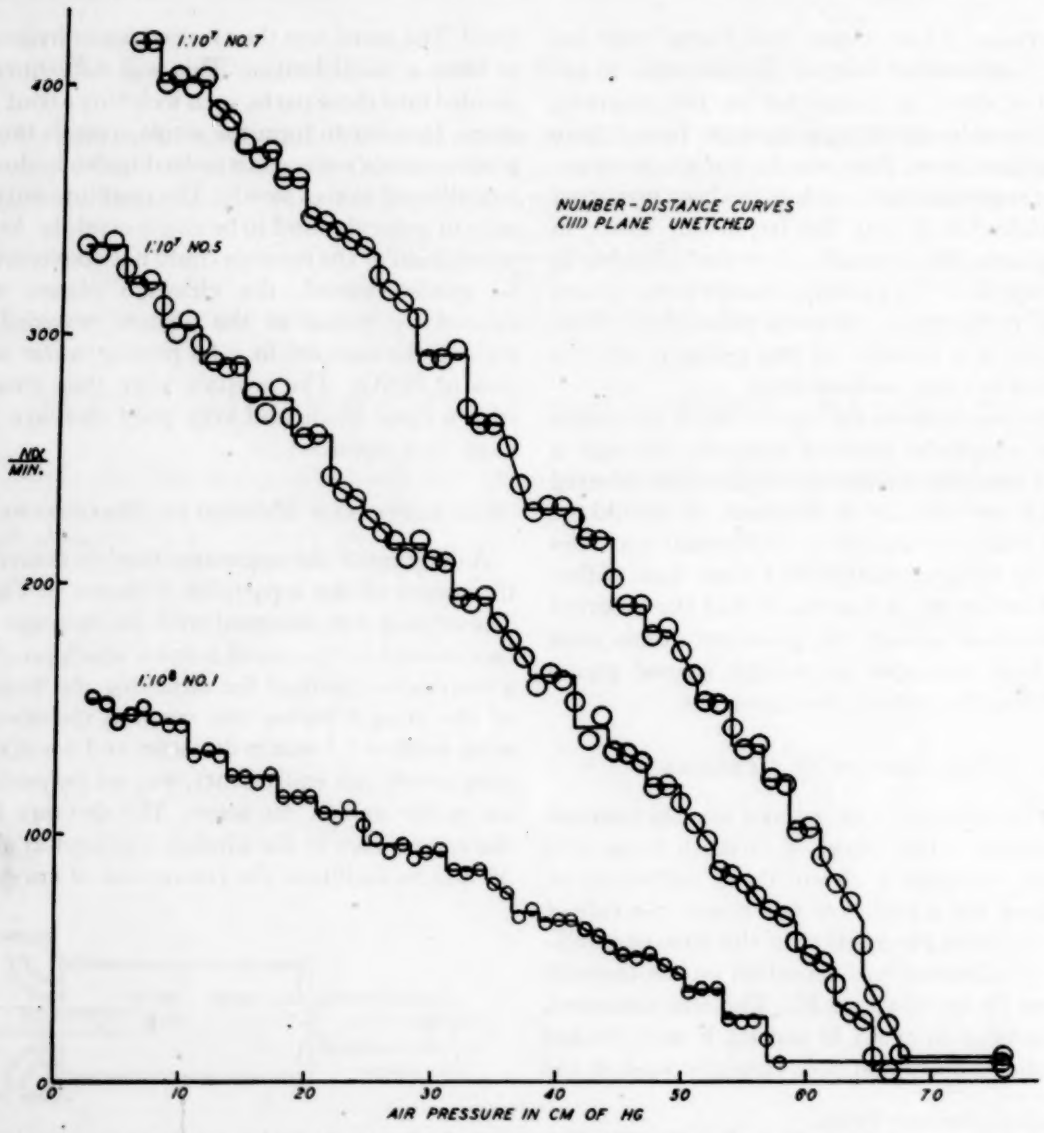

FIG. 2. Number-distance curves for α-particles emitted normally through (111) planes of bismuth crystals containing polonium.

although they were apparently constant for any one run, it was found that there was a gradual increase from 2 per minute to 10 per minute during the course of the whole series of experiments. This was probably due to the evaporation of a small amount of the polonium and its redeposition onto the walls of the vacuum chamber. Due to the very slow change of this residual contamination it caused no measurable error in the experiments.

Results and Discussion

Typical number-distance curves for bismuth crystals containing polonium alone, are given in Figs. 2 and 3. The data for Fig. 2 were taken for α-particles emerging normally through a perfect cleavage plane (111) and the data for Fig. 3 were taken for α-particles emerging normally through an imperfect cleavage plane ($11\bar{1}$). It may be seen at once that the polonium atoms were arranged

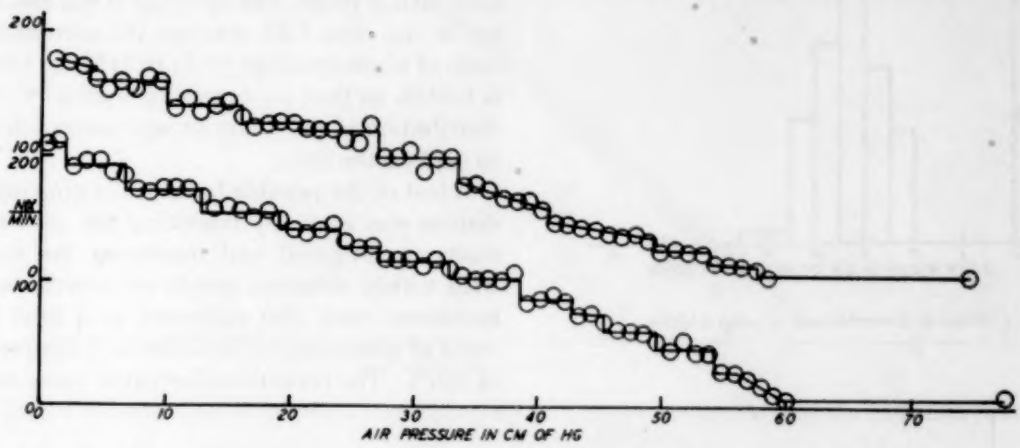

Fig. 3. Number-distance curves for α-particles emitted normally through ($11\bar{1}$) planes of bismuth crystals containing polonium.

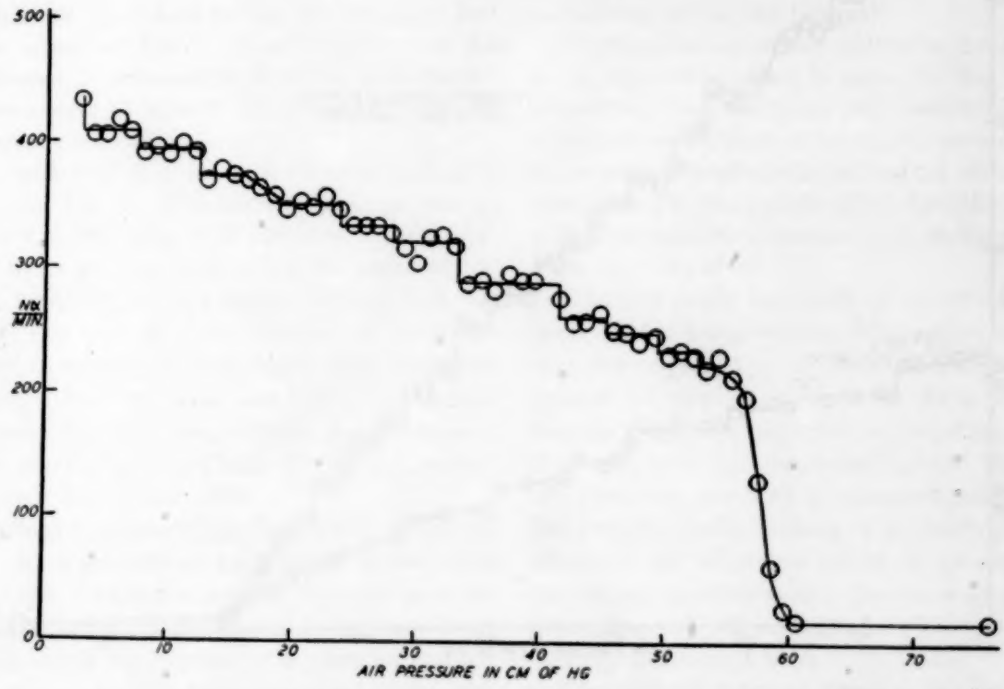

Fig. 4. Number-distance curve for α-particles emitted normally through an etched (111) plane.

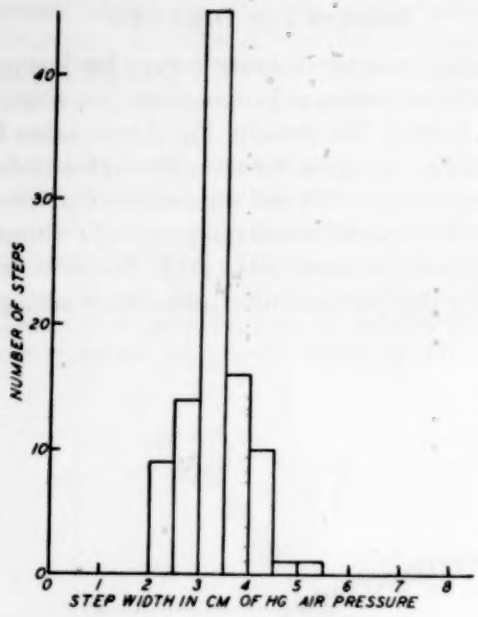

FIG. 5. Distribution of step widths.

in layers parallel to the surface in both cases. The distance between layers is indicated by the width of the steps parallel to the pressure axis. For 112 layers parallel to the (111) plane the average separation is $(0.54\pm0.03)\mu$. For 32 layers parallel to the $(11\bar{1})$ plane the average separation is $(0.90\pm0.10)\mu$.

The interpretation offered for these results is that the polonium is segregated into a kind of space lattice, with a large number of atoms at each lattice point. The spacings 0.90μ and 0.54μ are in the ratio 1.67, whereas the corresponding ratio of plane spacings $(11\bar{1})$ to (111) in bismuth is 0.9456, so that no crystallographically simple distribution of polonium groups seems adequate to explain the data.

A test of the possible influence of growing conditions was made by remelting the samples already investigated and regrowing the crystals with widely different speeds of growth. Several specimens were also subjected to a heat treatment of annealing for 48 hours at a temperature of 250°C. The crystals subjected to these various

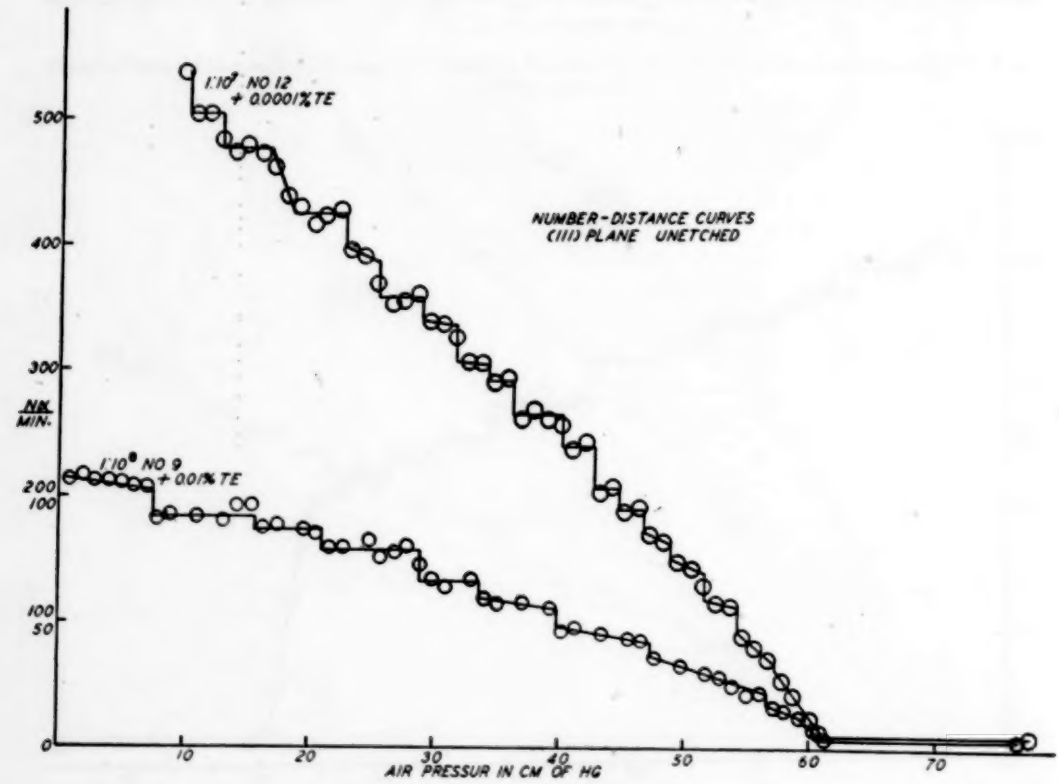

FIG. 6. Number-distance curves for α-particles emitted normally through (111) planes of bismuth crystals containing polonium and tellurium.

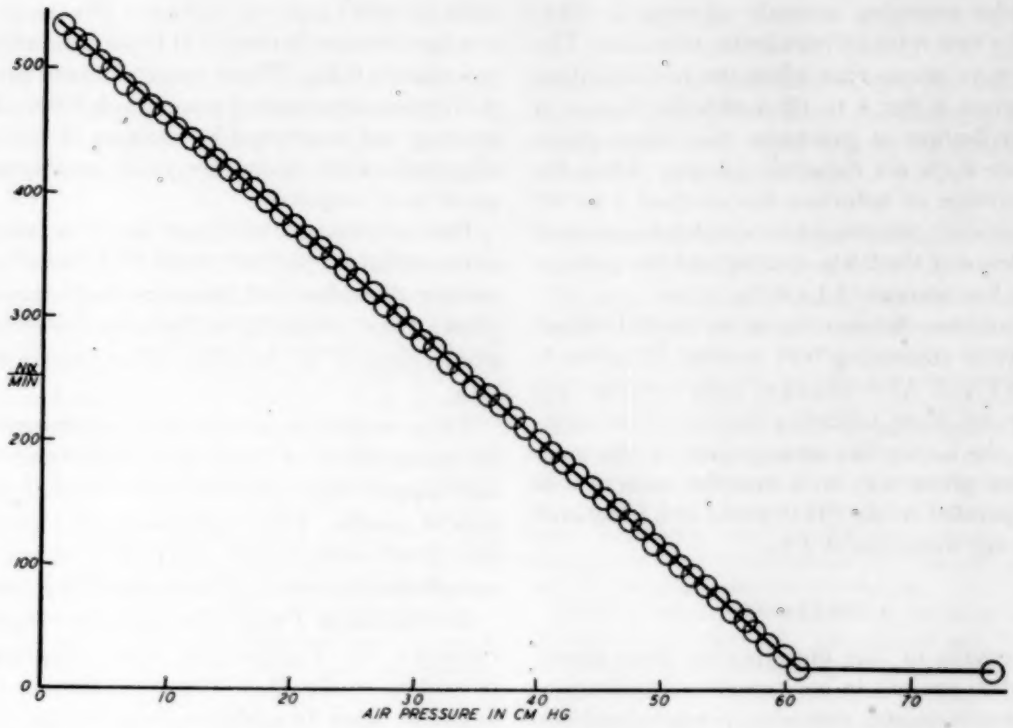

FIG. 7. Number-distance curve for α-particles emitted normally through a (11$\bar{1}$) plane of a bismuth crystal containing polonium and tellurium.

tests were found to have the same average distribution of polonium as the crystals first investigated, leading to the conclusion that the distribution of polonium in bismuth is unaffected by the speed of growth of the crystals or by subsequent annealing.

The effect of etching on a cleaved surface is shown in Fig. 4. The extremely large rise in numbers at the surface of the crystal occurs because in an acid solution polonium replaces bismuth. Therefore as the original surface was dissolved, the surface concentration of polonium rapidly increased. It had been suggested that smoother planes might be obtained by an etching treatment, but because precision was diminished by the greatly increased rate of counting, etched faces were not further used.

It should be noticed that the effect of straggling is very apparent in those parts of the curves which result from α-particles originating in or near the surface, whereas there seems to be very little evidence of it for groups of α-particles coming from greater depths. It would appear from this that there must be relatively little straggling of α-particles within the bismuth.

The distribution of step widths for layers parallel to the (111) plane is given in Fig. 5. The deviations from the mean are undoubtedly real, as several small steps or several large steps may occur consecutively in an individual crystal. The distribution is like a probability distribution with a definite maximum at about 3.2 cm Hg pressure of air or 0.54μ of Bi.

A further study was made of the effect of concentration of the polonium. More dilute mixtures than the original 1 to 10^7 Po to Bi were found to possess no new characteristics. As it was not feasible to make a more concentrated mixture of polonium, tellurium was added instead. Polonium and tellurium are both in the same subgroup of the periodic table, making it probable that the effects of the tellurium would be qualitatively, though not quantitatively, the same as those of polonium, and the polonium would serve to indicate the location of both.

Fig. 6 gives number-distance curves of the

α-particles emerging normally through a (111) plane for two crystals containing tellurium. The upper curve shows that when the concentration of tellurium is but 1 to 10^6 a definite change in the distribution of polonium has taken place. Alternate steps are definitely greater. When the concentration of tellurium has reached 1 to 10^4 (0.01 percent), this effect has completely removed all evidence of the 0.54μ spacing and the average spacing has become $(1.1\pm0.1)\mu$.

The number-distance curve for a $(11\bar{1})$ plane of a crystal containing 0.01 percent tellurium is given in Fig. 7. All evidence of layer structure has disappeared, thus indicating that for this concentration the lattice-like arrangement of the polonium has given way to a lamellar structure of planes parallel to the (111) plane and separated by average distances of 1.1μ.

Conclusion

The results of this investigation have shown that, when present in very small concentrations in a bismuth crystal, polonium is segregated into small regions which have nearly regular spacings when viewed in several different directions. The average distance between (111) planes containing polonium is 0.54μ. The average distance between $(11\bar{1})$ planes containing polonium is 0.90μ. These spacings are unaffected by changes in the speed of growth of the bismuth crystal, and by subsequent heat treatment.

The addition of tellurium tends to suppress alternate layers parallel to the (111) plane and to remove all evidence of layers parallel to the $(11\bar{1})$ plane, thus producing a lamellar structure of planes parallel to the (111) plane separated by 1.1μ.

These results are in excellent agreement with the assumptions of Goetz and Focke[1] and therefore support their interpretation of other experimental results. This experiment also gives the first direct evidence for a secondary structure in metals on the same scale as predicted by Zwicky.[2]

In conclusion I wish to express my thanks to Professor A. F. Kovarik, who supplied the polonium, to Dr. D. Cooksey for the use of the amplifier used in counting and to Dr. E. C. Pollard for many helpful suggestions.

LETTERS TO THE EDITOR

Prompt publication of brief reports of important discoveries in physics may be secured by addressing them to this department. Closing dates for this department are, for the first issue of the month, the twentieth of the preceding month; for the second issue, the fifth of the month. The Board of Editors does not hold itself responsible for the opinions expressed by the correspondents.

On the Doublet Separation in the Normal State of Nitric Oxide and Its Thermodynamic Quantities

A misunderstanding concerning the value of the doublet separation in the $^2\Pi$ state which constitutes the normal state of the nitric oxide molecule occurs in two recent papers, one by Johnston and Chapman[1] and the other by Gordon and Barnes.[2] In order to understand the situation it is necessary to write the formulas for the energy levels. These formulas are often written in the following form, which is convenient for the practical purposes of band-spectroscopy:

$$F_s'(v,J)=\sum_i A'_{si}(J+\tfrac{1}{2})^i+\sum_k a'_{sk}v^k+(s-1)D'. \qquad (1)$$

Here, as is well known, the A'_{si} are functions of v, the a'_{sk} are constants. The subscript s takes on the values 1 and 2, the former referring to the $^2\Pi_{1/2}$ state and the latter to the $^2\Pi_{3/2}$ state. Modern theory in Hund's case (a) requires, however, the following form:

$$F_s(v,J)=B_s(v)[(J+\tfrac{1}{2})^2-\Omega^2_s]+\omega_s(v+\tfrac{1}{2})-x_s\omega_s(v+\tfrac{1}{2})^2+\cdots+(s-1)D.$$

According to Miss Guillery[3] and Schmid[4] $D'=120.9$ cm^{-1}, which yields a value of $D=124.4$ cm^{-1}, the value given by Jenkins, Barton and Mulliken[5] who state that it was obtained from Miss Guillery's value by the addition of $(9/4)B_2''-(1/4)B_1''$ in their notation.

Johnston and Chapman, however, in calculating the specific heat, entropy, and free energy of nitric oxide from the spectroscopic data used the value 124.4 cm^{-1} for D', thereby obtaining results which are not quite correct. In an article to appear in a forthcoming issue of *The Journal of the American Chemical Society* the writer[6] gives a table of the values of these quantities from 1°K to 500°K computed with $D'=120.0$ cm^{-1}, which is very close to the value given by Schmid, Koenig and von Farkas.[7]

A similar misapprehension occurs on page 307 of the paper by Gordon and Barnes, where the value of the doublet separation 124.4 cm^{-1} is attributed to Jenkins, Barton and Mulliken and 120.0 cm^{-1} to Schmid, Koenig and von Farkas, thus indicating a disagreement which does not really exist.

ENOS E. WITMER

Randal Morgan Laboratory of Physics,
University of Pennsylvania,
Philadelphia, Pennsylvania,
August 31, 1934.

[1] H. L. Johnston and A. T. Chapman, J. Am. Chem. Soc. **55**, 153 (1933).
[2] A. R. Gordon and C. Barnes, J. Chem. Phys. **1**, 297 (1933).
[3] M. Guillery, Zeits. f. Physik **42**, 121 (1927).
[4] R. Schmid, Zeits. f. Physik **49**, 428 (1928).
[5] F. A. Jenkins, H. A. Barton and R. S. Mulliken, Phys. Rev. **30**, 150 (1927).
[6] Cf. E. E. Witmer, Phys. Rev. **29**, 918 (1927).
[7] R. Schmid, T. Koenig and D. von Farkas, Zeits. f. Physik **64**, 84 (1930).

Preliminary Report on a Quick Method of Depositing Polonium on Silver

The usual method of obtaining a polonium source from old radium emanation tubes has been described by I. Curie[1] and consists of a series of chemical operations in which the active residue is put into solution and the polonium salts separated from the rest of the solution by a series of precipitations. The polonium is finally separated from a solution containing its salts by deposition on a silver surface. Considerable care is necessary in the purification process or else the silver will become darkened and the deposition cease. Preliminary tests showed that variable valence material, contained in the solution in a high state of oxidation, stopped the deposition of polonium.

Radium D tubes were crushed and the active material dissolved in hot *aqua regia*. The solution was decanted, the residue again treated with *aqua regia*, and the resulting solution added to the first. Owing to the small supply of old emanation tubes available this solution did not contain enough active material for the tests, so some purified radium D solution was added. The resulting solution was purposely contaminated by adding impurities of Fe and Hg.

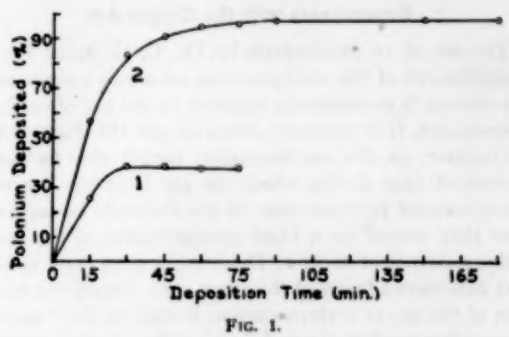

FIG. 1.

A silver disk (7/8 in. diam.) was rotated at 1400 r.p.m. in a 1/20 *N* HCl solution containing ½ millicurie of Ra D in equilibrium with its products. The activity of the disk was measured at 15 minute intervals and the results plotted in curve 1 Fig. 1. The deposit ceased when about 38 percent of the polonium had been deposited, and the silver appeared decidedly brown. In a second experiment the polonium was recovered from the silver and added to the remainder of the solution. This solution was evaporated to dryness, the residue dissolved in 1 cc of 1 *N* HCl, and 10 cc of water saturated with SO_2 added. This was boiled to reduce the Fe and Hg, and then diluted to 1/20 *N*. The silver disk was rotated in the solution as before. The results of the activity measurements are shown in curve 2. It will be noted that about 98 percent of the polonium was de-

posited. Furthermore the silver was bright and untarnished. These experiments were repeated using various acid concentrations from 1/20 *N* to 4 *N* without any noticeable difference in results. Other experiments made by using a disk 1/8 in. diameter (area 0.08 cm²) showed that the rate of deposition of polonium on this disk was slower than for the larger disk and that deposition stopped when 43.5 percent of the polonium had been deposited, the silver remaining bright. The amount of polonium deposited appears to be the maximum amount that can be deposited on a disk of this size. The density of the polonium deposit is 2.95 millicuries/cm² and is in good agreement with the work of Erbacher[2] who found the maximum obtainable deposit to be about 2.98 millicuries/cm², which he believed to correspond to one atomic layer of polonium on the silver.

The present method has the advantage of doing away with a great amount of time consuming purification and insures a clean deposit of polonium on the silver. A more detailed description of the experiments is being prepared for publication.

M. D. Whitaker
William Bjorksted
Allan C. G. Mitchell

Department of Physics,
New York University,
University Heights,
September 12, 1934.

[1] I. Curie, J. de chim. phys. **22**, 471 (1925).
[2] Erbacher, Zeits. f. physik. Chemie **A165**, 421 (1933).

Experiments with the Copper Arc

The use of an oscillograph by Dr. C. G. Suits[1] for the measurement of the voltage across an arc as a function of the current is undoubtedly superior to the use of ordinary instruments. It is necessary, however, for the observer also to register on the oscillographic record the particular periods of time during which the arc is in the "*normal*" form; running perpendicular to the electrode surfaces and near their center for a blind interpretation of the record will certainly lead to error. There are at least three distinct and well-known forms of the copper arc. During the operation of the arc at a given current it may be the "normal" form only a small fraction of the time since it often jumps in a random way from one form to another. As the cathode and anode spots run from place to place over the surface of the electrodes the arch stream is seldom vertical. It is only during these rare moments that readings have meaning as far as the *normal* arc characteristics are concerned. Since Dr. Suits has neglected to differentiate these particular intervals from the times during which the arc is operating in some undetermined way, his criticism of my work cannot be taken as final. A new determination of copper arc characteristic curves is to be undertaken here using an oscillograph.

W. B. Nottingham

Massachusetts Institute of Technology,
September 17, 1934.

[1] C. G. Suits, Phys. Rev. **46**, 252 (1934).

Arcs in Rare Gases*

In several recent papers[1, 2, 3] Doan and his associates have reported the difficulty of maintaining an arc in very pure rare gases. Their experiments and published data, unfortunately, are not of the type to furnish much definite* information about the stability of the arcs, except to show that removing the last trace of impurity (presumably oxide forming) renders the arc relatively unstable; the results, however, do admit an interpretation important in the theory of the cathode of an arc.

The stability of an arc depends not only upon its static characteristic, but also upon its dynamic response to any disturbance, and upon the electrical constants of the circuit. Since the electrode construction permitted the arc to elongate "several hundred percent," the extinction of the arc in the extremely pure gas may have been merely due to the increase in arc length to a static characteristic for which the circuit voltage used could not support the arc. The oscillogram[3] for an arc in impure argon shows a steady arc voltage, as if the arc remained constant in length, and so could be maintained by a much lower circuit voltage. The distinction between the two arcs, though, more probably may be explained by a difference in dynamic stability directly attributable to a fundamental difference in their cathode phenomena. The increased length of the one would then only indirectly increase the circuit voltage required, and the real instability would be caused by some occurrence at the cathode.

Both Compton[4] and the writer[5] have shown theoretically the cathode fall of a high field arc should be higher than that of a thermionic arc under the same conditions, and detailed calculations[5] put the excess as at least 4 to 6 volts. From a reasonable assumption, Doan and Thorne[3] have obtained volt-ampere characteristics for arcs of different lengths between iron electrodes in pure and impure argon. Under the same conditions, the arc voltage was from 5 to 7 volts higher for the pure gas than for the impure gas. This strongly suggests that in pure argon, a high field is responsible for the extraction of electrons from the cathode of the arc, while with a trace of impurity an oxide layer forms on the iron which emits electrons thermionically.

Factors rendering the cathode of the high field arc unstable might be lateral diffusion of ions or electrons from the cathode spot, or, more likely, disintegration of some surface irregularity on the cathode metal at which the increased electric field produced most of the electron emission. Very likely, the factors responsible for the instability also cause the erratic wandering of the cathode spot.

R. C. Mason

Westinghouse Research Laboratories,
East Pittsburgh, Pennsylvania,
August 14, 1934.

* Sci. Paper No. 740.

[1] Doan and Meyer, Phys. Rev. **40**, 36 (1932).
[2] Doan and Meyer, Elect. Eng. **51**, 624 (1932).
[3] Doan and Thorne, Phys. Rev. **46**, 49 (1934).
[4] K. T. Compton, Phys. Rev. **37**, 1077 (1931).
[5] R. C. Mason, Phys. Rev. **38**, 427 (1931).

Band Spectrum of Nitrogen

A continuation of the work on the new band systems of nitrogen, recently reported by me in these columns, has yielded new members for each system. The first system consisted of the four bands 2153(0,0), 2225(0,1), 2301(0,2) and 2381(0,3). As the pressure was gradually lowered, successive pictures showed these bands with increasing intensity. In addition the two bands 2288(1,3) and 2366(1,4) were observed. In the second system, which consisted of 2740 (0,3), 2365(0,2) and 2536(0,1), six new bands have been found. They were 2720(1,4), 2620(1,3), 2522(1,2) and 2432(1,1). Also, the two weaker bands 2421 and 2510 have been identified as 2,2 and 2,3, respectively.

In addition to these bands there are more than forty bands which do not seem to belong to any of the known systems of nitrogen. A few of these have been tentatively grouped together into progressions, but it must be pointed out that this grouping may have to be changed after further study. The five bands 2177, 2245, 2315, 2390 and 2468 degrade to the violet and resemble each other closely. Four more bands, 2236, 2297, 2360 and 2428 are grouped together and the bands 2198, 2280, 2367 and 2459 are also arranged in a progression. Two other sets of bands 2139, 2204, 2272 and 2309, 2391 and 2477 are also grouped together. Other bands at 2262, 2336, 2356, 2372, 2384, 2462, 2489, 2495, 2501, 2512, 2527, 2530, 2570, 2597, 2603, 2640, 2647, 2670 and 2682 have not been even tentatively identified. Further study of these bands is in progress.

JOSEPH KAPLAN

University of California at
Los Angeles, California,
September 12, 1934.